EFFECTS OF TRIMMING ON DAIRY-COW HOOF-PRESSURE DISTRIBUTIONS AND WEIGHT-BEARING DYNAMICS DURING STANCE PHASE

By

VICTOR RICARDO CIACO DE CARVALHO

A DISSERTATION PRESENTED TO THE GRADUATE SCHOOL OF THE
UNIVERSITY OF FLORIDA IN PARTIAL FULFILLMENT OF THE
REQUIREMENTS FOR THE DEGREE OF DOCTOR OF
PHILOSOPHY

UNIVERSITY OF FLORIDA

2004

I dedicate this dissertation to my wife and daughter, Flavia Zukemura de Carvalho and Maria Carolina Zukemura de Carvalho; and to my parents, José Augusto de Carvalho Neto and Ana Maria Ciaco de Carvalho. My most sincere gratitude goes to all of you for all the help and support during this journey.

ACKNOWLEDGMENTS

My most sincere gratitude and respect go to Dr. Ray Allen Bucklin, my graduate advisor and supervisory committee chair, for his outstanding guidance, exceptional graduate training, and most of all for his true friendship. I would also like to express great gratitude and admiration to Dr. Jan K. Shearer and his wife Leslie Shearer. They have always been by my side, providing me with support, guidance and friendship for all I have been through in pursuit of my Ph.D.

I thank my committee members, Dr. James D. Leary, Dr. Roger A. Nordstedt and Dr. H. Herbert Head, for their academic contributions and support. I would like to thank Dr. Charles J. Wilcox (Animal Science Department) for his collaboration in the statistical analyzes of my experimental data.

I will always be grateful to Robert (Bob) Tonkinson, Billy Duckworth, and Jimmy Rummel for their endless help and support during my Ph.D. program, and throughout the course of my graduate life at University of Florida. I would also like to thank my friends (Enoc Pallango, for his support during all these years; and Erin Wilkerson, for her support and help with data collection). I thank Vanessa Silva for all the time dedicated to one of our experiments, which became part of this dissertation.

I would like to express my appreciation to the agency CAPES-Brazil, which sponsored my entire Ph.D. program. I greatly acknowledge the support of Dairy Farmers for financial support via Check off Funds and Mr. Dave Bray.

TABLE OF CONTENTS

Page

AKNOWLEDGMENTS iii

LIST OF FIGURES vi

LIST OF TABLES x

ABSTRACT xii

CHAPTER

1 INTRODUCTION 1

2 LITERATURE REVIEW 4

- General Anatomy and Physiology of the Lower Limbs of Quadrupeds 4
- Biomechanics of the Bovine Foot 5
  - Loading of the Quick 6
  - Loading of the Claw 6
  - Mechanical Overloading due to Man-Made Conditions 7
  - Weight Distribution on Claws 8
  - Laminitis as an Aggravating Factor to Mechanical Overloading 12
- Large Animal Foot Kinetics 18
- Methods for Measuring Weight Bearing 24
- Ground Reaction Force (GRF) and Pressure Distribution Data Obtained With Thin Piezoelectric Crystals Film Technology 27
- Claw Trimming 31
- Functional Anatomy 33
- Enlarged Outer Hind Claw 34
- Mechanical Properties of the Claw Structures 35
- Fracture Mechanics 44
- Biomechanics of Anabolic Induced Musculoskeletal Overgrowth 49
- Influence of Incorrect Loading on Physiology of Bone Growth 50
- Pathogenesis of Joint Lesions and Joint Reaction Forces 51
- Joint Resultants 53
- Locomotion: Gait Analysis and Kinematics 60
  - Gait of Large Animals 65

3 MATERIAL AND METHODS 72

Preliminary Tests With the Sensor and Equipment Calibrations....72
Experimental Design....76
Statistical Analysis....86
Pressure....86
Gait....87

4 RESULTS AND DISCUSSION....89

Midstance Phase....89
Loading Response Phase....100
Push-off Phase....107
Linear and Angular Kinematics....117

5 SUMMARY AND CONCLUSIONS....123

REFERENCES....133

BIBLIOGRAPHICAL SKETCH....136

LIST OF FIGURES

Figure Page

2-1 Influence of load bearing on the quick 5

2-2 Quick and digital cushion 6

2-3 Overgrowth claw and weight shift schematic 8

2-4 Balance of weight on the claws of the hear quarter 9

2-5 Weigh shifting on legs due to sideways movements 10

2-6 Weight shifting on the claws due to sideways movements....11

2-7 Attachment of the suspensory ligament 14

2-8 Compression of the corium by the sinkage of distal phalanx 15

2-9 Top view of the actual sensor 27

2-10 Map of the sensor model 3120 used in this project 28

2-11 MID samples loaded at 3 cm/min speed 39

2-12 MID samples loaded at 1.5 cm/min speed 40

2-13 MID samples loaded at 0.3 cm/min speed 40

2-14 TOE samples loaded at 3 cm/min speed 41

2-15 TOE samples loaded at 1.5 cm/min speed 41

2-16 TOE samples loaded at 0.3 cm/min speed 42

2-17 SOLE samples loaded at 3 cm/min speed 42

2-18 SOLE samples loaded at 1.5 cm/min speed 43

2-19 TOE samples loaded at 0.3 cm/min speed 43

2-20 Mode I type of crack 46

2-21 FBD of the lower extremity of an equine front limb 58

2-22 Gait cycle of a Holstein cow...68

3-1 Footprint of simulated hoof using wooden blocks..73

3-2 New design of the force plate with drilled space for bolts 75

3-3 Restraint chute force plate 76

3-4 Matscan sensor attached to the Force plate..77

3-5 Force-pressure system mounted on the wooden platform 78

3-6 Digital video camera setup mounted at a distance from platform 79

3-7 Video capture system and field of view diagram...80

3-8 Claw divisions used in excel coordinate grid 82

3-9 Coordinate transformation schematic 83

3-10 Claw footprint rotation and pressure analysis...85

4-1 Main effect region (R) (midstance original set)..90

4-2 Group*Claw (G*C) interaction (Midstance original set) 91

4-3 Claw*Region (G*R) interaction (Midstance original set) 91

4-4 Group*Leg*Claw (G*L*C) interaction (Midstance original set)..........................91

4-5 Group*Claw*Region (G*C*R) (Midstance original set) 93

4-6 Main effect region (R) (midstance normalized set) 95

4-7 Group*Region (G*R) (Midstance normalized set)...95

4-8 Claw*Region (G*R) (Midstance normalized set)...96

4-9 Group*Leg*Region (G*L*R) (G1) (Midstance normalized set)...........................96

4-10 Group*Leg*Region (G*L*R) (G2) (Midstance normalized set)...........................96

4-11 Front left leg G*L*C*R interaction (G1) normalized set LSMeans (midstance)....97

4-12 Front left leg G*L*C*R interaction (G2) normalized set LSMeans (midstance)....97

4-13 Front right leg G*L*C*R interaction (G1) normalized set LSMeans (midstance)....98

4-14 Front right leg G*L*C*R interaction (G2) normalized set LSMeans (midstance)....98

4-15 Rear left leg G*L*C*R interaction (G1) normalized set LSMeans (midstance)....98

4-16 Rear left leg G*L*C*R interaction (G2) normalized set LSMeans (midstance)....99

4-17 Rear right leg G*L*C*R interaction (G1) normalized set LSMeans (midstance)....99

4-18 Rear right leg G*L*C*R interaction (G2) normalized set LSMeans (midstance)....99

4-19 Main effect region (R) (loading response original set)....102

4-20 Group*Claw (G*C) (loading response original set)....102

4-21 Group*Region (G*R) (loading response original set)....103

4-22 Claw*Region (C*R) (loading response original set)....104

4-23 Group*Leg*Region (G*L*R) (G1) (loading response original set)....105

4-24 Group*Leg*Region (G*L*R) (G2) (loading response original set)....105

4-25 Group*Leg*Region (G*L*R) (G2) (loading response normalized set)....107

4-26 Group*Leg*Region (G*L*R) (G1) (loading response normalized set)....107

4-27 Main effect region (R) (push-off original set)....109

4-28 Group*Claw (G*C) (push-off original set)....109

4-29 Group*Region (G*R) (push-off original set)....109

4-30 Group*Leg*Region (G*L*R) (G1) (push-off original set) 110

4-31 Group*Leg*Region (G*L*R) (G2) (push-off original set) 111

4-32 Main effect region (R) (push-off normalized set)....112

4-33 Group*Region (G*R) (push-off normalized set)....113

4-34 Group*Leg*Region (G*L*R) (G1) (push-off normalized set)....114

4-35 Group*Leg*Region (G*L*R) (G2) (push-off normalized set)....114

4-36 Front left leg G*L*C*R interaction (G1) normalized set LSMeans (push-off) 114

4-37 Front left leg G*L*C*R interaction (G2) normalized set LSMeans (push-off) 115

4-38 Front right leg G*L*C*R interaction (G1) normalized set LSMeans (push-off) 115

4-39 Front right leg G*L*C*R interaction (G2) normalized set LSMeans (push-off) 115

4-40 Rear left leg G*L*C*R interaction (G1) normalized set LSMeans (push-off) 116

4-41 Rear left leg G*L*C*R interaction (G2) normalized set LSMeans (push-off) 116

4-42 Rear right leg G*L*C*R interaction (G1) normalized set LSMeans (push-off) 116

4-43 Rear left leg G*L*C*R interaction (G2) normalized set LSMeans (push-off) 117

4-44 Stride time LSMeans for groups 118

4-45 Calculated velocity data set for the two groups 120

4-46 Video digitizing and lower limb digitized model 121

4-47 Group range of motion (ROM) during stance phase 122

4-48 Fetlock relative extension angle changes....122

LIST OF TABLES

Tables page

2-1 Housing influences on lameness disorders 12

2-2 Typical mechanical properties of Bovine cortical bone 37

2-3 Elastic Modulus for hoof keratin specimens at 3 cm/min....44

2-4 Experimental values of k_{ic} for bone 47

4-1 ANOVA table for midstance (original set) 89

4-2 Type III SS for midstance (original set) 90

4-3 Original set orthogonal contrasts for region (R) main effect and 2-way interactions (G*C) and (C*R) (midstance) 92

4-4 ANOVA table for midstance (normalized set) 94

4-5 Type III SS for midstance (normalized set) 94

4-6 Normalized set orthogonal contrasts for region (R) main effect (midstance) 95

4-7 ANOVA table for loading response (original set) 101

4-8 Type III SS for loading response (original set) 101

4-9 Original set orthogonal contrasts for region (R) and leg (L) main effects and 2-way interactions (G*C) and (C*R) (loading response) 103

4-10 ANOVA table for loading response (normalized set) 106

4-11 Type III SS for loading response (normalized set) 106

4-12 Normalized set orthogonal contrasts for region (R) main effect (loading response) 106

4-13 ANOVA table for push-off (original set) 108

4-14 Type III SS for push-off (original set) 108

4-15 Original set orthogonal contrasts for region (R) main effects (push-off) 110

4-16 ANOVA table for push-off (normalized set) 111

4-17 Type III SS for push-off (normalized set) 112

4-18 Normalized set orthogonal contrasts for region (R) main effect (push-off) 113

4-19 Stride time range values (sec.) for the two groups 118

4-20 Stride time orthogonal contrasts for leg (L) main effects 119

4-21 Stride length range values (m) for the two groups 119

4-22 Stride velocity range values (m/s) for the two groups 119

Abstract of Dissertation Presented to the Graduate School
of the University of Florida in Partial Fulfillment of the
Requirements for the Degree of Doctor of Philosophy

EFFECTS OF TRIMMING ON DAIRY-COW HOOF-PRESSURE DISTRIBUTIONS AND WEIGHT-BEARING DYNAMICS DURING STANCE PHASE

By

Victor Ricardo Ciaco de Carvalho

May 2004

Chair: Ray Allen Bucklin
Major Department: Agricultural and Biological Engineering

Accumulated economic losses resulting from treatment of claw diseases induced by lameness are among the major economic damages ($627.0 USD/cow) in dairy operations. Claw lameness can be associated with biomechanical factors caused by imbalances of pressure distribution under the hooves, when cows are confined in modern dairy operations with hard concrete flooring.

In the past, methods of measuring these imbalances relied on force plate experiments that were unable to measure how these forces were distributed on the contact surfaces under the claw. Trimming claws is the only known treatment to correct these imbalances but its efficacy is yet to be quantitatively determined.

Using a system that is based on thin pressure measurement film (Matscan®, Tekscan Inc. Boston- MA) developed for human-foot pressure-distribution analysis, the pressures under the hooves of 32 cows (divided into trimmed and untrimmed groups) were tested under dynamic conditions and compared, to evaluate the effects of trimming in repairing imbalances on claws.

Results indicated that pressure distribution under the hooves of trimmed cows was slightly different and had closer peak pressures values between regions as compared to un-trimmed (midstance phase G*L*R interaction, $p < 0.0043$). However, these differences were not tested by orthogonal contrasts and are based on least square means. Video kinematics of the cows' strides were also analyzed; results indicated that trimmed cows have a shorter overall stride time (1.29sec vs. 1.45sec; $p < 0.085$, for trimmed vs. un-trimmed, respectively). Angular kinematics of fetlock-joint was statistically significant at midstance phase ($p < 0.0045$). Trimmed cows presented more extension (162°) compared to un-trimmed (157°). It was concluded that trimming provides a slightly different pressure distribution under the hooves and may affect gait. Changes in weight-bearing indicated shifting of a small percentage of the pressures from heel and weight bearing border to the medial sole towards the fragile region (vulnerable spot). In this case, rather than benefit cows, it may be possible that this region will be even more stressed and prone to lameness. A more specific analysis, such as recalculation of this area (medial sole) with more subdivisions of this region is necessary to validate this assumption.

CHAPTER 1
INTRODUCTION

Lameness is among the most prevalent and costly of clinical disease conditions in dairy cattle. Causes include rations and/or feeding conditions that encourage rumen acidosis; confinement of cows to harder, wetter, more abrasive floors; or un-grooved floors that are smooth (and thus slippery, etc.). Flooring is of particular importance, because of pressure distribution and redistribution on claws. Uneven weight-bearing of hoof walls of cows managed on hard floors (i.e. concrete) lead to pressure redistribution on claws and thus causes greater pressure concentration and stress on claws.

Specific information concerning the incidence of foot diseases in cattle in the United States is limited. However, it is believed to be similar to that reported in the United Kingdom. Surveys involving 1821 herds reported that the average incidence of lameness requiring treatment by a veterinarian was 5.8% of cows. Of these, 88% involved the foot. Most of foot lesions involved the rear feet, with 85% of lesions occurring in the outer claw. Studies at University of Florida Dairy Research Herd in 1995 reported 178 clinical lameness events of 346 (51 cases/100 cows) affecting 120 (35%) cows; 27/120 had more than one clinical event (Shearer and van Amstel 2000). The economic loss incurred as a result of disease (i.e., sole ulcers) arises primarily from the consequences of the disease and not the cost of treatment. Walking impairment imposed by hoof lesions causes decreases in feed and water intake, resulting in marked losses in body weight and milk production; and also poor reproductive performance (Shearer

2003, Large Animal Clinical Sciences. Veterinary Medicine School. University of Florida. Gainesville. FL, personal communication). British researchers estimated the cost of lesions such as sole ulcers, white line disease and digital dermatitis to be $627/case, $257/case and $128/case, respectively (values converted to US dollars assuming the British pound to be at 1.6 to 1 US dollar). Lower milk yields, reduced reproductive performance, higher involuntary culling rates, discarded milk, among others, accounted for the majority of economic loss. Data from University of Florida (Gainesville, FL), with a herd of 346 cows computed losses of $58,266.00 due to clinical lameness during one-year study using the same figures (Shearer and van Amstel 2000).

Using platform-type scales, Raven (1989) was able to show that weight-bearing in cattle has a characteristic pattern whereby the extremes in weight distribution are borne primarily by the lateral claws of rear feet and the medial claws of front feet. However, what these studies were not able to measure was the amount of load concentrated on different regions of the claw. With improved technology measurements of load bearing are now possible. Tekscan Inc. (Boston, MA) developed a pressure mat that can measure the precise location and movement of loads on the human foot. These load-bearing measurements are displayed using a wide scale of colors in the shape of a footprint, which permits visual evaluation of weight-bearing forces on the foot. This device has been developed and tested to work with load-bearing forces within the human weight range. Adaptation of this technology to work with cattle permitted the pressure distribution analysis of stance phase of a cow stride. The software calculates the pressure in a given region at a given time.

Our first objective was to evaluate weight-bearing dynamics and pressure distributions under the hooves of dairy cattle for two groups of cows: Untrimmed (unbalanced) and trimmed (balanced). Second objective was to assess gait linear and angular kinematics changes (spatial and temporal gait characteristics, velocities, and joint range of motion) for each group and associate these changes in pressure distribution and gait kinematics, if any, to the lameness etiologies of biomechanical origin.

CHAPTER 2
LITERATURE REVIEW

General Anatomy and Physiology of the Lower Limbs of Quadrupeds

The most marked difference in locomotion of ruminants in contrast to humans is the lower limb configuration for load bearing. Ruminants bear weight on two digits in each foot; and humans bear weight on the sole of the foot. The bones that form the human foot from the calcaneus to the toes (tarsal bones) and the phalanxes; and are present in quadrupeds as well. In quadrupeds, some of these bones are fused and elongated (such as 3rd and 4th metatarsal bones); and become an extension of the tibia in the hind limbs and radius-ulna in the front limbs. The distal phalanx (P3), which is similar to any of the human toe bones, is the ultimate load-bearing structure of the leg of quadrupeds. The loads derived from the animal's weight while standing or during locomotion are transferred throughout the lower limbs to the distal phalanx in the claw and to the ground.

Below the distal phalanx and above the sole that contacts the ground, are structures that form a type of cushion to the pedal bone. In the heel (absent at the toe), this is a very important feature and directly affects the loading-bearing of the claw.

This cushion layer is formed primarily by fat and also by soft connective tissue, blood vessels, and nerves; and it is also called the quick. The quick functions as a supporting apparatus below the pedal bone and also for load bearing. The epidermis contain the germinative layer that forms the sole and the wall of the claw (horny shoe). The soft nature of the structures that comprise the quick makes it a vulnerable structure that is prone to damage if incorrectly loaded (Raven 1989).

Next section discusses weight-bearing and mechanics of loading of the bovine claw.

Biomechanics of the bovine foot

Figure 2-1 shows the influence of body weight on the quick in the claw. The main forces are indicated by arrows.

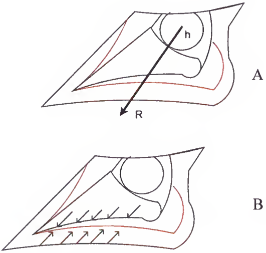

Figure 2-1. Influence of load bearing on the quick. A) Ground action. Forces B) Ground reaction forces. (Adapted from Raven T. E. 1989. Cattle foot care and claw trimming. Farming press. Ipswich.UK. Page 21.

Weight is transferred to distal phalanx via the short pastern bone (middle phalanx). The force (R) moves in the direction of the longitudinal axis of the short pastern bone and is applied at the center of rotation (h) of the distal interfalangeal joint. In the P3, it is resolved into a number of smaller forces, which sum to (R). This is the load P3 applies to the quick. This load only exists when the horny shoe, in contact with the ground, applies an equal force to the quick but in the opposite direction.

The distribution of the loads in the foot of a typical 460 kg cow is approximately 260 kg resting on the fore legs and the remaining 200 kg on the hind legs. This load must, to a large extent, be carried by a few centimeters of quick under the posterior margin of

P3. Therefore, the quick is under pressure between P3 and the horny sole of the weight-bearing claw. This scenario is the main cause of claw lameness of mechanical origin in cattle.

Loading of the Quick

The transition of corium into epidermis (horny shoe), in the lower half of the horny wall, is composed of laminae (folds). It is mainly abaxially and in the tip, and also in the anterior and axial area that the corium is firmly attached to P3. In this region, P3 is tightly and immovably fixed in the horny shoe (Figure 2-2).

The solear part of the tip also lacks digital cushion between corium and P3. This fixing of P3 enables a firm and steady gait. The axial wall and heel are loosely suspended due the presence of the digital cushion. Thus, there is a shock-absorbing buffer under the posterior part of P3 (Figure 2-2).

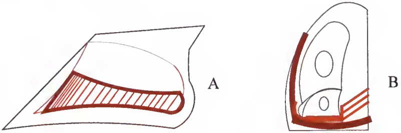

Figure 2-2 Quick and digital cushion. A) Lateral. B) Posterior. (Adapted from Raven T. E. 1989. Cattle foot care and claw trimming. Farming press. Ipswich. UK. Page 23.

Loading of the Claw

P3 rests on the corium of the sole and is suspended by the laminar corium in the horny wall. This suspension by the vertical wall is firmest on the outside front of the claw (abaxially in the anterior half); becomes less firm abaxially backwards; and is still present to a certain extent axially in the toe, but is absent axially in the heel. With this configuration, as a result of the normal loading caused by the body weight, the pedal bone tends to rotate axially and backwards. Thus, pressure on the corium of the sole is mainly applied by the posterior part of the P3.

Furthermore, there is a prominence on the axial side in the posterior margin of the P3. This is known as the flexotuberosity, which is the site of attachment of the deep flexor tendon. Under heavy loading, the quick under that region may become compressed (especially on the axial side). In normal weight-bearing conditions, a healthy claw is able to cope with this. However, under prolonged overloading, this region is likely to become vulnerable to this loading (by fatigue stress). This region is called the vulnerable spot and is the main site of the development of sole ulcers. This concept of the loading of the quick is supported by results of microscopic research on the corium; and helps to explain the defects often found on the claw at this site. This defect is referred as typical sole lesion (Raven 1989).

Mechanical Overloading due to Man-Made Conditions

Under natural conditions, cows walk on surfaces that are not flat and that vary in composition: sometimes hard, often yielding. Normally with the animal in good health, with intact claw horn, the support is stable. On hard surfaces, the claws are worn off. On soft ground, the claws project into the ground. With this scenario, lameness is accidental.

However, under conditions of insufficient wear, a claw tends to become overgrown along the abaxial wall and in the toe. The hard wall develops, whereas the sole shows a tendency to wear off (sole growth rate is slower). A long wall, abaxially in the toe (and a heel, which is axially under-developed or poorly developed) results in an unstable claw, which tilts over axially and backwards (Figure 2-3).

This scenario causes the body weight to shift axially and backwards, overloading the vulnerable region of the sole at its axial portion. This vulnerable region, under a prolonged period of excessive loading develops hemorrhages that lead to the typical sole lesion; which in turn, evolves into sole ulcers.

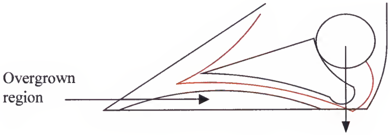

Figure 2-3. Overgrown claw and weight shift schematic. (Adapted from Raven T. E. 1989. Cattle foot care and claw trimming. Farming press. Ipswich. UK. Page 25.

Weight Distribution on Claws

Raven (1989), published work on weight-bearing mechanics in cattle, some of his findings are presented in the next section. He found that distribution of weight over the two claws of one foot depends mostly on whether the claw is situated on the outer or the inner side of the hoof.

Hind legs are connected with the pelvis by a ball-and-socket joints (Figure 2-4). In a squarely standing animal, the part of the body weight born by the hind legs (G) is evenly distributed over the two rear legs; and if the claws are equally high and stable over all four claws, the weight is evenly distributed over them. In other words, the 200 kg weight example mentioned earlier would be distributed equally (50 kg per claw) on the four claws of the hind legs (Figure 2-4).

In the ever-present small movements sideways (sideways deviations from the squared position mentioned), the following situation could change as shown in

Equations 2-1 and 2-2; and Figure 2-5.

$$\text{Weight left} = G * b / (a + b) = 200 * 10 / 25 = 80 \text{ kg} \tag{2-1}$$
$$\text{Weight right} = G * a / (a + b) = 200 * 15 / 25 = 120 \text{ kg} \tag{2-2}$$

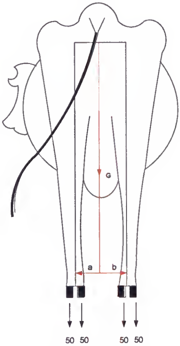

Figure 2-4. Balance of weight on the claws of the rear quarter. (Adapted from Raven T. E. 1989. Cattle foot care and claw trimming. Farming press. Ipswich. UK. Page 27.

If the two claws were attached to the leg in a perfectly elastic way, the weight, thus distributed over the two legs would be evenly sub-divided over the claws of each foot.

Outer left	inner left	outer right	inner right
40 kg	40 kg	60 kg	60kg

If the connection between the two claws and the leg were quite inflexible, the new weight would rest fully on the claws on the side to which the animal leans, resulting in:

Outer left	Inner left	Outer right	Inner right
0 kg	80 kg	0 kg	120kg

In reality what happens is somewhere in between these scenarios. The claws are connected with the leg in a stiffly elastic way, hence the distribution of the new weight over the two claws of the foot would be somewhere between 50%/50% and 0%/100%, for example, 40%/ 60%. This means that 3/5 of the new weight is born by the claw that the cow tilts onto; and 2/5 by the other claw (Figure 2-6)

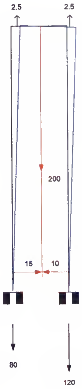

Figure 2-5. Weight shifting on legs due to sideways movements. (Adapted from Raven T. E. 1989. Cattle foot care and claw trimming. Farming press. Ipswich. UK. Page 27.

Outer left	inner left	outer right	inner right
2/5 * 80kg	3/5 * 80kg	2/5 * 120kg	3/5 *120kg
= 32kg	= 48kg	= 48kg	=72kg

In other words, the weight-bearing by the outer hind claws varies widely with the successive movements of the body. The load on the inner claws is far more even. According to Raven, the outer claws constantly correct the ever-shifting distribution of the weight over the two hind limbs. Hard surfaces, such as concrete encountered in modern housing, enhance this effect.

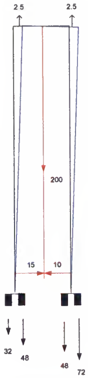

Figure 2-6. Weight shifting on the claws due to movements sideways .(Adapted from Raven T.E. 1989. Cattle foot care and claw trimming. Farming press. Ipswich. UK. Page 28

The front legs are not subjected to the same biomechanics. Instead they are inflexibly connected with the body by a rigid ball-and-socket joint: Their connection is cushioned by the tendons and ligaments of the shoulder blades.

Peterse (1986) subdivided lameness into two classifications: infectious and metabolic. He said that whether lameness is infectious or metabolic, housing plays an important role (Figure 2-1).

The claw disorder of metabolic origin is called pododermatitis aseptica diffusa (laminitis). Symptoms vary from sole ulcers, to white line ulcers and underrun soles. The trigger mechanism is thought to be in the digestive tract (discussed in detail later). Resorption of toxic fermentation products into the circulation causes the burden of the pododerm tissue. Burden of this tissue manifests itself in latter stages in the claw sole.

Table 2-1. Housing influences on lameness disorders. (Adapted from Peterse D. J. 1986. Aetiology of claw disorders in Dairy cattle. Cattle housing systems, lameness and behavior. Martnus Nijhoff Publishers. Netherlands. Page 4.

Origin	Pathway	Housing component
Infectious	Infection pressure	Group size and contact, density, indoor climate, disinfection possibilities
	Susceptibility	Stall floor conditions
Metabolic	Burdening	Movement, roughness, softness of surface
	Quality and quantity nutrition	Layout and feeding management
	Stress	Ranking, group formation and transport

The type of floor of the housing system may have influence on the burden of the pododerm under symptoms of laminitis: For instance, observations make clear that cows walk differently on slatted floors compared to concrete floors. The consequence of this is a different-shaped claw that is steeper and shorter.

Lameness of infectious origin is not the scope of this work. However, it is important to emphasize that claw disorders due to weight bearing dynamics (whether associated with laminitis or not) opens a portal for infections and therefore aggravating further the process.

Laminitis as an Aggravating Factor to the Mechanical Overloading

Metabolic laminitis is a vascular disease caused by rumen acidosis. Rumen acidosis can be caused by either nutritional factors or by heat stress. Consumption of large amounts of starches (such as corn) in the ration will acidify the rumen compartment and thus overload the lactolytic bacterial flora (bacteria that neutralize the pH (neutral =

7.0), acidic < 7.0). The pH of the rumen is thus lowered by the action of lactogenic bacteria (produces lactic acid) acidifying the environment inside the rumen. This scenario results in the death of some of the lactolytic bacteria with consequent release of endotoxins and histamines. At a microcirculatory level, claw connective tissue, endotoxins cause an inflammatory cascade process that results in the P3 to sink within the claw capsule. Lischer and Ossent (2002), suggested a theory for the pathway of the laminitis process that acts as an aggravating factor to the mechanical aspect of loading bearing leading to claw lameness and sole lesions. They divided into three phases. Phase one is initiated by an impairment of the blood supply to the corium due to the action of the vasoactive substances (histamines, endotoxins) in the bloodstream. Vessel wall paralysis and vasodilatation cause the blood to stagnate, depriving the corium tissue of blood. Hypoxia of the surrounding tissues occurs; blood-vessel in the walls start to leak (causing edema, hemorrhages, thrombi, and necrosis of the lamellar junction; and finally the claw's suspensory apparatus fails). The links begin to separate (Figure 2-7) and the whole foot sinks within its horn capsule to enter phase two.

Sinkage of the P3 compresses the corium in the sole and heel and further episodes of capillary damage, hemorrhage, and thrombosis leading to ischaemic necrosis results. Chronic edema combined with compression of the corium from the weight of the animal result in actual sinkage (Figure 2-8). The lesions result in a serious threat to the animal's life, for they may induce extensive damage, with severe pain and lameness.

Lesions at this stage are still confined to the inner surface of the horn capsule and are not visible to the clinician yet. Phase three occurs at about eight weeks after the onset of the process, where the lesions become apparent in the horn capsule. Accumulation of exudates between lamellae or lamellar hyperplasia or a separation of the epidermal-dermal junction causes the white line to disrupt and become wider; and leads to the appearance of friable layers at the bearing edges that provide a portal to environmental debris and infection. (white line disease).

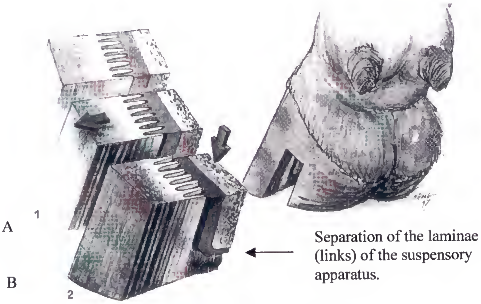

Separation of the laminae (links) of the suspensory apparatus.

Figure 2-7. Attachment of the suspensory ligament. A) healthy. B) separation. (Adapted from Lischer and Ossent 2002. Pathogenesis of sole lesions attributed to lameness in cattle. Proceedings of the 12th International Symposium on Lameness in Ruminants. Orlando. FL. Page 84.

Necrotic tissue masses and accumulation of blood at the surfaces of the corium retard or hinder horn production. Once the growth continues, the detritus is incorporated into the new horn that gradually grows out to the surface and appear as red patches (or when hematomas are extensive, a double sole). An ulcer develops when production of horn is totally blocked. The weakest link of the attachment of the P3 to claw capsule (locus minoris resistentiae) has yet to be demonstrated.

Disturbances in the microcirculation by vasoactive agents and the insult of the lamellar region have not yet been demonstrated in cattle. It seems indisputable that inflammatory mechanisms are responsible for Phase one lesions. However, there are alternative pathways for Phase two. A mechanical separation of the suspensory apparatus through excessive load is highly unlikely, since the force required to rupture the connective tissue between the distal phalanx (P3) and the wall of the hoof is about 20 times greater than that exerted by normal loads.

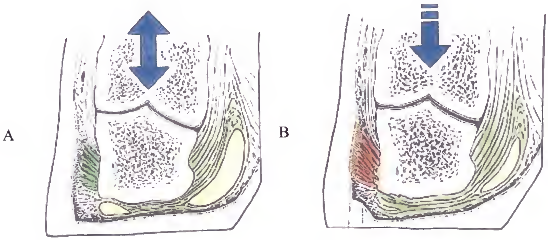

Figure 2-8. Compression of the corium by the sinkage of distal phalanx. A) healthy. B) compressed (Adapted from Lischer and Ossent 2002. Pathogenesis of sole lesions attributed to lameness in cattle. Proceedings of the 12th International Symposium on Lameness in Ruminants. Orlando. FL. Page 84.

A more likely explanation is softening and increases of elasticity of the collagen fibers of the suspensory ligament due to hormones of pregnancy at the perinatal period such as relaxin for instance. Relaxin has a broad spectrum of biological actions; one of such is the induction of collagen remodeling and consequent softening of tissues of the birth canal. Fibrous tissue in general may be affected and possibly the fibers of the suspensory apparatus (Lischer and Ossent 2002).

Christmann et al., 2002, conducted an experiment to evaluate hemodynamics of microvasculature of normal and laminitic bovine digit that may reinforce the theory presented by Ossent et al (2002). Eleven steers were divided into control and grain overloaded animal groups. Control group were administered only water during the experiment and grain overloaded group were administered a diet consisting of barley, wheat and oat at 3.5% of their body weight through a protocol that induced laminitis (not described by the author). The animals of the two groups were anesthetized either after drop of 50% of central venous pressure for the laminitic group (grain fed group) or after 6-8 hr after administration of water for the control group. Digital hemodynamics was evaluated through a digit extracorporeal pump-perfused and heparin (anticoagulant agent) administration intravenously before cannulating the vessels. Digital arterial and venous blood pressures were recorded by pressure transducers connected to a physiograph. Through his experiment, Christmann observed that capillary pressures and post-capillary resistance were significantly higher ($p < 0.05$) in the digital microvasculature in the grain-overloaded steers compared to control animals. The increase in capillary pressure and post-capillary resistance facilitates transvascular movement of fluid and increase in tissue pressure. Furthermore, digital venous constriction is thought to be the initiating step for these events (Christmann et al., 2002).

Another interesting experiment accounted for evaluating the deterioration of the basement membrane in ulcerated sites of the bovine hoof (keratin distribution in ulcerated and sound sole of the bovine claws) and was done by Hendry et al. 2002. He looked for histological confirmation of basement membrane deterioration in association with sole ulcers in vivo using samples of sole tissue obtained *post mortem* from dairy cows of various ages and culled for a variety or reasons and in vitro. In vitro study was undertaken to reproduce a loss of basement membrane signaling and investigate keratinization in sole tissue.

Histological examination of stained (acid-Schiff stained cryosections) ulcerated and non-ulcerated sole tissues revealed deterioration of the epidermal basement membrane of ulcer sites and immediately adjacent tissues. Basement membrane breakdown and remodeling are associated in many cases with activation of matrix metalloproteinases (MMps). In the bovine claws, the results showed increased activities of MMP-2 and MMP-9 at ulcer sites compared to that of healthy sole tissues from the same animals. In addition, a reduction in levels of Tissue Inhibitor of Metalloproteinases 2 (TIMP-2) at sole ulcer sites was accompanied. These reciprocal changes strongly suggest that proteolytic activity was increased at the sites of sole ulcer.

Changes in a cow's behavior and acid-base balance during heat stress predispose her to ruminal acidosis. Heat stress will cause alteration of this acid-base balance. In case of heat stress, as a cow pants and exhales carbon dioxide, the total amount of buffering capacity within her system is decreased (Hall 2002). Acid-base imbalance is caused by an excessive amount of saliva lost due to the increased respiration rate (panting) as a mechanism of heat stress relief (Shearer et al., 1999).

This imbalance causes a similar scenario of bacterial death and release of substances triggering the same cascade of events. In addition, changes in feeding behavior such as consuming fewer meals (slug feeding) and decreased rumination may lead to decreases in ruminal pH even in rations containing adequate fiber (Hall 2002).

In a study that tested the effect of ambient temperature in rumen environment (Misha et al., 1970 cited by Hall 2002), lactating Holstein cows were fed high roughage or high concentrate diets at ambient temperatures of 65° F (cool) and 85° F (hot) with relative humidities of 50% and 85% respectively. Ruminal pH was lower at the higher temperature and on the higher concentrate diet ($p < 0.01$). Interaction of diet with temperature was significant ($p < 0.01$). It was also noticed that ruminal ammonia and lactic acid concentrations were higher for the hot treatment ($p < 0.01$).

Large animal foot kinetics

The basis of large animal biomechanics used in this manuscript was obtained, mostly, through studies done in equines. The reason for that lies in the extensive amount of literature of equine biomechanics due to the frequent problems of foot and lower limb lameness of racehorses and the associated high value of these animals. Literature on biomechanics of dairy cattle, on the other hand, is very scarce. Nonetheless, muscular and skeletal anatomy between both horses and cattle are similar and so is their biomechanics.

Scott (1986), measured variation in pressure contact area and load distribution on hooves of six Friesian heifers. Force vs. time data were obtained using a pedobaroscope system (technology is discussed in further sections). The areas of the different pressure zones were evaluated and recorded. Analysis indicated that for the most part of the vertical force – time curves for the front feet were similar for the left and the right feet with a single peak whereas those for the rear feet exhibited two separate peaks as occur with human stride. The magnitudes of the two peaks were similar.

There were no differences between the vertical force time curves for left and right feet. There was a short initial peak corresponding to the percussive heel strike on the ground. In normal walking it was observed that the heel contacted the ground initially, though the contact region moved forward to the toe region as the cadence (rate of foot steps) increased.

The (Fx) force time curve represents the forces in the fore and aft directions. The forces in the aft and fore directions (Fx) presented an initial deceleration followed by acceleration as the foot contacted the ground and then pushed off. A greater push off peak value (Fx) force was shown for rear feet as compared to the front feet.

The positive peak that characterizes push off impulse, which was greater for the rear feet as compared to front feet suggests a greater thrust from the hind feet. The deceleration (negative peak) phase had similar values (Fx) for front and back feet.
For the Fy curves, perpendicular to the direction of walking, the curves suggested that after ground contact the calf swayed over the leg being loaded. Front and back feet force vs. time curves were significant different ($p < 0.01$). This was reflected in the peak vertical forces applied to front and back feet. According to data, hind feet carried 51% of body weight and front feet carried loads from 60% to 61% of body weight.

There was no significant increase in step duration of the calves as they aged (over time) nor on step time from the front and rear, left or right during the period. However, step duration was significant among calves for data taken on the first month alone.

Hoof-ground contact areas between front and back feet were not significant. However, the outer digits had significantly ($p < 0.01$) larger contact areas (319 mm^2) as compared to inner digits (285 mm^2). Preliminary analysis also suggested that the peak vertical load increased significantly ($p < 0.01$) over the six-month period as body mass increased.

Peterse 1986, has measured the weight distribution between inner and outer claw of hind legs in first calf heifers using double-scale that allows simultaneous weight bearing recordings from the inner and outer claws. Twenty-four Dutch Friesian heifers were evaluated before and after calving. During the trial these calves were housed in free stalls with concrete alleys. Measurements in the group of pregnant heifers showed an under-burdening of the lateral claw or an equal distribution between both claws. However, after calving the situation has completely changed to an adverse situation for the lateral claw.

Statistical evidence ($p< 0.05$) was assessed by groups of digits that were sound and digits with minor sole lesions. According to the author, these results suggest that digits with severe sole lesions were on average more loaded before calving. The loading of lateral hoof was expressed as a % of total weight (mean ± SD) of total load on the hind foot. A significant increase ($p< 0.05$) 42% ± 14 was observed before calving against 57% ± 13 after calving for minor or absent lesions. Moderate lesions after calving showed a difference of 43% ± 15 against 47% ± 14 before calving (not significant) and severe lesions were 49% ± 11 against 53% ± 13 (also not significant).

Raven 1973 (cited by Peterse 1986), based on his experience with the load distribution in hind claws, suggested trimming the claws in such a way that overloading of the affected outer claws can be limited. The effect of preventive trimming was also tested for these groups of heifers according to Raven's method on their first and second lactation. It follows that on the first lactation, this beneficial effect was not demonstrated, but during the second lactation less sole lesions were registered in the trimmed animals.

Several investigators have suggested that stationary fore legs of fully-grown cows carry about 60% of the body weight and the hind legs carry about 45 to 50%. It is also suggested that the loads applied on the fore legs exceed that of the hind legs because of the center of mass of the body is displaced forward by the mass of head and neck. It is expected that these loads would increase about 20% during slow walking (Irps, 1982 cited by Scott 1988). Scott (1988), studied gait of Friesian heifers during gait over a period of six months with the same group of animals. Most of the data collected were ground reaction forces during stance phase of gait using a Kistler Multicomponent force platform coupled with a pedobaroscope system. The pedobaroscope system will be discussed further in the methods for weight bearing measurements section.

Animals were allowed to pass freely over the platform without interference. Data could only be obtained from one foot in contact with the ground at any time. Hence, it was assumed that the force and pressure data were the same for individual feet both on and off the pressure platform. The greater pressures were mainly applied to the lateral digits, but that was not the case for every single step. Commonly the outer edges and heel of the digits were mainly involved in support. The hoof horn of the sole was generally not load-bearing on hard surfaces.

The peak vertical ground reaction force for the front legs occurred about half way through the step, while in hind feet it occurred in the first quarter to a third of the step. Apart from the data of the fourth month, there was no significance that the contact pressures were different for lateral or medial digits of the front feet or rear feet. In the forth month however, the contact pressures of the fore medial digit was significantly higher that of the hind medial digit.

In general, the contact areas of the lateral digits were greater than of the medial digits for the same hoof but only for the third and fourth months. The contact areas for the fore digits were generally the same whereas the contact area for lateral digit of the hind feet was greater than the medial digit by 25 to 50%. The total contact area of the fore feet was usually greater than the hind feet.

The relationship between the contact area and live weight was established through a log-log regression analysis. There was a highly significant relationship between contact area and live weight ($p < 0.001$, $R^2 = .67$). The relationship obtained by a similar regression analysis for pressure and body weight accounted for only 6% of the variance and suggested that there is no significant relationship between pressure and live weight. These relationships suggest that area of contact between hoof and the ground increase with live weight, whereas hoof pressure was almost independent of body weight.

The force time curves obtained in this experiment suggested that cattle hind feet have walking patterns similar to humans in that the legs remain straight through the support phase of the step. Also that the hind legs are more involved in propulsion whereas the front legs are more involved in steering and support of the body. Scott's data also suggest that cows have a plane of symmetry dorsoventrally since there were no significant differences in loads carried by contralateral legs. The heel area of cattle hoof consists of soft horn and may be able to compress under load to reduce the increase in applied pressure.

Some researchers (Feszl 1974 and Weaver 1979 both cited by Scott 1986) showed that the interdigital space increases during locomotion and Scott (1988) showed that the interdigital space increases with increasing load. The normal concave surface of the sole may then be increasingly in contact to the ground and reduce the increase in pressure.

Another important factor affecting weight distribution on claws may be attributed to velocity of walking during gait. Unfortunately, there is little data that account for speed of walking affecting ground reaction forces of cows. Most of studies involving ground reaction forces and kinematics variables were completed using horses. However, such data can be safely assumed to apply for cows as well, because they are governed by laws of physics that apply for any body in movement in this case.

Khumsap et al. (2001) studied the effect of subject velocity on ground reaction force in the hind limb of walking horses with the objective of developing a model for calculating the expected ground reaction force at any walking velocity. His hypothesis was that the subject velocities affect GRF in a predictable manner. Five clinically normal horses were used for the study. Force data was obtained using force platform and normalized to the body weight expressed as N/kg, and velocities were also normalized to height of the leg from hoof to shoulder (AVG 1.42m to 1.59m at the shoulder). Velocities were then expressed as VDU (dimensionless units). Impulse and stance time were also obtained through the video recordings and processing of kinematics data and calculated by methods of integration.

In Dutch warmblood horses walking at 1.44 m/s and 1.79 m/s the longitudinal impulses and forces had lower SD (standard deviation) than vertical force and impulse. The author believes that this could be interpreted as supporting his findings that velocity had more effect on the vertical force component than in the longitudinal component. The ground reaction forces distribution between the four limbs of walking horses is such that one limb provides braking forces while the other provides propulsive forces at any time. Therefore the longitudinal forces of different limbs act in opposition to each other and this is why changes in velocity do not depend on changes in longitudinal ground reaction forces (Merkins et al., 1988). This is confirmed by the fact that is his study, longitudinal ground reaction forces of the hind limbs did not change with velocity. Theoretically a prerequisite for maintaining a constant speed of progression is that the longitudinal breaking peak forces (L1) and the longitudinal propulsive peak force (L2) are equal, which were found to be true in the study (means L1 = 0.77N/kg vs. L2 = 0.69N/kg).

The first peak of vertical ground reaction forces (V1) was most apparent in the first half of the stance. V1 increased in a quadratic manner with VDU. This relationship has been observed in humans walking at different velocities (Thorstensson 1989 cited by Khumsap et al., 2001). The quadratic regression pattern of V1 mirrors the pattern of kinetic energy, which is proportional to velocity squared. Results of electromyography studies in the hind limbs of walking horses indicate that there is muscle activity in several muscles (gluteus medius, biceps femoris, gastrocnemius, etc.) during early stance with activity ceasing just before midstance. This quadratic pattern of V1 may reflect greater muscle activity together with increasing kinetic energy during early stance as velocity increases. During late stance, fewer muscles are active and V3 may reflect the release of the elastic energy stored during early stance by tendons. The vertical dip forces V2 correlated negatively with VDU and showed that the dip between the 2 peaks of the vertical force became more distinct as velocity increased.

In normal locomotion, the equine limb functions like a mass-spring mechanism during stance. At midstance the limb is unloaded (V2) caused partially by the rebound of the more heavily loaded limb spring combined to the contralateral hind limb midswing phase.

Methods for measuring weight bearing

Force measurement equipments usually consist of force plates or platform scales.

The general configuration of a force plate includes metal plates of known thickness that can withstand the amount of weight to be measured without deflecting, measuring units consisting of strain gauges or force transducers placed on a certain design that allows capture of one, two or all three components (Fz-vertical, Fx-medio-lateral, and Fy-anteroposterior) of the force and moments in the three-dimensional plane as well.

Peterse (1986) used the method of two platform scales for measuring pressure distribution. Two platforms taking up to 120 kg maximum each and placed next to each other. The unit is assembled behind the floor of a chute in a movable way so it can be adjusted to the stance of the animal. The inner and outer claw of one leg each has to rest on the scale indicating the weight distribution between the two claws and fluctuations of weight on each claw caused by slight movements of the animal.

The two parallel-platform scale system was also used by Rajkondawar (2000) to assess lameness in cattle. A symmetry factor (SF) was calculated based on peak ground reaction force values obtained with the system and lameness was associated to it.
The system was used with 3 lame and 3 sound dairy cows. A zero SF value corresponded to symmetry, whereas negative or positive values indicated dominance of one limb. Lame cows presented negative SF values and sound cows presented near zero values.
According to the author, the magnitude of the SF values was indicative of the degree of lameness.

Scott (1986) used a force plate with a pedobaroscope. The force plate had a solid aluminum top plate with a hole in the center for a pedobaroscope platform. The basic assumption of a pedobaroscope is that the intensity of scattered light is directly related to applied pressure. The apparatus depends upon the optical properties of glass. Light is totally internally reflected within polished sheet of cabin-glass because its refractive index is very different from that of the air at the boundary. When white membrane is pressed onto the glass surface, light escapes and is picked by a video camera. Extraneous light is eliminated by the two membranes, one of black PVC and the other of silicon carbide paper, applied over the system. The light transmitted into the camera is then recorded in videotape and digitized later. The range of light intensities, and grayness values within a footprint is then arranged into a series of color bands each corresponding to a pressure band. The area of each band is then measured electronically.

A new and more accurate form of measurement has been developed recently by the Massachusetts Institute of Technology (MIT). It consists of ultra thin films containing several arrays of piezoelectric crystal sensors has been developed and used for human gait analysis (Figure 2-9). Matscan (Tekscan Inc.-Boston Ma) pressure assessment system is based on this technology. MatScan is comprised of both software and hardware components. The hardware component collects pressure data from a sensor and inputs it into the Matscan software. The software allows the collected pressure data to be viewed, record as a movie and to be analyzed as force and pressure. The sensor component (pressure mat) is made up of over 2,000 individual pressure-sensing locations (piezoelectric crystal sensing elements or sensels). These sensels are arranged as arrays of rows and columns on the sensor. The output of each sensel is divided into 256 increments and displayed as a value (raw sum) in the range of 0 to 255 by the software. The software uses a map (Figure 2-10) to convert the pressure detected by the hardware into pressure data displayed in a real time window.

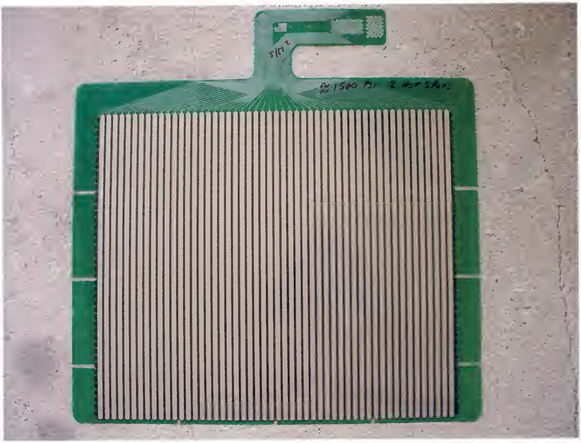

Figure 2-9. Top view of the sensor.

Ground Reaction Force (GRF) and Pressure Distribution Data Obtained with thin Piezoelectric Crystals Film Technology.

Instrumented shoes (in-shoes) have been used to quantify GRF in horses. These shoes have been limited in their use by their complexity and their weight. However, they have the advantage of providing vertical GRF and temporal analysis of hoof strike over successive strides. The most current instrumented in-shoe was constructed using three transducers embedded in the shoe. With the development of more sophisticated ultra thin films, these shoes became lighter and more accurate providing more reliable measurements.

Carter et al. (1999) tested the first in-shoe constructed using the ultra thin film technology (Tekscan Inc.- Boston, MA) with six horses walking on treadmills in a repeated measures experiment with the horses unshod vs. shod. Maximum GRF (kg), peak area (cm^2) of sole in contact with the sensor and stride time (s) were examined for each forelimb for ten successive hoof strikes. Horses did not object to the equipment and trotted as they did previously without the in shoe equipment.

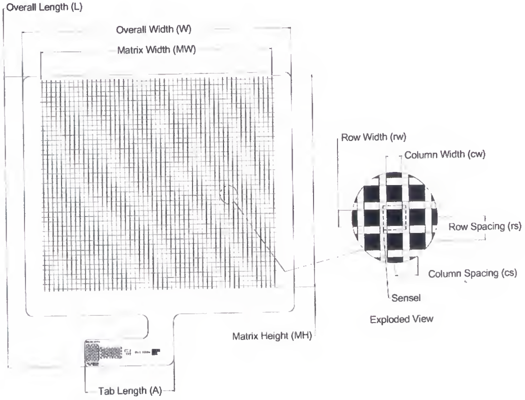

Figure 2-10. Map of the sensor model 3120 used in this project.

There were no significant differences for the maximum force or stance times in shod and unshod horses using independent data for each forelimb. However, the peak contact area decreased significantly for each successive trial for shod ($p < 0.006$) and ($p < 0.012$) for unshod horses. When the limbs were evaluated simultaneously, there were significant differences ($p < 0.001$) for the two treatments between right and left forelimbs for maximum forces (627.5 ± 118.3 kg vs. 594 ± 93 kg respectively) for the shod treatment and (590.6 ± 73 kg vs. 630 ± 104.4 kg respectively) for unshod horses. Stance time ($p < 0.011$) and peak contact area ($p < 0.001$) were also significant. Peak contact areas ranged from 53.6 ± 10.2 cm^2 to 59.1 ± 8.8 cm^2. According to Carter et al. (1999), when evaluating peak contact area data, it is recommended that each sensor to be used for a maximum of three trials prior to recalibration due to fatigue of the sensel elements. Results indicated that the system is viable and useful for evaluating vertical GRF in horses. Values for maximum force seemed to supply the most accurate correlation between observed clinical lameness and measured lameness (by differences in symmetry between left and right side).

Van der Tol et al., (2001) measured the pressure distribution on claws of 8 dairy Holstein cows during square standing on a flat substrate using a similar system (RsScan International, Olen, Belgium – Footscan Clinical Version®). Data was collected with the cows being positioned on the plate with one foot until stability was acquired and the measurement recorded. Five successful similar measurements for each limb were measured. Van der Tol et al., (2001) classified the location of the maximum pressure in each sole according to the diagram of claw region division proposed in the 6th International symposium on the Disease of the Ruminant Digit (Liverpool, UK, 1990). With the aid of an overlay of the diagram the location of the maximum pressures on the lateral and medial claws was accessed. Hind limbs maximum pressures occurred on the sole at region 3 (towards the heel on the lateral wall) of the lateral claw rather than at the wall (weight bearing border) and region 5 (sole portion towards the toe) of the medial claw.

On the front limbs, the maximum pressures occurred on the medial claw. Lateral claws for all limbs presented a higher incidence of maximum pressure concentrations on region 5 and 6 (front sole near to the toe and heel) except for right hind limb, which had higher incidence on region 3 (towards the heel on the lateral wall). Medial claws presented almost the same with highest incidences of maximum pressures at regions 5 and 6 and to a lesser degree in region 3. He showed that, regardless of outer or inner claw, front limbs were loaded maximally in region 6 (heel) and hind limbs on region 5 (front sole near to the toe).

A year later, Van der Tol et al., (2002) (Pathobiology Department. Veterinary Medicine School. University of Utrecht. Utrecht, personal communication) repeated its initial experiment using a combined Kistler force platform mounted underneath a Footscan Pressure Assessment System, to evaluate the pressure distribution of dairy Holsteins during walking on a flat substrate. A total of 9 cows were lead by a handler through the path hitting the foot on the force platform pressure measurement system recording the force-pressure data from the step. The passage was repeated 8 times for each foot. Erroneous measurements, such as both feet on the force plate while only one on the pressure film area, were discarded. Five moments of stance (step) were selected for analysis: heel strike, maximum deceleration phase, midstance, maximum propulsion and push off. According to his results, front and hind limbs behave differently throughout the stance phase. In the fore limbs, cows landed and strike the floor with the bulb of the lateral claw and to a lesser extend the bulb area of the medial claw, as stride progresses they both lateral and medial claw achieve a similar force magnitude at the bulb area and at the walls. From midstance to maximum propulsion, the loads shift somewhat towards the medial claw. At push off, the forces became equally distributed on the anterior wall and sole. On the hind limbs however, the maximum loads at heel strike are 95% on the lateral claw on the outer side (weight bearing border and lateral sole). From maximum deceleration to maximum propulsion the loads shift to the medial claw but the greatest part of the force remains on the lateral claw (sole and bulb). At push off, the forces equalize on the anterior wall and sole of both caws.

The distribution of total forces observed in this study agrees with literature in that front limbs carries most of the weight with 61% and rear limbs with 39% (Peterse 1986 and Scott 1988). These total forces are more evenly distributed over the two claws (lateral and medial) for the front limb but completely over the lateral claw during the first part of the stride moving to the medial claw and balancing between the two claws at push off. Fore limbs carried the greatest contact areas at heel strike and midstance but presented no differences at the other phases of the stance. Average pressure did not change much throughout the first 4 moments (time steps) of the stance for fore limbs and rear limbs. The pressures were highest at the moments of maximum deceleration, midstance and maximum propulsion for the fore limbs. Maximum pressures were highest at the maximum deceleration, midstance and maximum propulsion for both front and hind limbs.

Claw Trimming

The principal objective of trimming the foot is to restore its balance and functionability altered by excessive horn formation. Hoof growth is relatively slow (5mm per month) and the shape of the hoof is a product of the rate of growth versus rate of wear. Overgrowth is manifested primarily at the toe with a faster growth rate as compared to the heel where the rate of growth is slower and the horn is softer. The softer horn at the heel region produces a faster rate of wear as well. The result is a lengthening and rising of the toe with a corresponding lowering of the heel. The angle of the front wall is altered from a normal 45° to 30° or less (Shearer et al., 2000). Shearer also recommends that the functional trimming of the claws to be performed twice a year. Trimming only at the dry off period can lead to lameness problems depending upon housing conditions and prevalence of laminitis.

Raven (1989) stated that the incorrect weight bearing caused by claw overgrowth can be corrected by trimming thus creating a better distribution of weight within and between claws, Functional trimming (chiropody) may also be described as reducing claws to their normal shape and proportions by shortening and leveling the claws.

A functional trimming procedure, which was presented by Raven in1989, is described in a more practical manner by Shearer et al. (2000) who subdivides functional claw trimming into four steps. The fourth step here is introduced by Van Amstel et al., 2002 as an adaptation of the Dutch trimming method proposed by Raven.

First: the length of the toe is the most important starting point. Since the inner hind claw represents the more normal claw, this claw is used as a parameter for the correction of the outer more abnormal claw. The front wall of the medial claw (from the skin horn junction to the tip of the toe) should be 7.5 cm long for an adult Friesian Holstein cow. Thickness of the sole should be at least 0.64 cm. sparing as much of the heel in the medial claw as possible. Sparing the heel horn will provide the outer claw with some resting surface by increasing weight bearing on the inner claw. Next, the bearing surface (sole and wall but not the heel) is stabilized (pared flat) to be at right angles to the long axis of the chin bone (fused metatarsal bone) in the standing position.

Second: using the medial claw as a guide, trim the outer claw of the rear foot to the same length. Next, pare the weight-bearing surface of the sole of the outer claw to the same level as the inner claw (both at the toe and at the heel). The bearing surface at this stage should be flat and balanced with the inner claw.

Third: shape and slope the sole so that the innermost back portion of the sole slopes towards the center of the claws. The sole and axial wall at the toe region should be preserved for weight-bearing purposes. Also on the sole, excessive sloping or cupping should be avoided not to remove weight bearing on the lateral walls.

Fourth: biomechanics of weight bearing usually in combination with claw disease, such as laminitis, results in heel horn overgrowth and was demonstrated by Mair (1988) cited by van Amstel et al. (2002) using a pressure measurement device to verify the pressure distribution on claws. The reestablishment of the heel balance between the claws became an important consideration in the application of claw trimming procedures. To achieve balance, trimming of the heel of the medial claw should be avoided in most cases unless overgrowth is observed. The heels of both claws should be balanced and perpendicular to the long axis of the leg. The final conformation of the weight-bearing surfaces of the feet should be flat at the toes, along the walls and across the heels.

Functional Anatomy

A rough surface on a bone indicates regular forces exerted on the bone by the attached tissue. Correspondingly this tissue will be constantly submitted to the same forces. These tissues consist not only of tendons and ligaments, but also of the quick where it is attached to the P3. The smoother the surface of the bone is, the smaller the forces; the rougher the surfaces, the greater the forces. This is the relationship between the bone structure and its function.

An examination of the pedal bones of hind claws shows that those of the outer claws are always rougher than the inner claws. In young animals, these differences are minimal, however they increase with age as the forces exert their influence over a longer period of time. The P3 of outer hind claws grow increasingly rough, indicating that the forces affecting the outer claws are greater than those affecting the inner.

These findings support the biomechanical observations suggesting that the outer claw is more heavily stressed than the inner. Such irregular load-bearing on P3 of the hind claw must be very "tiring" for the quick in this claw. The corium will easily become "over-exerted" and irritated. Such condition is often accompanied by an increased tissue activity. In the fore legs there is no such obvious systematic differences in roughness between P3 bones.

Enlarged Outer Hind Claw

Irritation of the corium may cause excessive growth (hypertrophy) of the corium layer, as well as increased cell division (hyperplasia) of the germinal layer resulting in an enlarged outer hind claw. This Process is commonly encountered in cattle under prevalent farm conditions. The resulting process shows a higher wall and the horn of the bulb and sole thicker. It turns out that the outer higher claw will start to bear a greater part of the body weight (particularly on hard surfaces) and after some time it will be, not only unfavorably loaded, but also greatly overloaded. This scenario will lead to more irritation accompanied by more hypertrophy and hyperplasia creating a vicious cycle that causes the outer claw to be under constant stress from overloading.

It seems reasonable to think that the extra height of the wall, produced by increased weight-bearing, would be counterbalanced by wear until the point at which height and weight are approximately equal. This however, is not the case. Actually, the higher claw remains higher and more heavily loaded. This process will make the vulnerable spot favorable for developing a typical sole-lesion due to the excessive weight bearing in that region over time.

It is important to consider as well that not only the claw itself is subjected to loading but also the joints that follow above it. Joint reaction forces and some consideration regarding upper limb lameness as a consequence of incorrect weight bearing mechanics will be discussed in further sections.

Mechanical Properties of the Claw Structures

The mechanical properties of a certain material explain how the material can withstand certain types of loading. Strength, toughness, hardness, elastic and shear moduli and so forth are fundamental properties of every material including biological materials. The claw structures, mostly the horn and bones, are subjected to cyclic compressive axial loading due to the weight of the body when the animal is standing and to cyclic bending and shear loading when the animal walks.

The understanding of the mechanical properties of biological tissues under cyclic loading is important in order to estimate the life span of this material under a given situation of stress. The material under cyclic loading has a certain fatigue life that can be greatly shortened under unusual type of loading. Typical mechanical properties of cortical bone are presented in Table 2-2.

Baggot et al. (1988) (cited by van der Tol et al. (2002)) determined the shore hardness (SD) of horn samples of the wall, central sole and bulb area of the hind claws for normal and lame cows. At all sample sites the lame cows had significantly softer horn. In normal cows the bulb area has the softest horn (SD = 31.0), followed by the sole area (SD = 43.7), and walls (SD = 65.5). Younger animals (2 years old) seem to have harder walls (SD = 70 to 75) according to (Russke 2001). The modulus of elasticity (E), a measure of stiffness, of horn samples taken at the dorsal wall, abaxial wall and sole of the claws of all limbs were significantly higher at the fore limbs. Horn at the sole of hind limbs had modulus of elasticity $E = 106.4\ N/mm^2$ whereas the same site at the fore limbs showed $E = 162.3\ N/mm^2$ (Zöscher 2000 cited by Van der Tol et al., 2002).

Hedges et al. (2002) tested the tensile strength of hoof keratin of the white line region of the hind feet of dairy cows supplemented with biotin. Biotin it is believed to increase strength of hoof and reduce white line disease in dairy herd. In his experiment, hoof samples where removed by claw trimming at 0, 53, 90, 117, 147 and 187 days after start supplementation with biotin. The specimens were kept in sterile water frozen at -20° C. The tensile strength was tested using a Davenport-Nene T10 Test Frame. The specimens were loaded in tension using tensile test grips with load of 260N until failure. According to their findings, the time of sampling after supplementation with biotin had a significant effect and the tensile strength was increased over the six months period on medial claws from 3.8MPa to 6.5MPa and lateral claws from 3.1MPa to 4.7MPa. Zone 2, which corresponds to the white line at the sole area, had an increase of 4.41MPa to 7.02MPa and zone 3, corresponds to sole, heel and wall junction, had an increase of 3.18MPa to 4.15MPa. However, there was a depletion of these values at day 53 and 147 for medial claws and at day 53 for lateral claws.

A significant difference was observed for lateral claws vs. medial claws in their study. Medial claws presented significantly higher tensile strength than the lateral claws (4.8MPa vs. 3.6MPa, $p < 0.01$). The left foot white line was also significantly stronger than the right foot (4.35MPa vs. 4.04MPa, $p < 0.02$); however, supplementation with biotin did not have a significant effect on tensile strength of hoof keratin samples of white line in their study.

Table 2-2. Typical mechanical properties of Bovine cortical bone.

Property	Bovine
Elastic modulus, GPa	
Longitudinal	20.4
Transverse	11.7
Bending	19.9
Shear modulus, Gpa	4.14
Tensile yield stress, Mpa	
Longitudinal	141
Compressive yield Stress, MPa	
Longitudinal	196
Transverse	150
Shear yield stress, MPa	57
Tensile ultimate stress, MPa	
Longitudinal	156
Transverse	50
Compressive ultimate stress, MPa	
Longitudinal	237
Transverse	178
Shear ultimate stress, MPa	73
Bending ultimate stress, MPa	223.8
Tensile ultimate strain	
Longitudinal	0.0072
Transverse	0.0067
Compressive ultimate strain	
Longitudinal	0.0253
Transverse	0.0517
Shear ultimate strain	0.39
Bending ultimate strain	0.0178

This study highlighted the significance of tensile strength of the white line regions at zones 2 and 3 from medial claws and lateral claws. The weight transferred to the hind limbs of cows is carried primarily by the sole and heel border at zone 3 and mainly in the lateral claw and is the most common site for the white line disease. This is the area of highest horn production and therefore less keratinization and potentially the site for greatest hoof expansion during locomotion and may explain the differences found in tensile strength in this study. In this study, white line production at day 53 corresponded to the peak lactation and may explain the lower tensile strength of hoof samples at the time of highest energy demand for milk production. The authors believe that changes in tensile strength found in this study may have reflected the stage of lactation.

Reilly et al. (2002) emphasizes the importance in the utilization of methods of preparation of specimens for further analysis and conducted a comparative experiment on methods for measuring moisture loss of hoof wall samples. Methods tested were, freeze drying, vacuum drying, phosphorous pentoxide desiccation and room temperature drying at 90, 100, 105, 110 and 120°C. They observed that all the different drying methods produced different absolute median values for hoof horn moisture content and comment that although each method has its specific advantages and disadvantages, the implication of each of them must be understood before it can be used for research purposes.

Carvalho et al. (2003) (University of Florida. Agricultural and Biological Engineering Department. Gainesville. FL, personal communication) collected data from horn samples (keratin) of a single cow at and tested under compressive loading. Three locations were taken from the outer and inner claws from front and rear legs of one cow totaling 24 specimens. Mid section from the weight-bearing surface (MID), toe section from the weight bearing surface (TOE) and SOLE. These specimens were tested under three different velocities (0.3, 1.5 and 3 cm/min). The polynomial fits obtained for the stress-strain curves from the MID, TOE and SOLE specimens were differentiated with respect to strain (ε) and used to calculate modulus of elasticity (E). The modulus (E) was obtained for the fastest rate of loading and for three different stress ranges of each obtained from the testing (Table 2-3). Figures 2-11 to 2-19) show the stress-strain curves for the three specimens at the three speeds tested. The MID sections were the more compliant and presented the lowest moduli for its particular stress range followed by SOLE specimens and TOE specimens with the highest moduli. Within each specimen location, front inner claws were the strongest specimens followed by front outer, rear outer and the weakest being rear inner specimens. SOLE and MID sections reached the 30% preset strain (~0.076 cm) with a load of approximately 13.78 MPa and the TOE sections reached this strain at almost 41.36 MPa.

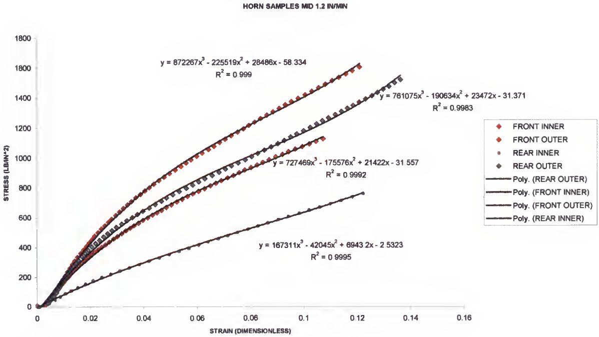

Figure 2-11. MID samples loaded at 3cm/min speed.

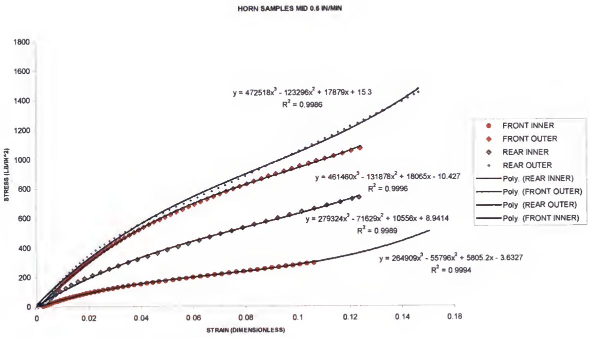

Figure 2-12. MID samples loaded at 1.5cm/min speed.

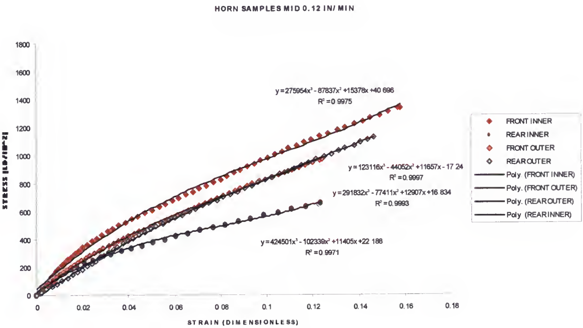

Figure 2-13. MID samples loaded at 0.3cm/min speed

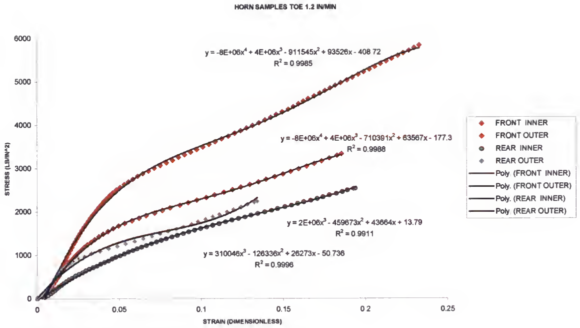

Figure 2-14. Toe samples loaded at 3cm/min speed.

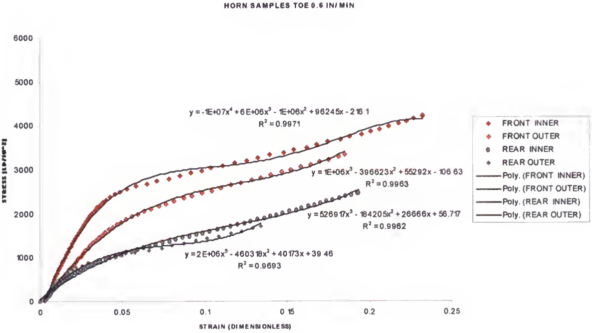

Figure 2-15. Toe samples loaded at 1.5cm/min speed.

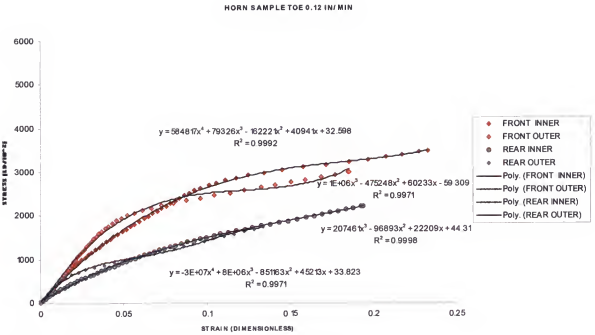

Figure 2-16. Toe samples loaded at 0.3cm/min speed.

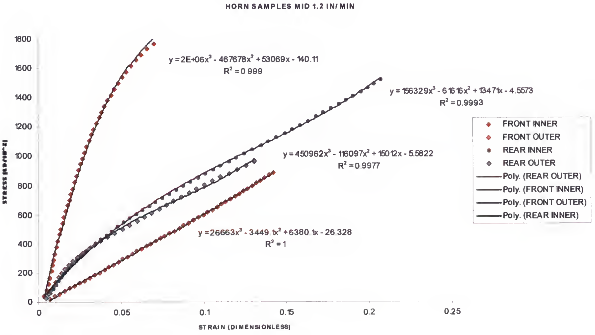

Figure 2-17. Sole samples loaded at 3cm/min speed.

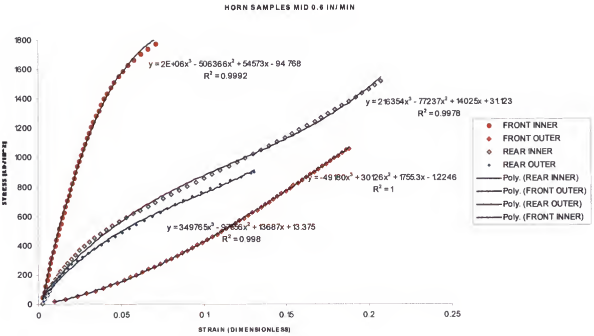

Figure 2-18. Sole samples loaded at 1.5cm/min speed.

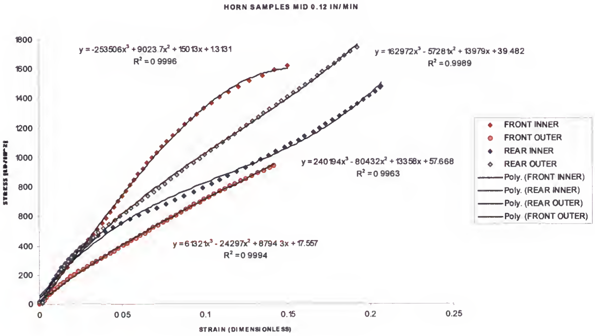

Figure 2-19. Sole samples loaded at 0.3cm/min speed.

Table 2-3. Elastic Modulus for hoof keratin specimens at 3 cm/min.

	Claw		FI		FO		RI		RO
Section	Stress (MPa)	Strain	E (MPa)		E (MPa)		E (MPa)		E (MPa)
MID	2.75	0.02	146.17	0.02	98.19	0.06	39.31	0.02	115.48
	4.13	0.03	125.51	0.04	73.68	0.09	37.49	0.03	97.07
	6.89	0.06	75.68	0.09	51.37		-	0.08	52.25
TOE	6.89	0.02	434.07	0.02	273.50	0.05	110.00	0.03	155.90
	13.78	0.04	289.06	0.08	74.77	0.14	62.82	0.12	119.12
	20.68	0.07	94.63	0.16	85.47		-		-
SOLE	4.13	0.02	278.21	0.10	44.66	0.06	53.50	0.07	37.75
	5.51	0.02	248.47	0.13	47.00	0.09	42.57	0.10	36.66
	6.89	0.03	225.96		-	0.12	37.46		-

Fracture Mechanics

There are two types of fracture that a material (e.g., bone) displays. Monotonic fractures which are the fractures that occur when the failure stress of the bone material under a given type of loading is exceeded. These fractures are abrupt and occur usually during accidents where impact is the major factor. The other type of failure of a material occurs more gradually and under cyclic loading. Creep and fatigue are the two ways in which failure of a structure can occur gradually. In both cases, stress less than the ultimate stress is applied and damage from this stress grows and accumulates until failure occurs. In Creep the stress is applied continuously and in fatigue the stress is applied cyclically. Both are closely related, an example is the vertebral bodies of the spine that support a constant weight while sitting or standing or cyclic loading when someone walks (Martin et al., 1998).

Bone has the ability, under normal conditions, of repair itself. This process is called remodeling and is accomplished by Basic Multicellular Units (BMUs), which are formation and resorbing type of cells (osteoblasts and osteoclasts) grouped in pairs. Their function is to repairs microcracks in the skeleton as they appear in a fully grown individual. If fatigue damage accumulates more rapidly than remodeling can remove it, fatigue failure (stress fracture) can occur.

Dairy cattle, under intensive housing conditions may also be affected in a long run by fatigue of structures such as bones and joints mostly with scenarios of incorrect load bearing on claws. Biological materials that are not designed to withstand certain load magnitudes could fail under cyclic loading.

For example, a lame claw of a dairy cow can be considered to have undergone fatigue failure on the corium structures due to fatigue of the biological tissues that comprise the corium under unusual cyclic loading. The fatigue damage (microcracks) propagates until catastrophic failure if the unusual cyclic loading of the structure in question is not removed.

Biomedical engineers normally use a model of an infinite metal plate with an elliptical hole in the center under Fairfield tensile stress to study fatigue damage and fracture in bone. The stress concentration on an elliptical hole in an infinite plate normal to the long axis of the ellipse is given by:

$$\sigma_A = s\,(1 + 2a / b) \qquad (2\text{-}3)$$

Where b and a are the minor and major radii of the ellipse and s is the nominal stress.

A crack may be thought of as a very eccentric elliptical hole where a in this case becomes very large and the ellipse becomes cracklike. In this case, the equation is given by polar coordinates (r, θ) relative to the end of the b –axis:

$$\sigma_x = s\,(a / 2r)^{1/2}\ \cos\theta / 2\,(1 - \sin\theta / 2\,\sin 3\theta / 2) \qquad (2\text{-}4)$$
$$\sigma_y = s\,(a / 2r)^{1/2}\ \cos\theta / 2\,(1 + \sin\theta / 2\,\sin 3\theta / 2) \qquad (2\text{-}5)$$

$\sigma_{xy} = s\,(a / 2r)^{1/2} \cos \theta / 2 \sin \theta / 2 \sin 3\theta / 2$ (2-6)

Where r is the distance from the stress at a given point to the crack tip and θ is the angle made between r and the *b*-axis.

Taking the stresses in the y direction along the line $\theta = 0$ gives:

$\sigma_y = s\,(a / 2r)^{1/2}$ (2-7)

Approaching the crack tip, r becomes very small relative to the crack length *a*, and the stress concentration becomes very large.

The stress intensity at the vicinity of the crack tip is proportional to the nominal stress, *s*, and the square root of the crack length *a*. This stress intensity is what drives the crack forward and causes the bone structure to failure.

Stress intensity (k) $= \sigma_y (2r)^{1/2} = s\,a^{1/2}$ (2-8)

Rearranging Equation 2-8, $\sigma_y = k\,(2\pi r)^{-1/2}$ and

$k = C\,s\,(\pi a)^{1/2}$ (2-9)

Where C is a dimensionless constant and depends on size and shape of the flaw, and mode of loading of the specimen.

There are basically three different equations for calculating C according to the crack geometry (mode I, II, III). A simple example is the mode I cracking (Figure 2-20).

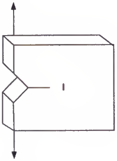

Figure 2-20. Mode I type of crack

Equation 2-10 is used for calculating C for this type of loading:

$$C = \{(\tan q)/q\}^{1/2}\ \{0.752 + 2.02\,(a / b) + 0.37(1 - \sin q)\}/ \cos q, \tag{2-10}$$

Where $q = \pi a / 2b$

If after these calculations the resulting value of k exceeds maximum critical value (k_{ic}), the crack will propagate to catastrophic failure otherwise it will not.

Maximum tolerable flaw size can be computed from k by setting the stress intensity factor k equal to the critical stress intensity factor k_{ic} (fracture toughness), and solving for *a*. Table 2-4 shows experimental k_{ic} for cortical bone with crack propagation parallel to the grain direction obtained from several investigators.

Table 2-4. Experimental values of k_{ic} for bone.

Bone type	k_{ic}, Mpa – $m^{1/2}$	Source
Mode I, transverse fracture		
Bovine femur	5.49	Melvin and Evans, 1973
Bovine tibia	2.2 – 4.6	Bonfield and Datta, 1976
Equine metacarpus	7.5	Alto and Pope, 1979
Human tibia	2.2 – 5.7	Norman et al, 1992
Mod I, longitudinal fracture		
Bovine femur	3.21	Melvin and Evans, 1973
Bovine tibia	2.8 – 6.3	Behiri and Bonfield, 1984
Human femur	2.2 – 5.7	Norman et al, 1992

$$K_i = 2\,(a / \pi)^{1/2}\ s\ \{1.211 - 0.186\,(\cos\theta)^{1/2}\},$$

For $\theta = 0$, maximum tolerable crack radius and solving the stress intensity factor for *a*, Equation 2-9 becomes:

$$a = a_c = 0.238\,\pi\,k_{ic}^{\,2} / s^2 \tag{2-11}$$

Assuming that $k_{ic} = 4$ Mpa – m ½ (Table 3), E = 20 Gpa and $\varepsilon = 2000\ \mu\varepsilon$, therefore $s = E\varepsilon = 40$ Mpa. Substituting into Equation 2-11:

$a_c = 0.238\ \pi\ (4^2 / 40^2) = 0.0075\ \text{m} = 7.5\ \text{mm}$

This would be the maximum tolerable crack size for human tibial cortical bone with a semi-circular crack loaded in tension before catastrophic failure of the bone structure in question (Martin et al., 1998).

Paris (1964) (cited by Martin et al., 1998) proposed that the number of cycles required for fatigue failure of a specimen with a crack could be related to the crack's stress intensity factor. His idea was that the crack length increase per load cycle, da/dN, is proportional to the range of k values experienced with the loading:

$$\Delta k = k_{max} - k_{min} \qquad (2\text{-}12)$$

A common suggested form for such relationship is given by Paris Crack Growth Law (PCGL):

$$da/dN = \xi(\Delta k)^{\eta} \qquad (2\text{-}13)$$

Where ξ and η are constants. However, the Paris equation has failed to maintain the relationship for high or low values of da/dN. Within intermediate crack grow rates; slopes and intercepts of log plots of da/dN vs. Δk yield the given constants predicted by the Paris crack-grow rate. Modifications for PCGL to fit low and high values of da/dN are presented in Skeletal Tissue Mechanics (Martin et al., 1998).

In practice, Equation 2-13 can be written as:

$$\Delta k = k_{max} - k_{min,} = C\ \Delta\sigma\ (\pi a)^{1/2} \text{ and}$$

$$dN = \{1 / \xi(C\ \Delta\sigma\ (\pi a)^{1/2})^{\eta}\}\ da, \qquad (2\text{-}14)$$

Integrating the equation within ranges of initial and final crack sizes (ai, af), dN gives the number of loading cycles required to fracture under a particular stress, bone geometry and mode of loading.

In sum, it is possible to calculate the fatigue life of bones that will lead to the origin of cracks and with crack propagation estimates calculated from parameters already studied and presented in the literature it is possible to predict failure of bones under a particular stress and mode of loading. This can be useful to understand and predict fatigue damage and failure through crack propagation in bones that are unusually loaded due to incorrect weight bearing dynamics.

Biomechanics of Anabolic Induced Musculoskeletal Overgrowth

Intrinsic and extrinsic forces determine the shape, dimension and strength of bones. Intrinsic forces follow from weight bearing and extrinsic forces result from muscles pressure and tension. During growth period, the increase in intrinsic and extrinsic forces correlate with the development of bone structures (arrangement of bone tissue including cartilage and quality of bone material).

Generally the development of bones and the influence of forces are in balance. However under the condition of intensive animal production this balance is very often disturbed and the resulting imbalances between strength of bones and operation stress lead to skeletal lesions with locomotory disorders or lameness (Dammrich 1986).

The influence of operating stressors and the reaction of the skeletal structures in fattened bulls treated with anabolic feeding in a diet that contained a high content of protein and energy was tested.

Growth hormone and anabolic feeding induce accelerated growth of muscles and bones resulting in the increase in the dimensions of bones because the endochondral bone growth and periostal osteogenesis are accelerated. As a result, bone quality was a little lower than in controls. It was noticed that the trabecular bone (spongy bone forming

mostly the head of long bones) was composed of thinner fibers than in control and the metaphyseal part of the corticalis (part below the head of a long bone) was elongated and the diaphyseal corticalis (middle portion of a long bone) was thinner than in controls. The author theorized that in enlarged bones, osteogenesis (bone formation) is not accelerated and the same or only a little increased quantity of bone tissue is distributed to the enlarged bone volume. However, the osteoclastic activity of remodeling (bone resorption) is more accelerated and bone resorption is more prominent than osteogenesis.
Hence, the result of accelerated growth is that the increased intrinsic and extrinsic forces influence bone structures of lower resistance against mechanical stressors.

In fattened bulls, the lower resistance of skeleton to these forces is complicated by incorrect load of bones, which is caused by faulty locomotion behavior and overloading (influenced by housing systems).

Different housing systems, stanchion stable, loose housing having either concrete floor and straw or slatted floors were investigated. The most severe lesion was observed in bulls housed on stanchion stable followed by slatted flooring.

Influence of Incorrect Loading on Physiology of Bone Growth

Unphysiological movement with faulty loads causes adaptational and pathological bone structures. Endochondral bone growth, osteogenesis and remodeling are affected.

The mediators of increased or decreased cell activity are pressure circulatory changes and bioelectric effects, which transduce mechanical to electrical energy in cellular membrane systems (Dammrich 1986) and Rapoff (2003) (Aerospace Engineering Department. University of Florida. Gainesville. FL, personal communication).

Overloading induces bone changes, which are characterized by action of compression and decompression. Under compression, endochondral bone growth is

retarded and endochondral ossification is accelerated, and sometimes, premature closure is observed. Under decompression, the retarded endochondral ossification is accompanied by a low increase of chondrocytic proliferation. Regularly the disorder of one epiphyseal plate is determined by the influence of compression and decompression. In such ways the bone grows unequally in length and deformed bones occur (Dammrich 1989).

Frost 1964 (cited by Martin et al., 1998) proposed a theory for the influence of mechanical loads in the remodeling of bones. He proposed an algorithm that would give the desired remodeling results for a long bone loaded in bending where remodeling is controlled by the polarity of the tangential walls (compression promotes formation and tension promotes resorption) and included terms for the tendency of the applied end load that alters the relative curvature of the surface. In his theory, rather than tension and compression promoting resorption and formation, this process is also influenced by surface convexity. Increased surface convexity would promote resorption and vice-versa. This scheme, allows both the internal and external surfaces of bone to remodel to reduce the curvature and high stresses associated with excessive bending. This theory explains why abnormally curved bones end up straightening themselves.

Deformed bones are one of important factors in the pathogenesis of articular lesions and consequently upper limb lameness.

Pathogenesis of Joint Lesions and Joint Reaction Forces

Synovial or diarthroidal joints are those joints that move freely and contain synovial fluid. Examples of these joints are the knee and elbow joints. These joints are comprised of synovial membrane that produces the synovial fluid within the fibrous joint capsule. The bone surfaces within the joint capsule are covered by articular cartilage (hyaline cartilage). The purpose of the articular cartilage is to provide suitable surface for lubrication and wear protection rather than shock absorbing capabilities (Martin et al., 1998). Synovial joints provide frictionless motion between limb segments while transmitting high loads between them. Joint forces are quite large and are due to not only the body weight in movement but due to the stresses promoted by tendons and ligaments that work to stabilize the joint during motion. These relatively high forces are also transferred to the articular cartilage that can hold loads in the order of 2 to 11MPa in normal situations (Afoke et al., 1990 cited by Martin et al., 1998).

Arthritis is one of the most common joint diseases and is related to mechanical damage and inflammatory processes. It is postulated that mechanical overuse may create fatigue damage in cartilage and this damage may induce an inflammatory process that activates bone and cartilage cells to not only repair but also to attempt to reshape the involved tissues as to improve mechanical efficiency (Martin et al., 1998).

The nutrition of the articular cartilage depends on the supply over the synovial fluid. In the cartilage tissue, the nutrition of the condrocytes depends on the diffusion and inner flow of the ground substance, supported by compression and decompression during moving (Dammrich 1987). In the fattening bulls experiment presented before, Dammrich also looked at the articular cartilage physiology and mechanics.

Under conditions of accelerated growth the extrinsic and intrinsic forces increase much more than the size of the articular surface. The increased load of the articular surface makes difficult the nutrition of the condrocytes, because the inner flow of the ground substance is diminished and the system of collagen fibers is overstressed. The accompanied reduction of the thickness of the articular cartilage is not sufficient to supply nutrition to the condrocytes.

The articular cartilage is supported by subchondral bone tissue and becomes more fragile in fattening bulls due to remodeling imperfections given with this scenario. The result is the decreased support of the articular cartilage and the lower resistance against mechanical stressors. The malnutrition of the condrocytes is further complicated by deformed bones. The equal distribution of load on the articular surface is essential for normal joint physiology and in cases of deformed bones the articular cartilage surface loading is uneven and the functional structure is disturbed resulting in even greater malnutrition of the chondrocytes.

The lesions of the articular cartilage start with traumatic injuries, mechanical overuse or with alterations of the chondrocytes that leads to painful inflammatory process with the development of aseptic arthritis. Traumatic injuries are clefts and cracks of the articular cartilage whereas alterations of the chondrocytes caused by malnutrition lead to loss of matrix synthesis, proliferation and regular regeneration. Regressive changes of the articular cartilage irritate the joint capsule by detached particles of necrotic cartilage (consequences of inflammatory and necrotic process from altered physiology of chondrocytes), release of lysosomal enzymes, etc.

Joint Resultants

The joint resultants are also referred to as intersegmental resultants and joint reaction forces and moments. At a given articulation, the joint resultants depict the net kinetic effect that the two adjoining body segments have upon each other

(Chow 2002, Exercise and Sports Sciences. University of Florida. Gainesville. FL, personal communication). Knowledge of loads in joints structures is very useful in understanding mechanical effects of musculoskeletal injuries. Joint resultants (resultant joint force and resultant joint moment or torque) are commonly used to evaluate the overall loads at a joint.

In a static body, the forces acting on a joint are generated mostly by the action of the body weight but when motion occurs other forces are involved. Dynamically, the simple concept of body weight, the product of the mass of body times the acceleration due to the gravity of earth, is replaced by the product of the mass of the body times the acceleration due to the motion. In addition, great force magnitudes are exerted by the action of muscles and ligaments that counteract one another to provide balance to the joint and keep it together. Joints are subjected to high stress magnitudes. They withstand these stresses mostly due to viscoelastic properties of the articular cartilage that has the ability of transferring these forces through the bone surfaces and in normal conditions works as a self-renewing, well lubricated, load-bearing surface (Martin et al., 1998).

Muscle and ligament action places a great amount of shearing forces on the joints. Joint shear is an important mechanical quantity and is usually regarded when investigating the causes of joint trauma and disease, and the efficacy of treatment modalities. In many joints, the resistance to transversely applied shearing forces is primarily by the soft tissues that comprise the joint neighborhood.

Joint shear values are often regarded as a measure of the exposure of the joint to soft tissue damage leading to loss of kinematic and kinetic integrity (Chow 2002, exercise and Sports Sciences. University of Florida. Gainesville. FL, personal communication).

Shear forces are parallel or tangent to the surface upon which they act and cause angular distortion. They tend to shear or displace one segment in a transverse direction Relative to the other segment.

Problems in the joints of large animals such as cattle and horses can be examined taking the example of racehorse joint problems. Racehorses place extraordinary high loads on their forelimbs, which are thought to carry about 60% of the weight of the animal. Racehorses are seriously injured by mechanical failures of the structures in the distal forelimb particularly the fetlock joint. Its biomechanical importance derives largely from the fact that the bones above it rise straight up to the torso, but the phalangeal bones below it angle sharply forward in a springy cantilever arrangement (Martin et al., 1998).

Upper limb conditions cause lameness less frequently than do hoof problems. In some cases primary hoof problems may result in secondary upper limb problems. Some problems such as degenerative arthritis or osteoarthritis occur in older cattle. Major weight-bearing joints are most commonly affected in bulls and heavier cows.

In the event of a lame cow, depending upon the stage of lameness, much of the weight is redistributed to the unaffected limbs, creating a high stress concentration in the joints. High stresses in joints can, over time, develop pathological conditions. Previous investigators have supported the idea that conditions such laminitis, fracture, bowed tendons, and certain forms of degenerative joint disease occur because the biological and mechanical capabilities of the tissues involved are exceeded as single or multiple events. The magnitudes of the forces at specific sites may be modified by conformational defects, the type of physical activity, and the surfaces on which the activity is performed

(Bartel et al., 1978).

In a horse, the primary load-carrying structures in the digit during the supporting phase of gait (hoof contact) are: the deep flexor tendon, superficial flexor tendon and suspensory ligament. The contribution of the extensor is considered negligible during support (Bartel et. al., 1978). The suspensory ligament and the suspensory navicular ligament are the act as springs that resist extension of the fetlock and coffin joint respectively. Also when writing a model of the lower leg for kinetic analysis, Bartel and co-workers consider the joints and ligaments below the fetlock joint to be frictionless pinned points connected to the fetlock joint and the motion is assumed to be planar. That is due to the hypothesis that there is little or no relative motion between proximal sesamoids, first phalanx and second phalanx. Another assumption commonly made for this type of analysis is that ligaments of similar diameter are able to withstand about the same amount of strain and therefore have equal load.

Riemersma et al. (1987), studied tendon loads for the stance phase of gait of ponies. Mercury strain gauges (MISS) were implanted inside the tendons and the loads were compared to the actual tendon strain measured after the animal was sacrificed. The results reported are that the deep digital flexor tendon (DDFT) was loaded maximally at the second half of the stance phase, the superficial digital flexor tendon (SDFT) reaches maximum load in the first half of stance. Both tendon loads are minimal at swing phase. The long digital extensor tendon (LDET) was a mirror of the SDFT having maximal loads at the swing phase and minimal loads at the stance phase. These results are similar work done in horses that are cited by the author. In humans, the motion of foot and ankle during the walking cycle occur primarily as a result of passive constraints of joints and ligaments. Electromyography has shown that muscle activity does occur during normal gait. At the heel strike, the pretibial musculature fires eccentrically to slow down the descend of the forefoot and prevent a foot slap. At midstance, the calf musculature contracts to slow down the forward movement of the body over the foot and prevent crouch gait. The intrinsic also contracts during to toe-off to aid the rigidity of the fore foot. The pretibial musculature again contracts during swing phase to ensure that the foot clears the floor during swing-through. The muscles of the lower extremity are more active during running. The gluteus maximus and hamstrings are active in midstance through toe-off and increase their activity 30 to 50% to decelerate the stance phase limb. Dorsiflexors and the foot and ankle are active in 70% of the running cycle. The intrinsic, plantar flexors, and peroneals are important stabilizers of the plantar surface and hind foot during the foot flat phase.

Muscle activity in gait of large animals has not been reported as frequently as tendon loads. This may be because problems of lameness are primarily on the lower extremity at the foot, coffin joint and fetlock joint where tendon actions are more evident and muscle activity is not a primary concern.

The forces at a joint are calculated through equations of equilibrium (Equations 2-15 to 2-17 for static and 2-18 to 2-19 for dynamic) in static and dynamic conditions and also accounting for muscles and ligament forces and torques when necessary.

$$\sum Mo = 0 \tag{2-15}$$
$$\sum Fx = 0 \tag{2-16}$$
$$\sum Fy = 0 \tag{2-17}$$
$$\sum Mo = I\alpha \tag{2-18}$$
$$\sum Fx = ma_x \tag{2-19}$$
$$\sum Fy = ma_y \tag{2-20}$$

Where for static analysis the sum of the forces and moments equal to zero and in case of dynamic analysis the sum of the forces equals the product of mass (m) and acceleration (a) and the same for the moments where in static equilibrium the moments sum to zero and in case of dynamic, they equal to the product of moment of inertia (I) and angular acceleration (α).

In animal gait analysis is also common to assume that, for normal walking speed, during the support phase of gait, the accelerations at a digit level are small and can be neglected, reducing the problem of determining forces in the digit to a static equilibrium at various digit configurations.

A simple calculation of the fetlock joint reaction force starts with a Free Body Diagram (FBD) of the segment being analyzed and the rest of the body replaced by a system of forces (Figure 2-21).

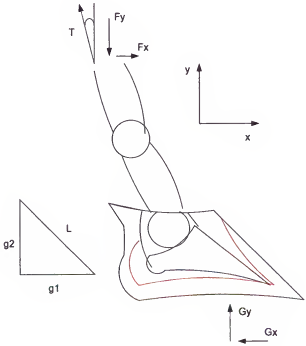

Figure 2-21. FBD of the lower extremity of an equine front limb

Let (T) be the flexor tendons and suspensory ligaments combined force and its direction assumed that the longitudinal direction of the fibers define the direction that the ligament or tendon is loaded (in this case two or three tendons are lumped together as one for simplifying the calculations), (Gx) and (Gy) are the ground reaction force measured by force plates and (Fx) and (Fy) are the two components of the joint reaction force and (*T*) is the angle teta that the tendon makes with the vertical axis. The FBD would be such: For a standing position and static analysis the moment equation (Equation 2-15) is:

$\sum Mo = -Gx\ g2 + Gy\ g1 - tT = 0$;

Where g1, g2 and t are the moment arms measured from the point of application of forces to the joint center.

$\sum Fx = Fx - Gx - Tx = 0$,
$\sum Fy = -Fy + Gy + Ty - W = 0$,

Where Fx, Fy, Gx, Gy, Tx, Ty are the forces and W is the force due to the weight and is negligible and is assumed to be equal to zero.

Assuming that the animal weighs 6000N, the weight for a standing position on one foot at the front quarter would be Gy = 6000 * 30% = 1800N (60% of total in the front quarter divided by two for each leg).

Assuming that theta is 0, that is T is parallel to the longitudinal axis and also given values for the moment arms to be t = 0.05m, g1= L cos 40 = 0.153m and g2 = L sin 40 = 0.128m (L is the distance from the application of the ground reaction force to the joint center and is assumed to be 0.2m), then from the moment equation:

$T = 1800(0.153)/0.05 = 5508N$

And therefore solving for Fx and Fy from the other equations (Equations 2-16 and 2-17),

$$\sum Fx = Fx - Gx = 0,$$
$$Fx = Gx = 1800 \cos 90 = 0$$
$$\sum Fy = -Fy + 1800 + 5508N = 0,$$
$$Fy = 1800N + 5508N = 7308N$$

The shear force (F^{sh}) can be calculated knowing the angle (Ω) made by two specific vectors. The fetlock joint resultant F vector intersected with the vector made by the relative location of the fetlock joint center and the point of application of the ground reaction force. This angle can be found by locating the angular position of each vector. In the case of the joint resultant (F) vector, its angular position can be found by taking the tangent inverse of the quotient of the vector components ($\tan^{-1}(Fy/Fx)$). The relative location vector from the joint center to the point of application of the ground reaction force can be found by taking the tangent inverse of the quotient of its planar coordinates ($\tan^{-1}(y\ joint - y\ grf)i / (x\ joint - x\ grf)j$). After these angles are found, Ω can be calculated and the axial and shear components of the joint force are respectively:

$$F^{ax} = F \cos \Omega \qquad (2\text{-}21)$$
$$F^{sh} = F \sin \Omega \qquad (2\text{-}22)$$

Locomotion: Gait Analysis and Kinematics

Locomotion is the act of moving (dislocating) from one place to another by means of one's own mechanism of power. Gait can be defined as the manner or style of walking during locomotion (Chow 2003, Exercise and Sports Sciences Department. University of Florida. Gainesville. FL, personal communication) or simply the limb coordination pattern used in locomotion (Dalin et al., 1995). A normal gait repeats a basic sequence of limb motions that serves to progress the body along a desired path while maintaining a weight-bearing stability, conserving energy, and absorbing the shock of floor impact.

Gait analysis can be defined as the systematic analysis of locomotion either by an experienced observer (clinician) or by means of quantitative parameters obtained through video analysis and ground reaction force and pressure measurements. Clinical (observational) or biomechanical (engineering) gait analysis has many applications such as pretreatment assessment, surgical decision making, post operative follow-up and it has proven to be useful tool in studies of neuromuscular disorders, evaluation of prosthetic joint replacement, athletic injuries, orthotics, etc (Harris et al., 1994). Nevertheless, the most useful application of gait analysis is the evaluation of walking disorders and understanding the impact of them on an individual's health. Observational gait analysis is done by observing the patient without the aid of any equipment. It is best done by systematically concentrating on one body part and then another. A trained observer can recognize many gait deviations during stance and swing phases of gait. An obvious limitation of observational gait analysis is the difficulty of observing multiple events and multiple body segments concurrently because the human eye cannot perceive events happening faster than 1/12 of a second (Harris et al., 1994). This problem is overcome with introduction of cinematography, where videos of the patients can be played frame by frame or slow motion videotape replay using cameras with typically 60 frames per second resolution.

Biomechanical gait analysis is a quantitative analysis and incorporates the use of a more detailed video technology by means of digitizing landmarks in the body and performing calculations of linear and angular kinematics. Linear and angular positions, velocities and accelerations can be calculated using differentiation methods from the positions of the landmarks on the body in the video frames. In addition, the angular positions of joints can be used for evaluating degrees of flexion and extension of limbs as they change from normal patient population to patients with walking disorders.

Digitization of landmarks in the body can be done using marker systems, where markers (reflective tape, commercial reflective balls with belt attachments, etc) are placed on top of joint centers in one, two or three different planes (saggital, coronal and transverse planes) to help identify the movements of the body segments. By digitizing the location of the markers placed on the anatomical landmarks, the marker position can be quantitatively determined with respect to the focal plane of the camera or cameras. The most common and less expensive video kinematics analysis is done using one single camera that captures video on the saggital plane (subject walking in the direction perpendicular to the focal plane of the camera).

An important issue in quantitative (biomechanical) gait analysis is the form of digitizing of the body landmarks. Manual digitizing has an overwhelming disadvantage, which is the extensive processing time necessary to digitize the data (all landmarks in a frame by frame basis). That situation is even complicated when digitizing landmarks without the aid of any markers.

An option to manual digitizing is the use of automated motion tracking systems, which offers the most sophisticated method for motion analysis. These systems (i.e., Peak Motus System – Peak Technologies Co.) use either passive reflective or active illuminated (optoeletric) markers that are tracked by and automated multicamera system. Active marker systems offer the advantage of higher sampling rates (200 to 300Hz), and uses a larger number of markers and frequency coded data sorting. The markers in these systems require that the subject use a power pack on the body for the LEDs.

Passive markers on the other hand do not require power pack, but they require an illumination source (typically infrared or stroboscopic light) near the camera and they also require the use of algorithms to identify the center marker position. Irrespective whether performing observational or biomechanical (quantitative) gait analysis, the gait is evaluated by the assessment of several parameters within a gait cycle.

The gait cycle is defined as being the time interval between two consecutives occurrences of one of the repetitive events of walking. Usually initial contact (heel strike most of the times in humans) or toe-off are the choices for they are well defined and therefore easily identified. When one of the foot strikes the ground (right foot for example), the gait cycle will last until the right foot strikes the ground again. The left foot goes through the same series of events but displaced by half a cycle in time.

The gait cycle is divided into stance phase and swing phase. Stance phase is the period in which the foot is in contact to the ground and swing phase is the period in which the foot moves through the air. The stance phase, also called support phase or contact phase, lasts from initial contact of the foot with the ground until the foot leaves the ground (toe-off) and is subdivided into four sub-phases. The stance phase subdivision varies according to literature but the most complete terminology can be defined as being:

1 - Initial contact (IC), the moment when the foot contacts the ground.

2 - Loading response (LR), weight is rapidly transferred onto the outstretched limb. Is the first period of double limb support (humans).

3 - Mid-stance (Mst), the body progresses over a single limb (humans).

4 - Terminal stance (Tst), progression over a single limb continues. The body moves ahead of the limb and weight is transferred onto the fore foot.

The swing phase lasts from the toe-off to the moment the foot contacts the ground again and it can be subdivided into another four sub-phases:

5 – Pre-swing (Psw), a rapid unload of the limb occurs as the weight is transferred to the contralateral limb. Characterizes the second period of double limb support (humans).

6 – Initial swing (Isw), the limb begins to advance as the as the foot comes off the ground.

7 – Mid-swing (Msw), the limb continues to advance as the knee begins to extend.

8 – Terminal swing (Tsw), the knee extends and the foot prepares to contact the ground for initial contact.

In gait analysis, temporal and spatial parameters are obtained from the digitization of the foot landmarks and are useful for characterizing and comparing some specific gait with normative data (range of values for normal subjects). Spatial data is obtained from the position of the video landmarks with respect to the camera's field of view. For instance, Step length is the longitudinal x-axis distance from one heel strike (IC) to the next contralateral (IC). Its distance is measure by subtracting the x-coordinate of the of the heel landmark of the contralateral foot at IC from the heel landmark at IC of the foot the stroke the ground initially. Temporal data uses the product of the frame elapsed between two events (i.e., two heel strikes in the latter step length calculation example) and the frequency of the camera use for capturing it (30Hz = 30 fps = 1/30 = 0.03333) and yield the step time. These calculations can be performed not only for steps, but also for the whole stride using the ipsilateral consecutive events (right heel strike to the next right heel strike) rather then contralateral consecutive events (right heel strike to the following left heel strike). Step speed and stride speed are calculated easily once step length and time or stride length and time are obtained from video data by dividing the distance of either parameter by its respective time.

Another useful parameter is the cadence of a stride, or the number of steps taken in a given time usually measured as steps per minute. Cadence can be computed by taking the inverse of step time (1/ step time (s)) and multiplying it by 60 seconds).

Gait in normal circumstances is influenced by factors other than locomotory diseases. Factors such as aging and velocity of walk have major impact in gait dynamics. Elder individuals tend to walk slower and spend more time in stance phase. Stance phase becomes longer because elders spend a longer time in an intermediate phase called double support phase. Double support phase is a short period that occurs when any given foot (left or right) strikes the ground (heel strike) but the contralateral foot has not left the ground (toe-off). Elders tend to spend more time in double support phase in an attempt to preserve stability.

Velocity of walking affects other gait variables and are different for certain velocity ranges. In humans, cadence and step demonstrate linear relationship at speeds ranging from 0.8 to 2m/s and is curvilinear in ranges of 0.3 to 0.8m/s. Also, single and double support are inversely proportional to velocity. Double support time decreases with increased velocity and becomes near zero in race walking. In very low velocities stance time can occupy as much as 80% of the gait cycle. Normally it occupies around 60% and swing 40% for normal walking.

Gait of Large Animals

The walk of horses is a natural symmetrical gait in which the foot falls occur in a 4-beat rhythm with a lateral sequence of hoof placements: left hind, left fore, right hind, right fore. The limb support sequence alternates between tripedal (two hind limbs vs. one fore limb and two fore limbs vs. one hind limb) and bipedal (lateral pair or diagonal pair) support (Hodson et al., 2000).

Gait of horses and cattle are similar during normal walk. Looking closely to the pattern of walking of cows and horses is evident that these animals spend more time in stance phase than swing phase. Their gait at normal walk is comprised of three different stance phases; triple stance, double lateral stance and double diagonal stance and one swing for each of the stance phase.

Triple stance occurs at the impact of any leg. It is a brief period in which three of the legs are in contact with the ground. Diagonal double stance occurs at liftoff of hind legs only. Either left or right hind leg liftoff will put its adjacent leg into diagonal double stance. For instance, hind right leg liftoff will put left hind leg together with right front leg into double limb support and vice-versa. Lateral double stance occurs at liftoff of front legs only. At the same token as the diagonal double stance, either left or right front leg liftoff will put its adjacent leg into lateral double stance. For instance, front left leg liftoff will cause the right front leg to go into double limb support with the right hind leg and vice-versa. Figures 14 shows a complete full stride of a normal cow and its phases during walking.

Changes in limb weight-bearing, propulsion and deceleration forces are expected as a moving horse compensates for lameness. Abnormal gait maybe detected by lack of symmetry between limbs, reduced or non-uniform rates of loading and unloading, reduced maximal and minimal forces and changed duration of force application (Leach 1987).

Kinematics of gait describes quantitatively the movement of limbs. It describes position, velocities, and accelerations of linear motion and angular motion. Parameters usually described are the segment range of motion in space relative to a reference frame that can be local with respect to some point on the animal itself or global with respect to some point in the environment. Other good examples of the use of cinematography and kinematics is in stress/strain analysis for the development of prosthesis, design of plates for fracture fixation and surgery recovery.

The same methods used for kinetic and kinematics of human gait described previously have been used for studies of gait in horses and recently in cattle (Leach 1987, Clayton et al., 2000, Merkens et al., 1985, Bartel et al., 1978, Keegan et al., 1999, Flower et al., 2003 (University of British Columbia. Ontario, Canada, personal communication)).

Hodson et al. (2000), described kinematics and ground reaction forces on the forelimb of walking horses to demonstrate the relationships between kinematics variables and ground reaction forces. With a sample of five clinically sound horses data was collected during eight passages of each horse. The data obtained for left and right fore limbs were collapsed into a single variable according to symmetry trends between limbs presented by earlier research (Merkens et al., 1986).

Temporal characteristics of the walk in individual horses were remarkably consistent both within and between horses. Spatial and temporal average data showed that stride length was 1.75±0.09m, velocity was 1.39±0.07m/s, stride time was 1.27±0.08s and stance duration was 66.2±1.4%. The angular kinematics (joint angle) was associated with the respective GRF at various points of the stride. Coffin joint was flexed maximally at the time of peak of the longitudinal breaking force which occurred at during breakover of the contralateral forelimb. The metacarpus was vertical at 28% of the stride and, according to the author, was considerably earlier than the change from braking (~13% of stride) to propulsive longitudinal force (34% of stride), which coincided with maximal extension of the fetlock joint. Longitudinal propulsive force peaked just after the contact of the contralateral forelimb.

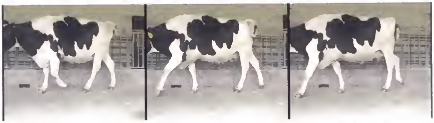

A Hind left impact, start of hind triple stance
FR MSt HR TSt
FL ISw HL IC

B Hind right liftoff, start of left diagonal double stance
FR TSt HR PSw
FL TSw HL LR

C Front left impact, start of fore triple stance
FR TSt HR ISw
FL IC HL MSt

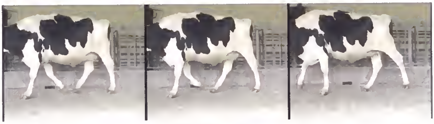

D Front right liftoff, Start of left double lateral stance
FR PSw HR TSw
FL LR HL TSt

E Hind right impact, start of hind triple stance
FR ISw HR IC
FL Mst HL TSt

F Hind left liftoff, start of right diagonal double stance
FR MSw HR LR
FL MSt HL PSw

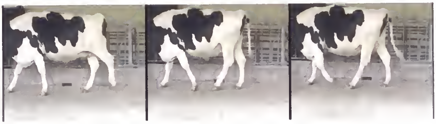

G Front right impact, start of fore triple stance
FR IC HR MSt
FL TSt HL ISw

H Front left liftoff, start of right double lateral stance
FR LR HR MSt
FL PSw HL TSw

A Hind left impact, start of hind triple stance
FR MSt HR TSt
FL ISw HL IC

Phase of gait	characteristics
IC	Foot contacts the ground.
LR	Weight is transferred to outstretched limb, first period of double limb support.
MSt	Body progresses over a single limb.
TSt	Body moves ahead the limb. Fore foot gets the weight.
PSw	Weight is transferred to the contralateral limb. Second period of double limb support.
Isw	Thigh begins to advance as the foot comes off the ground.
MSw	Thigh continues to advance as the knee begins to extend.
TSw	Knee extends and foot prepares to contact the ground.

Figure 2-21. Gait cycle of a Holstein cow

During the swing phase, the joints distal to the shoulder showed a single flexion cycle that peaked at 76% of the stride at the carpus joint, 81% of the stride at the fetlock and 84% of the stride at the elbow and coffin joint. Finally, the coffin and shoulder joints began to extend in the terminal swing phase and continued until contact to the ground and early stance phase. These data (Hodson et al., 2000) constitute normative data that can be used as a basis for similar studies with horses and can be applied to detect changes in kinematics associated with specific lameness.

The range of motion of the joint during stance phase is of particular importance for calculating the joint forces and moments and power and also stress/strain analysis of tissues such as the bone itself, tendons and ligaments. Comparisons can be made for different population of animals with locomotory diseases caused by different types of lameness.

In a preliminary study, Flower et al., (2002) (University of British Columbia. Ontario, Canada, personal communication)) compared spatial and temporal gait kinematics variables for three sample populations of dairy cows; healthy, sole lesion and cows with digital dermatitis. Gait was analyzed from video of 46 lactating cows over 7 consecutives days using reflective marker system and a commercial (Peak Motus – Peak Technologies) for analysis.

Stride length and stride duration were not significantly different among the three groups (1.39±0.09m, 1.36±0.13m, and 1.42±0.11m respectively for healthy, sole lesion and digital dermatitis) for stride length and (1.29±0.16s, 1.38±0.2s, and 1.28±0.19s) for stride duration. Speed was significant ($p < 0.067$) among population samples (1.10±0.19m/s, 1.01±0.22m/s, and 1.14±0.2m/s). Cows with sole lesions had shorter strides and smaller vertical displacements than healthy cows and were also slower taking the longest time (with agrees with human trends of gait biomechanics of velocity relationships).

Video data was obtained in a preliminary run test of a term project at the Department of Physical Therapy of the University of Florida (Gainesville, FL). Observational gait analysis was performed for a single severely lame cow at the Dairy Research Unit (Hague, FL). The following was observed: The major difference noted was the replacement of the triple stance phase for a period in which the four legs are in contact to the ground. Time taken for liftoff of right hind leg caused a delay on gait cycle. The four legs were now on the Ground with the front left impact. There was no diagonal double stance. The front right claw should have been on liftoff but it was still in contact to the ground. No double lateral stance was observed. The lame cow did not go into double lateral stance. Instead she remained in triple stance as the left hind foot fell quickly onto the floor and the left front leg still touched the ground. This was due to a decreased swing time and increased stance time taken by the limbs that were not lame in an attempt to remove most of the load from the lame limb. The consequence was the shift of the load bearing from the lame foot and redistributed to the other limbs.

In sum, lameness is a very serious problem and incurs considerable losses to animal welfare and productivity. Biomechanical aspects involving the initial damage of the tissues inside the claw due to incorrect loading are not yet clearly understood. Mechanical properties of horn keratin structures are of importance because of its interaction with floor materials used in modern housing and are directly related to the rate in which horn grows and wear. An assessment of the mechanical properties of horn structures combined to pressure distribution data will help understand the overburden these structures experience under modern housing and the development of better floor materials that will mitigate lameness problems. Finally, gait analysis lets you quantify animal locomotory behavior, which under foot lameness may influence other body parts.

CHAPTER 3
MATERIAL AND METHODS

Preliminary Tests With the Sensor and Equipment Calibrations

A set of preliminary tests was performed with the pressure mat. The Matscan was mounted under a cow restraint chute located at the Dairy Research Unit (DRU) University of Florida at Hague, FL. The Veterinary Medicine Department's Large Animal Clinical Sciences facility located in Gainesville, FL was used to collect the second set of data.

Data were collected in the first preliminary test at the DRU from a single Holstein cow. According to the farm's records, the cow hooves had been trimmed recently as part of the farm's routine management. The movie of the claw's footprint was recorded at first from the left front foot with the animal standing and subsequently of the left rear foot during gait. The second trial at the Veterinary School facility was done using two Holstein cows. Footprint movies were recorded of the left front foot in both of both cows. The animals at the Veterinary School had not been trimmed and presented different levels of claw overgrowth. A simple analysis of the movies was done using the MatScan software provided with the sensor.

Adaptation of the technology to match the loads imposed by large animals required several tests. The tests were necessary in order to obtain confidence in the accuracy of the sensor in converting raw data into standard force units that can be easily analyzed. Also, the tests were useful to predict the response of the sensor and the amount of hysterisis that the sensor displayed, if any, during loading and unloading of the same area many times.

This process consisted of several laboratory tests performed with the first sensor (861.8 KPa saturation pressure) using pieces of smooth wood blocks that represented the approximate average surface area (129 cm^2) under a hoof of a large Holstein cow. The piece of wood was loaded and unloaded with initially 889.6 N. The load was further increased to 300, 350, 1779, 2001, 2224 and 2446 N. Metal weights with increments of 222 N were used for the test. Several tests were conducted on different areas of the sensor with the same procedure. The same laboratory tests were performed using a second sensor (10.3 MPa saturation pressure). The first set of calibration tests performed with wooden blocks and predicted loads failed because they did not represent real loads and areas expected for a single limb of a cow (Figure 3-1).

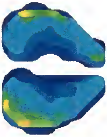

Figure 3-1. Footprint of simulated hoof using wooden blocks.

According to the manufacturer, to obtain optimal results in accuracy of the readings, the sensor should first be conditioned (break in) with the subject performing several walking trips across it. The next step was the correct calibration of the sensor, which was done individually for each subject. In order to do that, each subject should stand on the sensor and its known weight entered in the software's calibration process prior to each trial. This procedure assures the most accurate readings according to the user's manual. Nevertheless, one single calibration procedure can also be performed for collecting data from more than one subject with some degree of accuracy loss (user's manual).

To calibrate the sensor for working with cows, it was necessary to obtain the weight applied on a single foot with the cow standing on it. In order to do that, a force plate was designed specifically for this purpose. The force plate consisted of a metal plate base with four 1112 N load cells in each corner and a top metal plate supported only by the load cells that read the load. The top plate was first secured to the load cells with screws and free from any other contact. Next step was the calibration of the force plate for converting the voltage readings of the load cells into weight. The procedure was done using the same metal weights used previously for the Matscan calibration. A data logger was programmed for reading the voltage outputs and converting them into force values.

The first design presented a problem because when the plate was loaded and reloaded for the calibration, it would not maintain its initial zero value. This problem was due to an imbalance in placement of the load cells that caused it to accumulate different small torques when secured to the top plate. A new design was developed to mount the top plate so that it would move freely on top of load cell bolts in a manner resembling a ball and socket joint.

The new design required minimal modifications of the attachment of the top plate to the load cells. Four bolts were specially manufactured to go into the load cell attachment holes and had large round solid heads. The top plate had four holes, one in each corner, that were drilled in its bottom side in order to fit the four bolts.

The new modified design of the force plate is shown in Figure 3-2

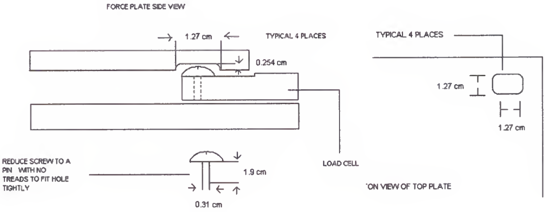

Figure 3-2. New design of the force plate with drilled spaces for bolts

The calibration using this new design was considered successful with readings matching the known loads measured with an industrial scale of 22,241 N maximum load. The calibration data was plotted and a regression fit, which gave a high correlation coefficient ($R^2 = 0.9998$).

A similar force plate on a larger scale was installed on a mobile cattle restraint chute to obtain the total weight of each cow. The total weights of the cows were used to normalize the forces obtained in the data collection process (express force as a % of body weight by dividing the forces by the total weight) to each cow's respective body weight and therefore make use of a more meaningful analysis.

This force plate was first calibrated using the same procedure for the small one but using loads up to 6672 N in drums filled with water. The force plate built on the restrain chute in the first calibration process is shown in Figure 3-3.

After the calibration tests with the force plates were concluded, the next step was to mount the Matscan sensor firmly to the small force plate and test the system.

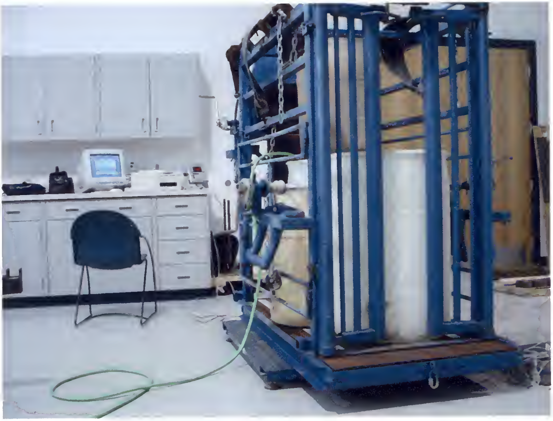

Figure 3-3. Restraint chute force plate

The best method for attaching both of them required that the sensor be glued to the force plate. The glue used for this purpose was silicone brand glue because it was easier to remove in case of damage to the sensor and the need for replacement. The sensor also needed to be glued in a manner that would not affect its readings by gluing its sensitive area. Therefore, according to the manufacturers recommendation, the sensor was glued only on its sides and the actual sensitive area remained free from the adhesive glue. In addition to the silicone glue, the sensor was taped with aluminum tape around the edges. The final attachment of the sensor to the force plate is shown in Figure 3-4.

Experimental Design

To analyze the pressure distribution on claws during the stance phase of a cow's walking stride, a wooden platform was built to house the force plate and Matscan system.

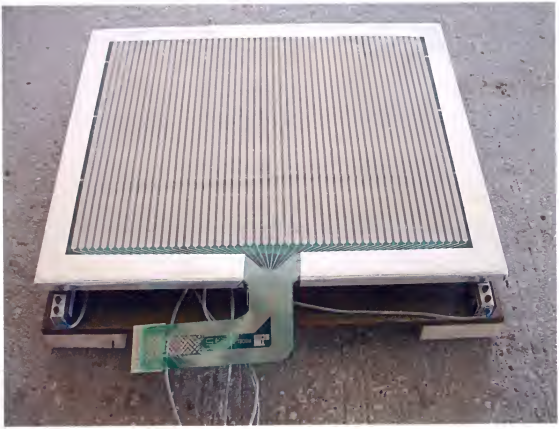

Figure 3-4. Matscan sensor attached to the Force plate

The wooden platform was designed with dimensions of 680 cm x 91 cm x 8.9 cm to fit inside a restraint corridor located in the feed animal barn (Building 216) of the Veterinary Medicine School Large Animal Clinical Sciences facilities.

The length of the platform was chosen according to the length of an average large Holstein cow (approximately 2.17 m) and to assure at least two complete strides before stepping onto the force/pressure system. The reason for that was to ensure a normal gait of the cow after having to step onto the wood platform with the embedded Matscan system.

In addition to the force-pressure system used for the weight bearing and pressure distribution analysis, a motion analysis system consisting of a digital video camera

(JVC GDR-120U – 30 Hz. 520 lines vertical resolution) placed at a distance of approximately at 6.7 m away from the plane of motion (wooden platform- force/pressure system section) was used for acquisition of 2D (two dimensional) video kinematics data. The camera was aligned on its vertical and horizontal axis and at a 90° angle from the plane of motion to record saggital plane kinematics of single stride during walking trips over the force-pressure system. The kinematics data provided spatial and temporal parameters of the cow's stride, angular range of motion of joints, displacement, velocities, acceleration of limbs, and aided in determining joint reaction forces with the camera synchronized with the pressure measurement system. Figure 3-5 and 3-6 and diagram in Figure 3-7 show the complete setup of the data acquisition system used for the experiment.

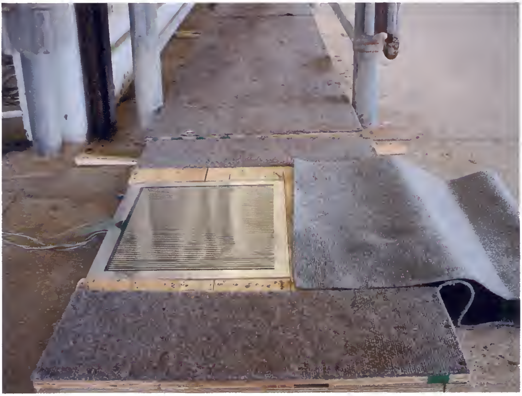

Figure 3-5 Force-pressure system mounted on the wooden platform

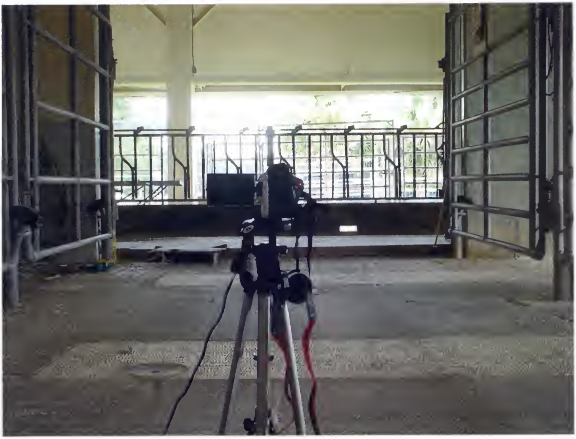

Figure 3-6. Digital video camera setup mounted at a distance from platform

The experiment consisted of 32 Holsteins cows divided into two groups: A – Balanced/Trimmed claws (Control) with 14 cows, and B – Unbalanced claws with 17 cows. All cows were obtained from the Dairy Research Unit (DRU) non-lactating herd. Data were collected during one month from June 5th to July 3rd of 2003. Five cows were transported from the DRU to the Veterinary Medicine Large Animal Clinical Sciences-Feed Animal Barn at a time on Mondays and Wednesdays. Un-trimmed group (17 cows) data collection started on 5th of June 2003 and lasted until the 26th of June 2003. The 14 cows belonging to the trimmed group were trimmed by Professor Jan K. Shearer (Veterinary Medicine School Large Animal Clinical Sciences Department. University of

Florida. Gainesville, FL) before starting the experiment every other day from 26 of June 2003 to 03 of July 2003. From trimming the cows, it was observed that their hooves were about 0.6cm overgrown in height at the heel and about 1.27cm to 1.9cm overgrown in length at the toe. Data on the un-trimmed group was not assessed, however they belonged to the same herd and therefore must have had similar degrees of overgrowth because they are trimmed at the same time (farm protocol). The average weight of the cows accounting for both groups was 6316.4 N.

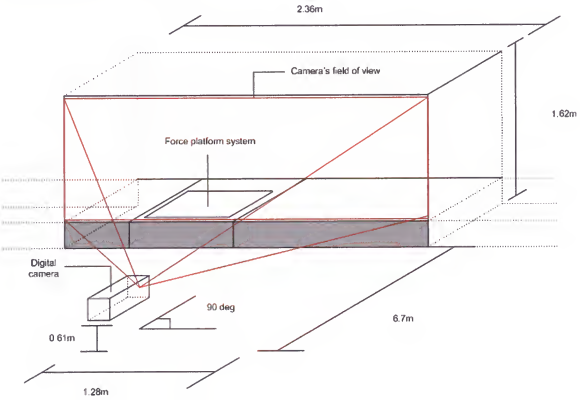

Figure 3-7. Video capture system and field of view diagram

After setting up the equipment, a single average large Holstein cow was brought to the platform and directed towards the sensor by an experienced handler until it stepped with a single foot (left front) on the sensor. The cow remained standing on top of the sensor for a few seconds until there was enough load on that leg and subsequently enough area for calibration. The weight on that limb was then read from the force plate display and entered into the calibration window of the Matscan software for calibration. The calibration took only a second after the process was started.

After the calibration was completed, the cow was released and the data collection started with the same cow walking back and forth on the platform without stopping until it eventually stepped on the sensor. Several walking trips per cow were necessary until there was at least one set of footprints recorded (one front foot and one back foot for that cow). Sometimes more than a set was obtained and in few cases it was possible to obtain footprints of all four feet of the same cow. The video data was collected simultaneously with each passage of a cow, recorded on the camera and downloaded afterwards into a PC using video editing software (Adobe® Premiere 6.5; Adobe Corporation®).

The Matscan software has limitations for research purposes. It does not allow manipulation of the images to correct for twisting of the foot on top of the mat as it strikes the ground or during the step. Another restriction is that it does not have any form of coordinate system or reference frame that allows the user to define the regions of interest proportionally for the different sizes and shapes of the pictures obtained. These problems complicated the analysis and comparison of pre-defined regions among a sample population, because there was no means to define the beginning and ending of a region. However, the Matscan software allows the use the raw or calibrated pressure data with other applications such as Excel.

In order to analyze the pressure under the regions, an Excel spreadsheet was designed and programmed with a coordinate system and predefined formulas for calculating the force under the one of the four proposed regions.

Pressure data can be entered into an Excel spreadsheet and the footprint displayed with the pressure values instead of color patterns. After that, the grid that corresponds to the footprint can be cut and dropped inside a grid containing a coordinate system with pre-defined formulas that calculates the forces under the regions of interest (analysis grid). The regions are pre-defined according to the following proportions:

Heel - 1/4 of the claw (longitudinally from heel to toe)

Sl (Sole lateral) - 2/4 of the claw (longitudinally from heel to toe) and 1/2 (vertically from abaxial wall to interdigital space)

Sm (Sole medial) - 2/4 of the claw (longitudinally from heel to toe) and 1/2 (vertically from abaxial wall to interdigital space)

Toe - 1/4 of the claw (longitudinally from heel to toe)

The division of the claws is shown below in Figure 3-8.

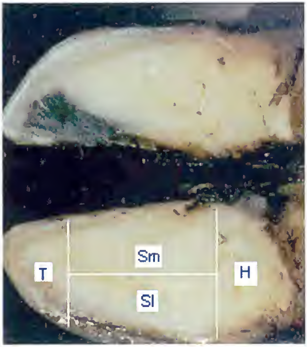

Figure 3-8. Claw divisions used in excel coordinate grid

The grid x – y coordinate is 17 cells in the y-axis by 16 cell in the x-axis. This dimension gives a horizontal proportion of 4 x 8 x 4 cells (1/4 x 2/4 x 1/4) in the x-axis and a vertical proportion of 4 x 4 cells (1/2 x 1/2) in the y-axis for the sole.

Heel and toe were well defined, in most of the cases, and visibly separated from each other on the vertical axis and did not need to be proportionally adjusted.

In many cases, due to gait patterns, where there was slight twisting of the foot during the step, the footprint was not oriented exactly with the line of motion's horizontal axis. When this was the case, an axis coordinate transformation was required in order for the regions to be well aligned and correctly calculated. A coordinate transformation matrix was developed in Excel that rotated the footprint to any angle (degrees) clockwise and counterclockwise in order to align the longitudinal axis of the foot (plus or minus the mid point between lateral and medial heel and lateral and medial toe) to the longitudinal axis (x –axis) of the Excel coordinate system. The diagram of the coordinate transformation algorithm is presented in Figure 3-9 and the Excel spreadsheet used to implement this is in Figures 3-10.

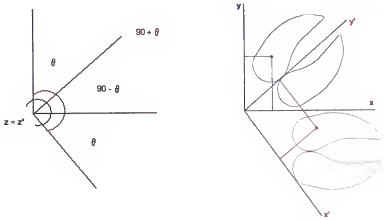

Figure 3-9. Coordinate transformation schematic

The on-plane coordinate transformation matrix in this case is:

$$[x , y] = \begin{array}{|ccc|c} x' & y' & z' & \\ \cos\theta & \cos(90-\theta) & 0 & x \\ \cos(90+\theta) & \cos\theta & 0 & y \\ 0 & 0 & 1 & z \end{array} = [x', y']$$

The calculation then becomes:

$$[\cos\theta * x] + [\cos(90-\theta) * y] = x' \tag{3-1}$$
$$[\cos\theta * y] + [\cos(90+\theta) * x] = y' \tag{3-2}$$

The four columns on the left hand side of the Figure 3-10 right below the blue row on top are the transformation matrix implemented and calculated according to the angle θ inputted in the green cell. To the left side of these columns are x and y original coordinates of the footprint captured. On the right hand side of the coordinate matrix columns are the calculated x' and y' coordinates for the pressure values that constituted the original picture. The result is presented by the two claw footprint images: before (left) and after (right).

A second adjustment may be necessary if the claw is larger or smaller than the dimensions of the analysis grid. In that case the regions needed to be adjusted to the size of that specific claw in order to maintain the same proportion. Adjusting the array of cells used by the formulas to calculate the regions does this. The arrays were adjusted proportionally to fit smaller claws or increased proportionally to fit larger claws. After these adjustments, the pressure values obtained for the regions were used for the analysis.

The gait kinematics data were obtained using the Human Movement Analysis Software (Hu-m-an™) developed by the HMA Technology Inc. – Ontario –Canada.

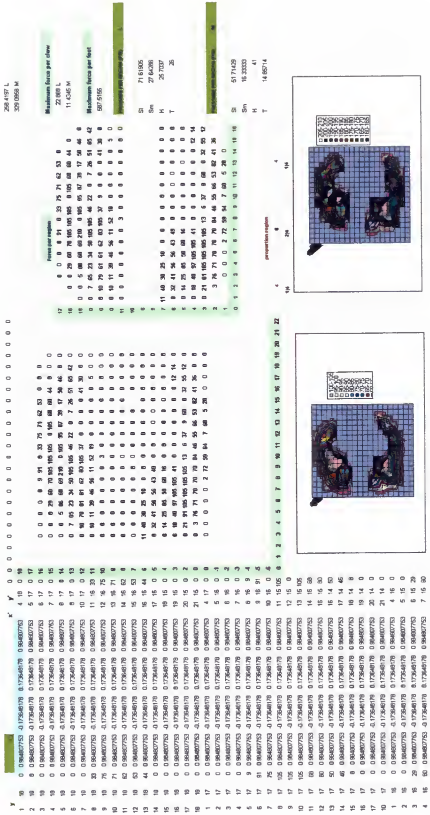

258.4197 L
309.0958 M

Maximum force per claw
22.869 L
11.4345 M

Maximum force per foot
587.5155

SI 71.61905
Sm 27.64286
H 25.7037
T 25

SI 51.71429
Sm 16.33333
H 41
T 14.85714

Figure 3-10. Claw footprint rotation and pressure analysis

The videos of the cows' strides on top of the force plate were loaded into the software and landmarks of the fetlock joint, pastern joint and foot were manually digitized in order to calculate fetlock joint flexion and extension ranges of samples of the two different groups (trimmed and un-trimmed).

The amount of frames recorded (± 30) and the displacements of the front and rear feet for a single stride in the clips of the cows were used to calculate spatial and temporal characteristics of each cow such as stride and step length, and stride and step times, respectively. In addition, velocities and accelerations can be obtained from the position of the feet landmarks and by applying a differentiation method. For simplicity and due to the large amount of data processing involved, only stride velocities were obtained by simple calculation of spatial and temporal characteristics of stride:

$$\text{Stride velocity} = \text{Stride length } (p_f - p_i) \,/\, \text{Stride time } (\Delta t) \tag{3-3}$$

Where:

p_f is the final position of the digitized midpoint of the foot at the beginning of the cycle,

p_i is the initial position of the digitized midpoint of the foot at the beginning of the gait cycle, and

Δt is the time elapsed during the gait cycle.

Statistical Analysis

Pressure

The statistical design used was a mixed model factorial design with two groups: A – Balanced claws (control) and B – Unbalanced claws. The arrangement used was 2 x 4 x 2 x 4. This represents: 2 groups of cows with 14 cows in group A and 21 cows in group B totaling 35 cows, 4 or less legs per cow (an average 2 legs per cow, one front and one rear), 2 claws per leg and 4 regions per claw yields 720 observations.

The SAS® V.8.2 was used for all the statistical analyzes, and the statistical design mentioned above was carried out using PROC MIXED at a default 95% confidence interval. The General Linear Model procedure PROC GLM was also used, and the ANOVA tables are presented in the results. This statistical design was supplied by Dr. Charles J. Wilcox (Professor Emeritus), geneticist from Animal Science Department – University of Florida.

The procedure tested the main fixed effects: Group (G), Leg (L), Claw (C) and Region (R) and their 2-way, 3-way and 4-way interactions:

G*L, G*C, L*C, G*L*C, G*R, L*R, G*L*R, C*R, G*C*R, L*C*R, G*L*C*R.

Some claws were discarded from the population sample because of noise to the consistency of footprint shape (abnormal shape). The two criteria used for discarding claw footprints were: First, because the conformation of the footprint represented a damaged claw, second: Some claws lacked their entire surface within the sensor measurement area. The resulting sample after discarding claws was 32 cows and 504 observations. These were used in subsequent statistical analyzes

Gait

For the gait kinematics, a simplification of the above design was used. A 2 x 4 mixed factorial (PROC MIXED) arranged with two groups, at least 2 legs (front and back) of each cow and 29 cows totaling 65 observations.

The model used in SAS accounted for the main effects G and L (group and leg respectively) and the 2-way interaction G*L.

CHAPTER 4
RESULTS AND DISCUSSION

Midstance Phase

The analysis performed with the reduced sample (32 cows, n = 504) of the original set of pressure values showed highly significant differences for claw (C) and region (R) main effects ($p < 0.0001$ for both effects). The 2-way interactions G*C were significant and C*R was highly significant ($p < 0.0165$ and $p< 0.0004$ respectively). The 3-way interaction G*L*C, tended to be significant ($p < 0.0825$) and L*C*R was highly significant ($p < .0001$). The above significance levels were obtained with PROC MIXED. The ANOVA table obtained using PROC GLM is Table 4-1.

Table 4-1. ANOVA table for midstance (original set).

Source	DF	SSQ	MSQ	F value	Pr > F
Model	353	306883.4047	869.3581	3.85	<.0001
Error	150	33831.6539	225.5444		
Corr. total	503	340715.0586			

R-Square	Coeff. Var	Root MSE	Y mean
0.900704	39.21913	15.01813	38.29288

➲ Values are based on PSI

The Type III SS for the interaction terms are presented in Table 4-2. Table 4-2 fixed main effects (C) and (R), and fixed interaction terms (G*C), (G*L*C), (C*R), (G*C*R) and (L*C*R) were statistically significant.

Table 4-2. Type III SS for midstance (original set).

Source	DF	Type III SS	Mean square	F value	Pr > F
Group (G)	1	33288.11577	33288.11577	147.59	<.0001
Animal (A)(G)	30	67040.37045	2234.67901	9.91	<.0001
Leg (L)	3	765.04074	255.01358	1.13	0.3387
G*L	3	964.25626	321.41875	1.43	0.2377
A*L(G)	25	4086.95313	163.47813	0.72	0.8255
Claw (C)	1	17997.49996	17997.49996	79.8	<.0001
G*C	1	2716.71215	2716.71215	12.05	0.0007
A*C(G)	30	12444.23698	414.8079	1.84	0.0093
L*C	3	751.16549	250.3885	1.11	0.347
G*L*C	3	2319.77396	773.25799	3.43	0.0187
A*L*C(G)	25	5471.95752	218.8783	0.97	0.5098
Region (R)	3	47575.66668	15858.55556	70.31	<.0001
G*R	3	1431.18396	477.06132	2.12	0.1007
A*R(G)	90	32982.51895	366.47243	1.62	0.0043
L*R	9	1162.60981	129.17887	0.57	0.8179
G*L*R	9	1892.43153	210.27017	0.93	0.499
C*R	3	4368.705	1456.235	6.46	0.0004
G*C*R	3	2207.98088	735.99363	3.26	0.0232
A*C*R(G)	90	21521.54414	239.12827	1.06	0.3722
L*C*R	9	7004.93074	778.32564	3.45	0.0007
G*L*C*R	9	3062.07609	340.23068	1.51	0.1497

➲ Values are based on PSI

Figures 4-1 to 4-5 summarizes the trends found for region (R) main effect, 2-way and 3-way interactions G*C, G*L*C, C*R and G*C*R using PROC MIXED (SAS ®).

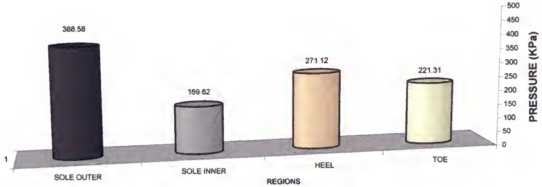

Figure 4-1. Main effect region (R) (midstance) LSMeans (original set)

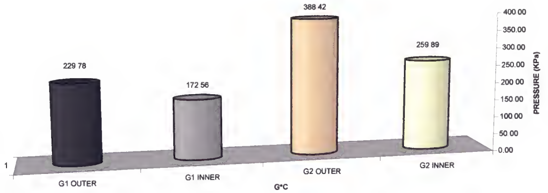

Figure 4-2. Group*Claw (G*C) interaction (Midstance original set)

Orthogonal contrasts for the main effect region (R) detected significant differences between the four regions tested. Orthogonal contrasts for main effect (R) and the 2-way interactions (G*C) and (C*R) are presented in Table 4-3.

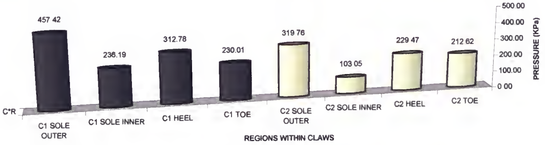

Figure 4-3. Claw*Region (G*R) interaction (Midstance original set)

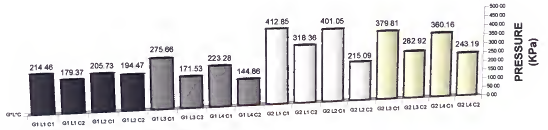

Figure 4-4. Group*Leg*Claw (G*L*C) interaction (Midstance original set)

In Figure 4-3, Claw vs. Region (C*R) LSMeans, there seems to be an average greater pressure concentration applied on sole lateral (R1) and Heel (R3) on the lateral claw (C1) whereas the medial claw (C2) the average pressures are more evenly concentrated on regions 1,3, and 4 (sole lateral, heel and toe). Sole medial (R2) consistently shows a smaller average pressure concentration for the two claws.

Table 4-3. Original set orthogonal contrasts for region (R) main effect and 2-way interactions (G*C) and (C*R) (midstance)

Contrast	Estimate	SE	DF	T value	Pr > |t|
Region (R)					
1 vs. 2, 3, 4	73.98	6.45	90	11.47	0.0001
2 vs 3, 4	-21.79	4.56	90	-4.78	0.0001
3 vs 4	7.21	2.63	90	2.74	0.0074
G*C					
G 1,2 vs C 1,2	-10.02	3.89	25	-2.57	0.0165
C*R					
C 1,2 vs R 2,4	9.34	4.25	90	2.19	0.03

In Figure 4-4, Group 2 (G2 – trimmed/balanced) appeared to have a consistent greater average pressure on the lateral claw (C1) in all four legs (L1, L2, L3 and L4), rather than only for the rear legs (L3 and L4) as shown by the un-trimmed/unbalanced group (G1). The front legs (L1 and L2) in group 1 (G1) appeared to have a similar average pressure for lateral and medial claws.

Group vs. claw vs. region (G*C*R) interaction (Figure 4-5), indicated a slightly better average pressure distribution for group 2 (trimmed/balanced) on the lateral claw (C1) among regions 2, 3, and 4 in a general form accounting for the four legs.

This trend is desired for trimmed claws and the greater the equalizing of average pressure among the regions of a claw the greater is the amount of balancing obtained. However, Orthogonal contrasts were not performed for any of the 3-way interaction levels. The significance levels were obtained using PROC MIXED type 3 tests of fixed effects only.

The same set of pressure data on the four regions, but normalized to total pressure applied in a given claw, was used under the same model design as previously. The General Linear Model ANOVA table and Type III SS are presented in Table 4-.4 and Table 4-5 respectively.

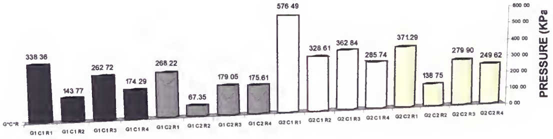

Figure 4-5. Group*Claw*Region (G*C*R) (Midstance original set)

Normalizing pressures to the total pressure (expressed as a percentage (%) by dividing the pressure at a given region by the total pressure applied on that claw), was performed in order to accommodate the results to the differences in cow weights and therefore the maximum pressures applied. Velocity of walking is another factor. Cows walking faster have greater force components (given by $F = m * a$) and not necessarily an increase in surface area (A) resulting in greater pressures ($P = F/A$) and differences due to this may influence some interpretation of the results.

For the normalized analysis, region is the factor that is normalized. Therefore, only region main effect and the 2, 3 and higher level 4- way interactions with respect to region have any importance.

Main effect region (R) was highly significant ($p < 0.0001$) and is shown in Figure 4-6. Interactions G*R ($p < 0.0266$) Figure 4-7, L*R ($p < 0.0305$), C*R ($p < 0.0001$) highly significant (Figure 4-8), G*L*R ($p < 0.0043$) highly significant (Figure 4-9 and

4-10), L*C*R ($p < 0.0001$) highly significant, and G*L*C*R ($p < 0.0465$) (Figures 4-11 to 4-18). The ANOVA table and Type III SS for this particular analysis is presented in Tables 4-4 and 4-5 respectively.

Table 4-4. ANOVA table for midstance (normalized set).

Source	DF	SSQ	MSQ	F value	Pr > F
Model	353	67749.44169	191.92476	2.08	<.0001
Error	150	13836.67602	92.24451		
Corr. Total	503	81586.1177			
R-Square	Coeff. Var	Root MSE	Y mean		
0.830404	38.32671	9.6044	25.05929		

➲ Values are based on PSI

Table 4-5. Type III SS for midstance (normalized set).

Source	DF	Type III SS	Mean square	F value	Pr > F
Group	1	5.16824	5.16824	0.06	0.8132
Animal (A)(G)	30	122.83909	4.09464	0.04	1
Leg (L)	3	0.10131	0.03377	0	1
G*L	3	0.10143	0.03381	0	1
A*L(G)	25	0.84802	0.03392	0	1
Claw (C)	1	4.94084	4.94084	0.05	0.8173
G*C	1	5.08223	5.08223	0.06	0.8147
A*C(G)	30	122.83909	4.09464	0.04	1
L*C	3	0.10131	0.03377	0	1
G*L*C	3	0.10143	0.03381	0	1
A*L*C(G)	25	0.84802	0.03392	0	1
Region (R)	3	22284.22085	7428.07362	80.53	<.0001
G*R	3	778.58426	259.52809	2.81	0.0413
A*R(G)	90	14053.54439	156.15049	1.69	0.0022
L*R	9	643.0656	71.45173	0.77	0.6401
G*L*R	9	1012.13718	112.45969	1.22	0.2873
C*R	3	1998.40393	666.13464	7.22	0.0001
G*C*R	3	204.92765	68.30922	0.74	0.5295
A*C*R(G)	90	6982.39394	77.58215	0.84	0.8141
L*C*R	9	3242.64612	360.29401	3.91	0.0002
G*L*C*R	9	1221.47154	135.71906	1.47	0.1634

➲ Values are based on PSI

Orthogonal contrasts performed for regions (R) were also significant in this analysis and for the 2-way interaction (C*R) was significant between region 2 (medial sole) and region 4 (toe). Orthogonal contrasts are presented in Table 4-6.

Table 4-6. Normalized set orthogonal contrasts for region (R) main effect (midstance)

Contrast	Estimate	SE	DF	T value	Pr > |t|
Region (R)					
1 vs. 2, 3, 4	73.98	6.45	90	11.47	0.0001
2 vs 3, 4	-21.79	4.56	90	-4.78	0.0001
3 vs 4	7.21	2.63	90	2.74	0.0254
C*R					
C 1,2 vs R 2,4	9.34	4.25	90	2.19	0.0007

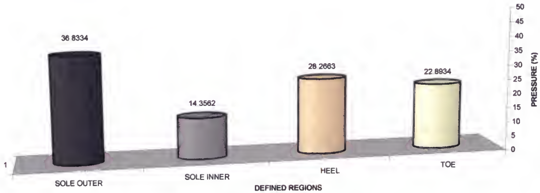

Figure 4-6. Main effect region (R) (midstance normalized set)

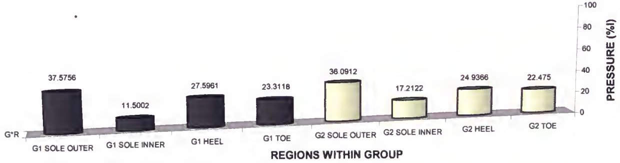

Figure 4-7. Group*Region (G*R) (Midstance normalized set)

The normalized LSMeans for the main effect region (R) displayed a similar pressure distribution over the four regions, to the original set of pressure values.

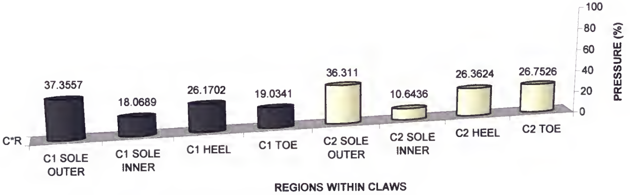

Figure 4-8. Claw*Region (G*R) (Midstance normalized set)

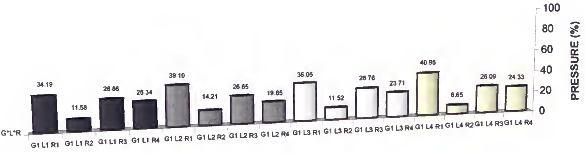

Figure 4-9. Group*Leg*Region (G*L*R) (G1) (Midstance normalized set)

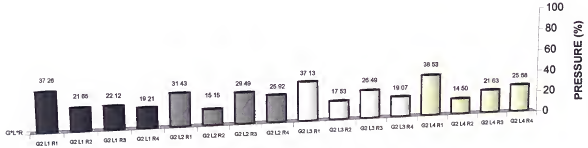

Figure 4-10 . Group*Leg*Region (G*L*R) (G2) (Midstance normalized set)

In Figure 4-7, Group vs. region interaction, the trimmed group (G2) pressure distribution appeared to have a slight reduction of the pressures applied to the regions of the heel (R4) and toe (R3) and the medial portion of the sole (R2) appears to be taking up these loads. Similarly with Figure 4-5, this trend tend to indicate a small regain of balance. The 3-way interaction G*L*R (Figure 4-9 and 4-10) provides a better comparison by visualization of the two groups because it has the effects of the four limbs and the higher level 4 – way interaction (Figures 4-11 to 4-18, below) provide visual trends that the major changes of trimming occur on the lateral claws of front and rear limbs. As it was shown with G*R interaction (Figure 4-7), the heel region on the lateral claws was the most affected by trimming. Its pressure concentration appeared to be reduced and transferred mostly to the medial sole (R2).

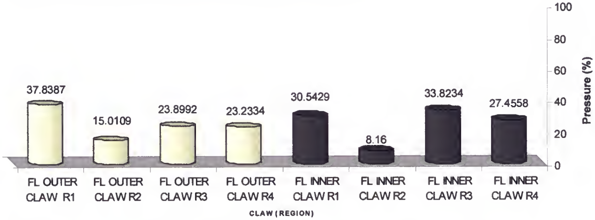

Figure 4-11. Front left leg G*L*C*R interaction (G1) normalized set LSMeans (midstance)

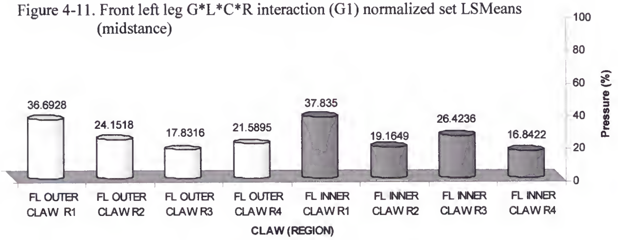

Figure 4-12. Front left leg G*L*C*R interaction (G2) normalized set LSMeans (midstance)

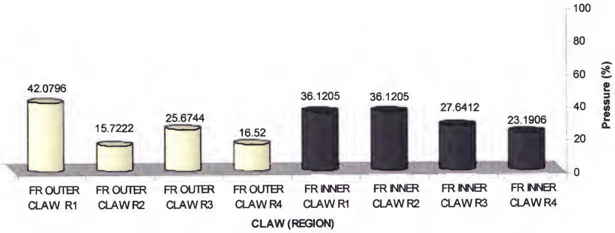

Figure 4-13. Front right leg G*L*C*R interaction (G1) normalized set LSMeans (midstance)

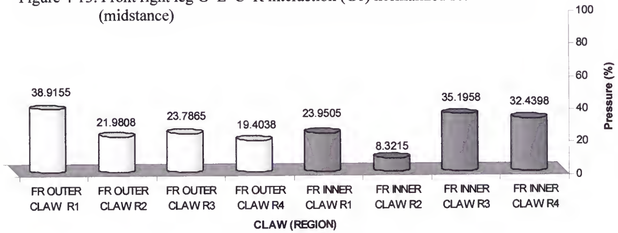

Figure 4-14. Front right leg G*L*C*R interaction (G2) normalized set LSMeans (midstance)

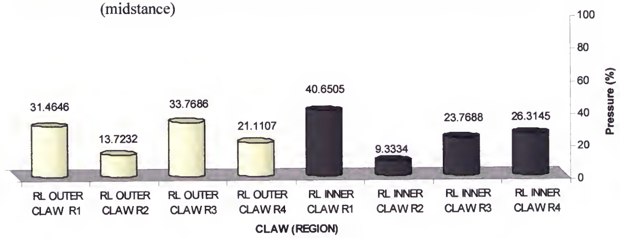

Figure 4-15. Rear left leg G*L*C*R interaction (G1) normalized set LSMeans (midstance)

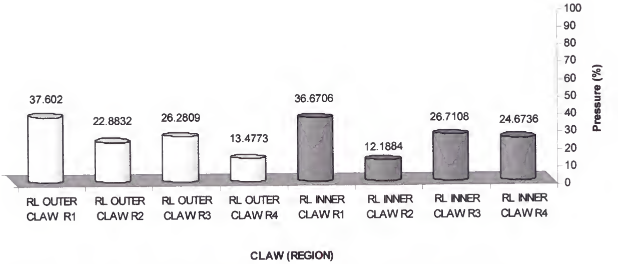

Figure 4-16. Rear left leg G*L*C*R interaction (G2) normalized set LSMeans (midstance)

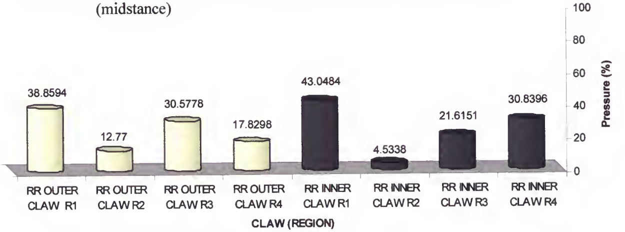

Figure 4-17. Rear right leg G*L*C*R interaction (G1) normalized set LSMeans (midstance)

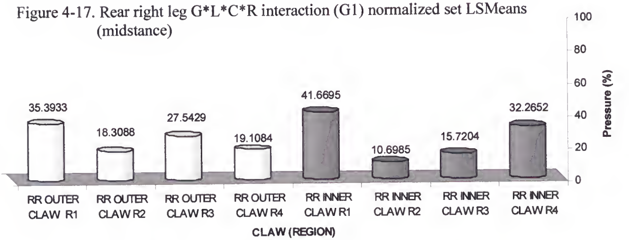

Figure 4-18. Rear right leg G*L*C*R interaction (G2) normalized set LSMeans (midstance)

The average reduction in pressure concentration on the heel area after trimming was about 5% of the total pressure applied on the lateral claws whereas the medial sole area had an increase of 7.5% of the total applied on the lateral claws. The average total pressure applied on the lateral claw of the un-trimmed group was 929.4±117.5 KPa. The average total pressure applied on the heel of the lateral claws was 262.7±29.4 KPa and the medial sole was 143.75±29.4 KPa (118.93±29.4 KPa difference). The average total pressure applied on the lateral claws of the trimmed group was 1577.52±129.2 KPa. The heel region average total pressure was 361.97±32.3 KPa and the medial sole had a total average pressure of 323.36±32.3 KPa (38.61±32.3 KPa difference). Orthogonal contrasts were not performed for the 3-way and 4-way higher interaction levels and the trends presented for this analysis are expeculation from visual observation of the graphs obtained with PROC MIXED LSMeans.

Loading Response Phase

The analysis performed with the original untransformed data for the Loading response (LR) point of the stance using PROC MIXED (SAS®) presented the following significant levels characteristics: Main factors G, L, C and R were all highly significant ($P < 0.0004$, 0.0003, 0.0001 and 0.0001 respectively).

The 2-way interaction levels G*C, G*R and C*R were highly significant and significant respectively ($p < 0.0017$, $p < 0.0405$ and $p < 0.0009$). The 3-way interaction level G*L*R was the only significant interaction on this order ($p < 0.0639$). The 4-way interaction level G*L*C*R was significant in this point of stance phase as well ($p < 0.0436$). The ANOVA table for this analysis is presented in Table 4-7.

Table 4-7. ANOVA table for loading response (original set)

Source	DF	SSQ	MSQ	F value	Pr > F
Model	355	330622.648	931.3314	5.71	<.0001
Error	156	25432.6883	163.0301		
Corr. Tot	511	356055.3363			
R-Square	Coeff. Var	Root MSE	Y mean		
0.928571	35.98352	12.76832	35.4838		

➲ Values are based on PSI

Table 4-8. Type III SS for loading response (original set).

Source	DF	Type III SS	Mean square	F value	Pr > F
G	1	28415.05	28415.05	174.29	<.0001
A(G)	30	57341.59	1911.386	11.72	<.0001
L	3	4155.456	1385.152	8.5	<.0001
G*L	3	1242.59	414.1968	2.54	0.0585
A*L(G)	26	3213.078	123.5799	0.76	0.7938
C	1	24322.17	24322.17	149.19	<.0001
G*C	1	5526.88	5526.88	33.9	<.0001
A*C(G)	30	13545.63	451.521	2.77	<.0001
L*C	3	2336.827	778.9422	4.78	0.0033
G*L*C	3	119.487	39.82901	0.24	0.8653
A*L*C(G)	26	2906.973	111.8067	0.69	0.8702
R	3	62411.48	20803.83	127.61	<.0001
G*R	3	2714.349	904.783	5.55	0.0012
A*R(G)	90	39650.07	440.5563	2.7	<.0001
L*R	9	1402.692	155.8547	0.96	0.4787
G*L*R	9	2031.729	225.7477	1.38	0.1993
C*R	3	3646.005	1215.335	7.45	0.0001
G*C*R	3	1036.339	345.4462	2.12	0.1
A*C*R(G)	90	23723.13	263.5903	1.62	0.0044
L*C*R	9	6063.83	673.7589	4.13	<.0001
G*L*C*R	9	1738.152	193.128	1.18	0.3084

➲ Values are based on PSI

The following figures indicate the most important trends for this analysis according to PROC MIXED (SAS®) type 3 test for fixed effects. Their important details will be emphasized individually based on visual observation of LSMeans plots. Main factor region (R) is presented in Figure 4-19.

The region LSMeans for the entire sample population in this particular moment of the stride did not have any significant changes in the loading of the regions when compared to midstance analysis. The regions at LR are still being loaded in the same proportion as Midstance. The same can be observed for the (G*C) interaction presented in Figure 4-20.

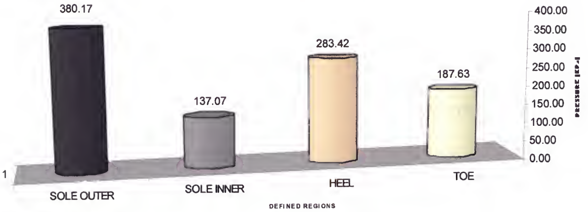

Figure 4-19. Main effect region (R) (loading response original set)

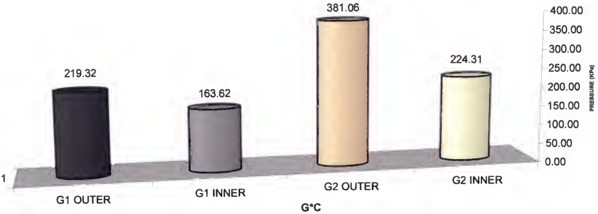

Figure 4-20. Group*Claw (G*C) (loading response original set)

Orthogonal contrasts for the significant main factors L and R and for the 2-way interaction factors, (G*C) and (C*R) are presented in Table 4-9. Some of the orthogonal contrasts tested were not estimable by PROC MIXED (SAS®) and were not included.

Table 4-9. Original set orthogonal contrasts for region (R) and leg (L) main effects and 2-way interactions (G*C) and (C*R) (loading response)

Contrast	Estimate	SE	DF	T value	Pr > |t|
Region (R)					
1 vs. 2, 3, 4	77.216	6.9292	90	11.14	<.0001
2 vs 3, 4	-28.5596	4.8997	90	-5.83	<.0001
3 vs 4	13.8932	2.8288	90	4.91	<.0001
Leg (L)					
1 vs. 2, 3, 4	-2.8299	4.8871	26	-0.58	0.5675
2 vs 3, 4	-15.6925	3.0504	26	-5.14	<.0001
3 vs 4	0.7272	1.9583	26	0.37	0.7134
G*C					
G 1,2 vs C 1,2	-14.6565	4.1976	26	-3.49	0.0017
C*R					
C 1,2 vs R 2,4	7.4095	4.3825	90	1.69	0.0944

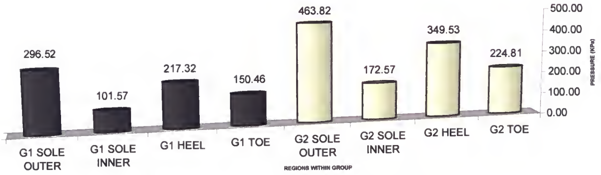

Figure 4-21. Group*Region (G*R) (loading response original set)

For the G*R interaction, heel and sole lateral are the regions that hold greater pressure concentration. Because of the negative acceleration at the moment of braking impulse caused by the slope of the longitudinal axis of the leg and a certain degree of dorsiflexion of the foot at heel strike, it would be expected that the heel region would carry the major pressures as opposed to lateral sole. However, loading response (LR) is not the same as heel strike. In LR most of the impulse breaking force is transferred to the front of the foot and the slope of the longitudinal axis of the leg and dorsiflexion of the foot are not as steep as in heel strike. The results may indicate that cow's normal gait at heel strike may be flat-foot, that is, it hits the ground with most of the foot surface rather than heel only like most humans.

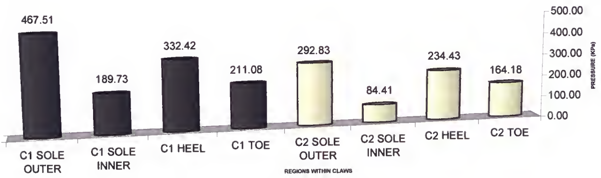

Figure 4-22. Claw*Region (C*R) (loading response original set)

In Figure 4-22, there seem to be no major changes in the concentration of the pressures compared to the midstance analysis. Heel and lateral sole still shows the majority of the pressures. It can be noticed, however, that heel may be slightly more loaded than toe as compared to Midstance. In Midstance, heel and toe differed with 82.7 KPa for the outer claw and only 17.23 KPa for the inner claw. In loading response, these differences accounted for 124.1 Kpa for the outer claw and slightly over 68.94 Kpa for the inner claw. The 3–way interaction G*L*R is summarized in Figures 4-23 and 4-24.

The pressure magnitude seemed to be the only factor that really changed between groups for the 3-way interaction G*L*R. The distribution of the total pressure among the 4 regions of interest seemed to have similar proportions. A better visualization of this can be seen by the transformed (normalized pressures) analysis that presented the same trend for that interaction and will be shown in the next set of results in Figures 4-25 and 4-26.

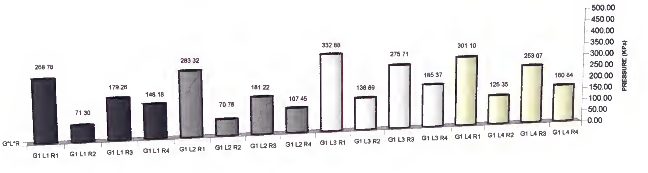

Figure 4-23. Group*Leg*Region (G*L*R) (G1) (loading response original set)

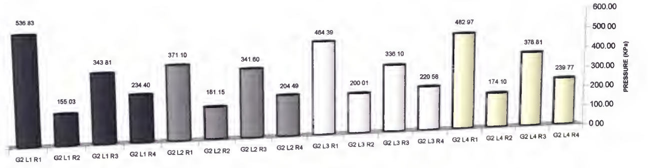

Figure 4-24. . Group*Leg*Region (G*L*R) (G2) (loading response original set)

The only three interactions that were significant for the set of normalized pressures were: the 2-way interaction C*R ($p < 0.0003$), the 3-way interaction G*L*R ($p < 0.00172$) and the 4-way interaction G*L*C*R ($p < 0.0033$). The significant levels were obtained with PROC MIXED (SAS®).The ANOVA table and the Type III SS table, obtained with PROC GLM (SAS®), for this set is presented on Tables 4-10 and 4-11.

Orthogonal contrasts for main effect region (R) in this analysis was significant for all the comparisons across regions (Table 4-12).

Table 4-10. ANOVA table for loading response (normalized set)

Source	DF	SSQ	MSQ	F value	Pr > F
Model	355	89520.7111	252.171	3.04	<.0001
Error	156	12942.9093	82.9674		
Corr. total	511	102463.6204			
R-Square	Coeff. Var	Root MSE	Y mean		
0.873683	36.42094	9.108642	25.00936		

➲ Values are based on PSI

Table 4-11. Type III SS for loading response (normalized set)

Source	DF	SSQ	MSQ	F value	Pr > F
G	1	0.66367	0.66367	0.01	0.9288
A(G)	30	3.70358	0.12345	0	1
L	3	7.16623	2.38874	0.03	0.9934
G*L	3	7.11533	2.37178	0.03	0.9935
A*L(G)	26	54.42768	2.09337	0.03	1
C	1	0.27133	0.27133	0	0.9545
G*C	1	0.28544	0.28544	0	0.9533
A*C(G)	30	11.97614	0.3992	0	1
L*C	3	1.01958	0.33986	0	0.9996
G*L*C	3	1.01449	0.33816	0	0.9996
A*L*C(G)	26	11.50422	0.44247	0.01	1
R	3	34286.85	11428.95	137.75	<.0001
G*R	3	93.64818	31.21606	0.38	0.7703
A*R(G)	90	22247.36	247.1929	2.98	<.0001
L*R	9	699.6074	77.73415	0.94	0.4949
G*L*R	9	956.1562	106.2396	1.28	0.2515
C*R	3	1029.519	343.1731	4.14	0.0075
G*C*R	3	402.4073	134.1358	1.62	0.1877
A*C*R(G)	90	9785.454	108.7273	1.31	0.0703
L*C*R	9	2888.621	320.9579	3.87	0.0002
G*L*C*R	9	1110.543	123.3936	1.49	0.157

➲ Values are based on PSI

Table 4-12. Normalized set orthogonal contrasts for region (R) main effect (loading response)

Contrast	Estimate	SE	DF	T value	Pr > |t|
Region (R)					
1 vs. 2, 3, 4	53.4419	4.52	90	11.82	<.0001
2 vs 3, 4	-26.1276	3.1962	90	-8.17	<.0001
3 vs 4	8.9684	1.8453	90	4.86	<.0001

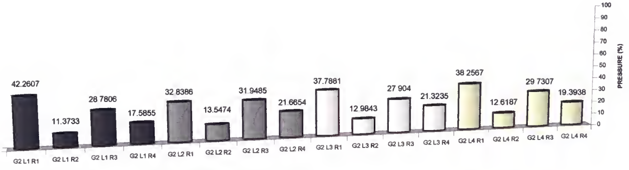

Figure 4-25. Group*Leg*Region (G*L*R) (G2) (loading response normalized set)

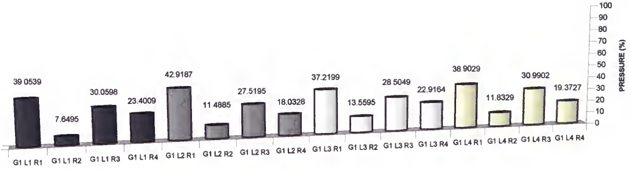

Figure 4-26. Group*Leg*Region (G*L*R) (G1) (loading response normalized set)

Push-off Phase

The analysis performed with the original data for the Push-off (PUSHOFF) phase of the stance using PROC MIXED (SAS®) presented the following significant levels characteristics: Main factors (G) and (R) were highly significant ($p < 0.0002$, and $p < 0.0001$ respectively). The 2-way interaction (G*R) was significant ($p < 0.0581$) and the only significant 3-way interaction was G*L*R ($p < 0.0262$). The 4-way interaction G*L*C*R was not significant ($p < 0.6172$).

Tables 4-13 and 4-14 present the ANOVA and Type III SS overall statistical results obtained for this analysis using PROC GLM (SAS®).

Table 4-13. ANOVA table for push-off (original set)

Source	DF	SSQ	MSQ	F value	Pr > F
Model	355	263535.7506	742.3542	2.93	<.0001
Error	156	39457.5921	252.9333		
Corr. Total	511	302993.3427			
R-Square	Coeff. Var	Root MSE	Y mean		
0.869774	46.61079	15.90388	34.12059		

➲ Values are based on PSI

Table 4-14. Type III SS for push-off (original set)

Source	DF	SSQ	MSQ	F value	Pr > F
G	1	28293.68	28293.68	111.86	<.0001
A(G)	30	51243.82	1708.127	6.75	<.0001
L	3	804.4754	268.1585	1.06	0.3678
G*L	3	2880.559	960.1865	3.8	0.0116
A*L(G)	26	5535.672	212.9104	0.84	0.6878
C	1	1517.93	1517.93	6	0.0154
G*C	1	560.0873	560.0873	2.21	0.1387
A*C(G)	30	18670.4	622.3467	2.46	0.0002
L*C	3	1012.034	337.3447	1.33	0.2655
G*L*C	3	2159.237	719.7455	2.85	0.0395
A*L*C(G)	26	20340.57	782.3295	3.09	<.0001
R	3	39944.24	13314.75	52.64	<.0001
G*R	3	1453.134	484.378	1.92	0.1294
A*R(G)	90	25264.74	280.7193	1.11	0.2827
L*R	9	1972.514	219.1682	0.87	0.5566
G*L*R	9	2796.165	310.685	1.23	0.2814
C*R	3	198.976	66.32534	0.26	0.8525
G*C*R	3	491.6037	163.8679	0.65	0.5854
A*C*R(G)	90	26843.25	298.2583	1.18	0.1837
L*C*R	9	2422.47	269.1634	1.06	0.3923
G*L*C*R	9	2215.191	246.1323	0.97	0.4644

➲ Values are based on PSI

The graph of LSMeans for the region (R) main effect (Figure 4-27) shows clearly the transference of the forces to the toe region (R4) as the stride progresses into push-off phase. Figure 4-28 shows the 2-way G*C significant interaction and Figure 4-29 shows the 2-way (G*R) significant interaction.

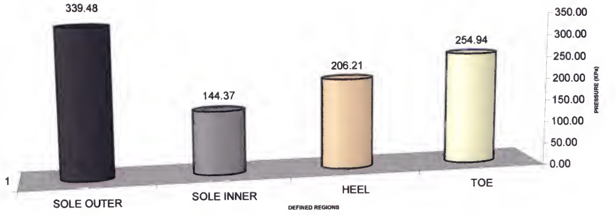

Figure 4-27. Main effect region (R) (push-off original set)

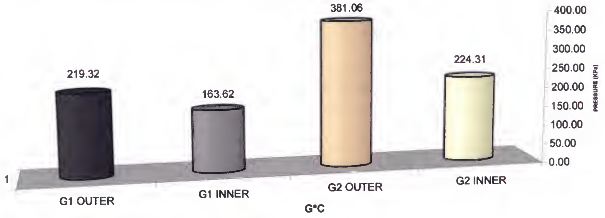

Figure 4-28. Group*Claw (G*C) (push-off original set)

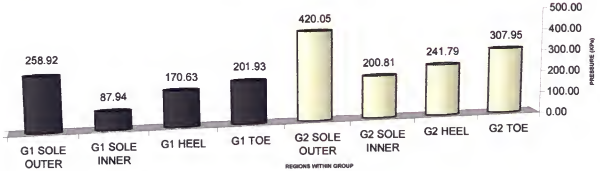

Figure 4-29. Group*Region (G*R) (push-off original set)

Orthogonal contrasts for the main effect region (R) was significant for all comparisons across regions. The 2-way significant interaction (G*R) was not significant.

Orthogonal contrasts for this analysis obtained with PROC MIXED (SAS®) are presented in Table 4-15.

Table 4-15. Original set orthogonal contrasts for region (R) main effects (push-off)

Contrast	Estimate	SE	DF	T value	Pr > |t|
Region (R)					
1 vs. 2, 3, 4	59.8887	5.7872	90	10.35	<.0001
2 vs 3, 4	-25.0062	4.0922	90	-6.11	<.0001
3 vs 4	-7.0677	2.3626	90	-2.99	0.0036

In Figure 4-29, trimmed cows (G2) medial sole (R2) presents the same trend that has been consistently shown in the other points of the stance phase, that is, an approximation to the pressures of the heel (R3) and toe (R4) and hence, a slight better balance of the claws after trimming them.

The 3-way interaction G*L*R shows that front legs at push-off load more the sole lateral and toe region and rear legs on the contrary load more consistently sole lateral and heel for the un-trimmed group. Trimmed cows consistently load more the sole lateral (R1) and toe (R4) region irrespective of the legs. This interaction is presented in Figures 4-30 and 4-31

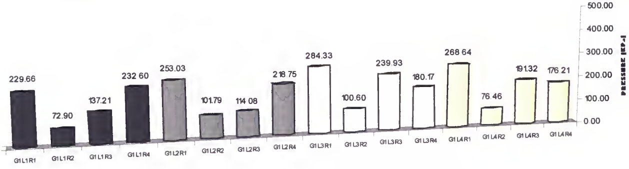

Figure 4-30. Group*Leg*Region (G*L*R) (G1) (push-off original set)

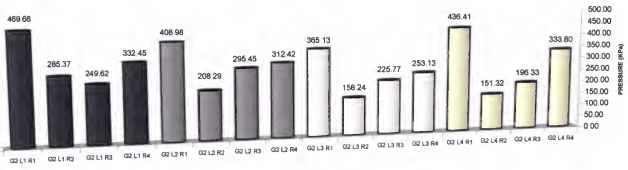

Figure 4-31. Group*Leg*Region (G*L*R) (G2) (push-off original set)

The analysis performed with the normalized data for the Push-off (PUSHOFF) phase of the stance using PROC MIXED (SAS®) presented the following significant levels characteristics: Main factor R was highly significant (P < 0.0001). The 2-way interaction G*R was once again the only significant interaction (p < 0.0205) and the only significant 3-way interaction was G*L*R (p < 0.0016). The 4-way interaction G*L*C*R was significant (p < 0.0452).

Tables 4-16 and 4-17 present the ANOVA table and Type III SS overall statistical results for this analysis obtained using PROC GLM (SAS ®).

Table 4-16. ANOVA table for push-off (normalized set)

Source	DF	SSQ	MSQ	F value	Pr > F
Model	355	88213.1872	248.4879	1.51	0.0016
Error	156	25619.1004	164.225		
Corr. Total	511	113832.2876			
R-Square	Coeff. Var	Root MSE	Y mean		
0.77494	51.15757	12.81503	25.05012		

➲ Values are based on PSI

Table 4-17. Type III SS for push-off (normalized set)

Source	DF	SSQ	MSQ	F value	Pr > F
G	1	1.31766	1.31766	0.01	0.9287
A(G)	30	38.2727	1.27576	0.01	1
L	3	3.18202	1.06067	0.01	0.9993
G*L	3	3.18569	1.0619	0.01	0.9993
A*L(G)	26	34.88162	1.3416	0.01	1
C	1	5.36209	5.36209	0.03	0.8568
G*C	1	5.7123	5.7123	0.03	0.8523
A*C(G)	30	165.9192	5.53064	0.03	1
L*C	3	13.79464	4.59821	0.03	0.9937
G*L*C	3	13.81055	4.60352	0.03	0.9936
A*L*C(G)	26	151.2182	5.81608	0.04	1
R	3	28393.89	9464.629	57.63	<.0001
G*R	3	637.2739	212.4246	1.29	0.2787
A*R(G)	90	16070.07	178.5563	1.09	0.3212
L*R	9	1196.223	132.9137	0.81	0.6083
G*L*R	9	2020.595	224.5106	1.37	0.2074
C*R	3	118.4825	39.49415	0.24	0.868
G*C*R	3	133.7307	44.5769	0.27	0.8459
A*C*R(G)	90	17868.32	198.5368	1.21	0.1501
L*C*R	9	2581.919	286.8799	1.75	0.0828
G*L*C*R	9	2657.673	295.297	1.8	0.0726

➲ Values are based on PSI

The LSMeans for the region (R) main effect is presented in Figure 4-32. Figure 4-32, similarly to Figure 4-27 (original set), also shows that the forces are transferred to toe region (R4) as the stride progresses into push-off phase. Figure 4-33 shows the 2-way significant interaction (G*R).

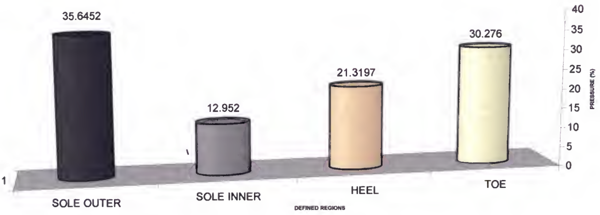

Figure 4-32. Main effect region (R) (push-off normalized set)

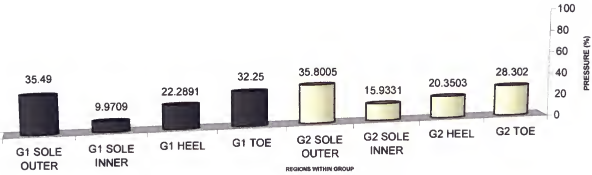

Figure 4-33. Group*Region (G*R) (push-off normalized set)

Orthogonal contrasts (PROC MIXED (SAS®)) for this analysis showed significant differences across regions (R) only. There was no significances for any other main effect or the tested 2-way interactions. Table 4-18 present the significant differences across regions obtained with the orthogonal contrasts.

Table 4-18. Normalized set orthogonal contrasts for region (R) main effect (push-off)

Contrast	Estimate	SE	DF	T value	Pr > |t|
Region (R)					
1 vs. 2, 3, 4	42.388	4.0053	90	10.58	<.0001
2 vs 3, 4	-25.6917	2.8322	90	-9.07	<.0001
3 vs 4	-8.9562	1.6352	90	-5.48	<.0001

Group vs. Leg vs. Region interaction (G*L*R) is summarized in Figures 4-34 and 4-35. As the pressure value analysis presented, un-trimmed cows front legs loaded more the sole lateral and toe region and rear legs loaded more sole lateral and heel. Trimmed cows loaded more the sole lateral and toe region irrespective of the legs.

The higher order 4-way interaction G*L*C*R (Figures 4-34 to 4-43) showed that the major changes noticed for the legs presented previously tended to occur primarily on the lateral claw. A similar trend for the lateral claw seemed to occur in the midstance analysis as well, where balance of the pressures although small, were noticed exclusively on the lateral claw. These expeculations were observed visually in the graphs presented since orthogonal contrasts were not performed for the 3 and 4-way interaction levels.

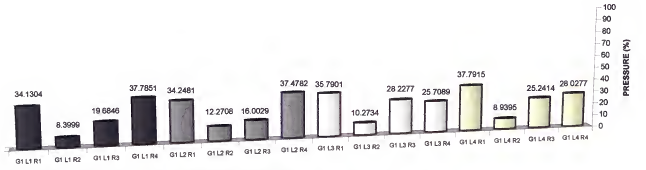

Figure 4-34. Group*Leg*Region (G*L*R) (G1) (push-off normalized set)

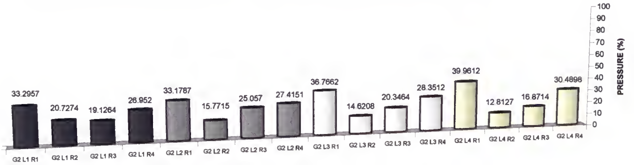

Figure 4-35. Group*Leg*Region (G*L*R) (G2) (push-off normalized set)

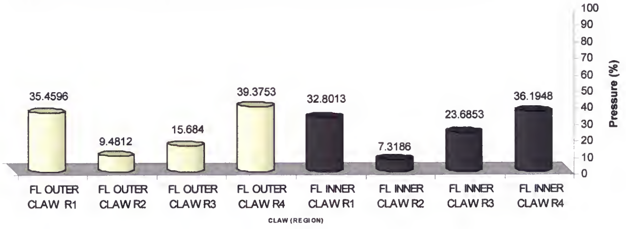

Figure 4-36. Front left leg G*L*C*R interaction (G1) normalized set LSMeans (push-off)

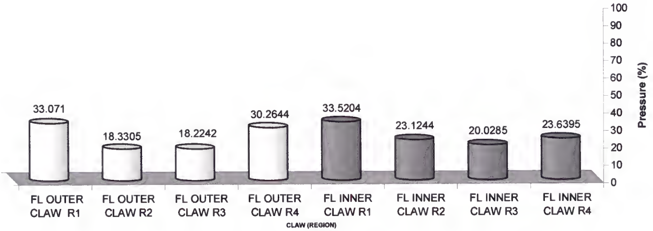

Figure 4-37. Front rear left leg G*L*C*R interaction (G2) normalized set LSMeans (push-off)

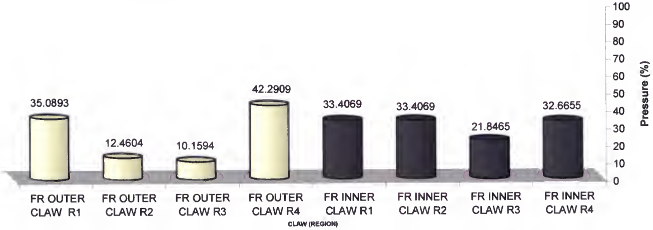

Figure 4-38. Front right leg G*L*C*R interaction (G1) normalized set LSMeans (push-off)

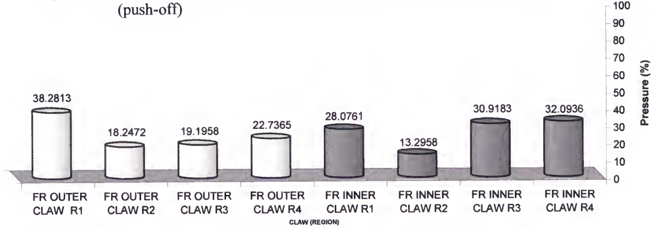

Figure 4-39. Front right leg G*L*C*R interaction (G2) normalized set LSMeans (push-off)

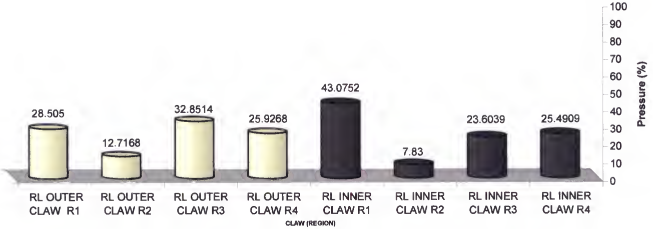

Figure 4-40. Rear left leg G*L*C*R interaction (G1) normalized set LSMeans (push-off)

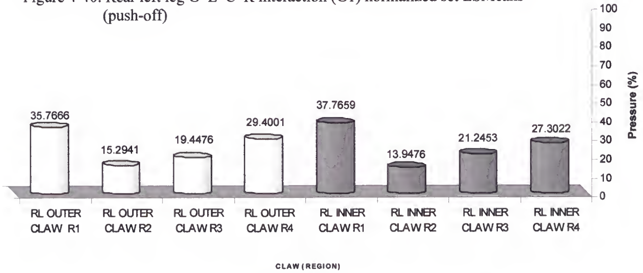

Figure 4-41. Rear left leg G*L*C*R interaction (G2) normalized set LSMeans (push-off)

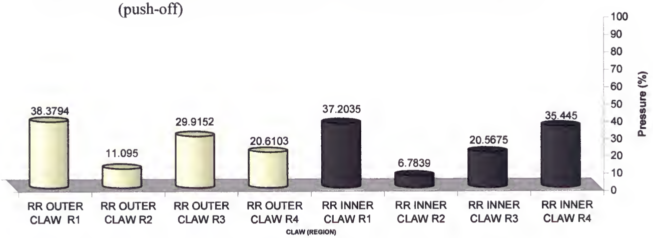

Figure 4-42. Rear right leg G*L*C*R interaction (G1) normalized set LSMeans (push-off)

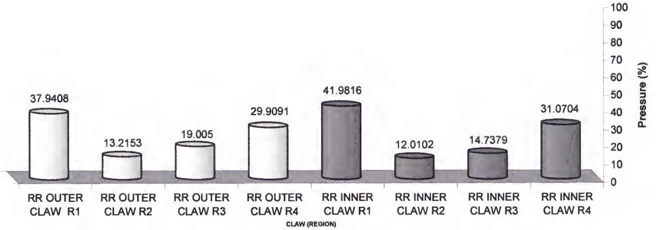

Figure 4-43. Rear right leg G*L*C*R interaction (G2) normalized set LSMeans (push-off)

Linear and Angular Kinematics

The video data collected during the cows' passage in front of the camera were used with Hu-m-an™ (Human Movement Analysis) software (HMA Technologies Inc.) for acquisition of the kinematics data used for this analysis. A total of 29 cows from the two groups were used for the data acquisition from the 32 cows used in the initial reduced sample pressure distribution analysis. Untrimmed group consisted of 17 cows and trimmed group consisted of 12 cows.

Some of the cows did not have either a two consecutive heel strike or a two consecutive toe-off to allow calculation of spatial and temporal kinematics (linear kinematics). Usually that happened because the stride was too long and the second heel strike fell outside the camera's field of view, thus preventing the digitizing of the foot landmark.

The analysis for stride time presented the main factors G and L close to significance ($p < 0.0857$ and $p < 0.0708$) according to PROC MIXED (SAS®).

The interaction term group*leg (G*L) was not significant ($p < 0.4687$). Stride time LSMeans for group are presented in the Figure 4-44. Values for stride time ranges are presented in Tables 4-19. Stride time was longer for the un-trimmed (G1) group of cows and indicated slower gait as compared to the trimmed (G2) group of cows. Orthogonal contrasts for stride time main effect Leg (L) were tested for differences across the 4 legs. There were significant differences across the 4 legs (Table 4-20).

Table 4-19. Stride time range values (sec.) for the two groups

Group	Min. (sec)	Max. (sec)
Un-trimmed	1.03	2.36
Trimmed	1	1.56

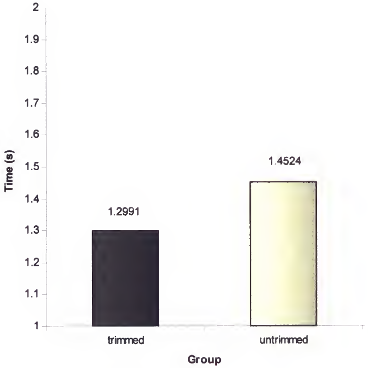

Figure 4-44. Stride time LSMeans for groups

The analysis for stride length was not significant for either of the main effects (G or L) ($p < 0.7216$ and $p < 0.6493$ respectively). The stride length LSMeans values for the untrimmed and trimmed groups were 1.6494 m and 1.6677 m respectively. Values for stride length ranges are presented in Tables 4-21. According to the analysis, stride length were not different between the two groups trimmed versus un-trimmed.

Table 4-20. Stride time orthogonal contrasts for leg (L) main effects.

Contrast	Estimate	SE	DF	T value	Pr > |t|
Leg (L)					
1 vs. 2, 3, 4	0.3764	0.1695	31	2.22	0.0338
2 vs 3, 4	-0.2182	0.08712	31	-2.5	0.0177
3 vs 4	0.2034	0.07704	31	2.64	0.0129

Table 4-21. Stride length range values (m) for the two groups

Group	Min. (m)	Max. (m)
Un-trimmed	1.28	2.29
Trimmed	1.4	1.92

The analysis for stride velocity was not significant for main effects group (G) and leg (L) or the interaction term (G*L) ($p < 0.1773$, $p < 0.1619$ and p , 0.2659 respectively). Stride velocity LSMeans for the un-trimmed and trimmed groups were 1.17 m/s and 1.29 m/s respectively. Table 4-22 shows the range of values for stride velocities. Figure 4-45 shows a representation of the velocity pattern of the two groups using the original calculated velocities.

Table 4-22. Stride velocity range values (m/s) for the two groups

Group	Min. (m/s)	Max. (m/s)
Un-trimmed	0.6	1.67
Trimmed	1.05	1.71

Although no significant changes were detected in kinematics of spatial and temporal data between the two groups, it was expected differences would exist for velocities between the two groups since untrimmed cows tended to have a longer time spent during stride. That would indicate that trimmed cows should have had faster stride. In fact they did walk slightly faster according to LSmeans obtained in the analysis from PROC MIXED (SAS®), however, the greater velocity was not statistically significant.

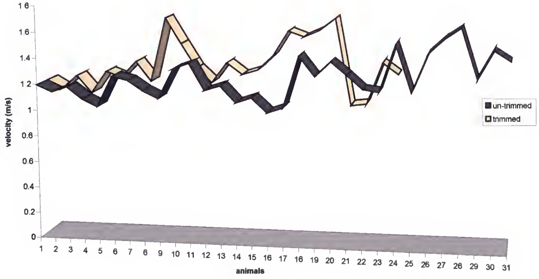

Figure 4-45. Calculated velocity data set for the two groups

Angular Kinematics analysis was performed using PROC MIXED (SAS®). The videos of 20 cows' stride were used for this analysis (10 trimmed cows and 10 un-trimmed cows). Five body landmarks on each lower portion of the front legs and rear legs of each cow were digitized frame by frame for each movie. Frames corresponding to the three phases used for the pressure analysis (midstance, loading response and push-off phases) were selected according to its position in the movie. An example of the digitizing is shown in Figures 4-46.

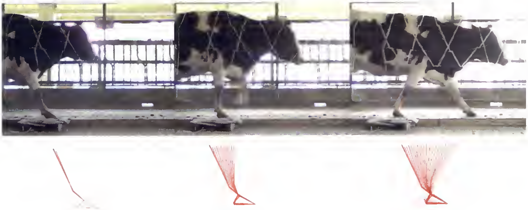

Figure 4-46. Video digitizing and lower limb digitized model

The analyses were performed for the three different phases individually. Midstance phase fetlock relative angle analysis was statistically significant for the main factor group (G) ($p < 0.0045$) according to PROC MIXED (SAS®). Fetlock relative angle LSMeans obtained for untrimmed cows presented significant smaller joint angle (157±1.8°) compared to trimmed cows (162±1.8°). This difference reflects a reduced amount of extension of the two body segments that form this joint presented by the untrimmed group. The increased extension angle at the fetlock joint shown by the trimmed cows may be due to the fact that trimming the foot brings the sole more parallel (level) with the pavement, thus extending these two segments. Maximum standard deviation obtained for the sampled population was (±6.1° deg) for trimmed cows and (±7.78° deg.) for untrimmed cows. Figure 4-47 shows the angular range of motion (maximum and minimum extension angles) of the data presented by each group during the three selected phases. Figure 4-48 shows a diagram of the changes in the relative fetlock joint extension angle between the two groups (trimmed and un-trimmed).

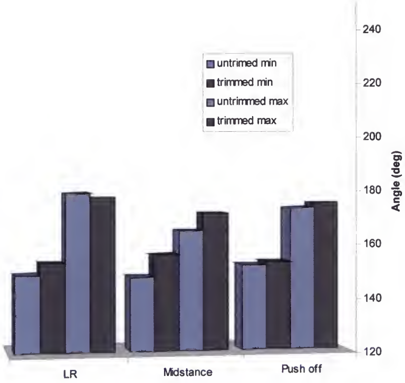

Figure 4-47. Group range of motion (ROM) during stance phase

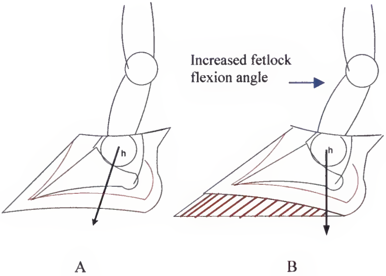

Figure 4-48. Fetlock relative extension angle changes. A) trimmed. B) un-trimmed

CHAPTER 5
SUMMARY AND CONCLUSIONS

The first objective of this study was to evaluate weight bearing dynamics and pressure distributions under the hooves of dairy cattle for two group of cows: Un-trimmed (unbalanced) and trimmed (balanced). The second objective was to assess the gait linear and angular kinematics changes (spatial and temporal gait characteristics, velocities and joint range of motion) for each group and associate these changes in pressure distribution and gait kinematics, if any, to the lameness etiologies of biomechanical origin.

This study tended to reinforce the fact that the highest loads on hind limbs of cows, irrespective of the trimming treatment, are applied on the lateral claw (close to significance G*L*C interaction, $p < 0.0825$) as seen in Figure 4-4 (Midstance analysis). The highest pressures for the left hind limbs of untrimmed cows were 268±31.7 KPa for the lateral claw vs. 171±31.7 KPa for the medial claw and the right hind limb pressures were 220±28.13 KPa for the lateral claw vs. 144.78±28.13 KPa for the medial claw. The front limbs had pressures that were more even between the two claws: front left averaged 214.4±26.88 KPa for lateral vs. 179±26.88 KPa for medial claw and front right averaged 205.4±24.8 KPa for lateral claw vs. 194.4±28.13 KPa for medial claw. Orthogonal contrasts for these trends were not tested, hence, these are assumptions based on visual interpretation of the graphs and LSMeans. However, the effect of trimming seemed to have shifted the highest pressures to the weight-bearing borders of the lateral claws of the front and hind limbs. The pressure differences were: 412.78±33.8 KPa vs. 318.3±33.8 KPa for the left front limb's lateral and medial claws respectively, and 401±28.54 Kpa vs. 215±28.54 KPa for the lateral and medial claws of the right front limb.

The hind limbs of the trimmed cows had a similar pressure distribution between claws as the front limbs. Left hind limb pressures were: 379.5±31.71 KPa vs. 262.89±31.71 KPa for the lateral and medial claws respectively. Right hind limb's pressures were: 360.1±28.26 KPa vs. 243.1±28.26 KPa for the lateral and medial claws respectively (Figure 4-4). The forces on the medial claw of the front foot of cows are consistently reported in literature to be somewhat greater for the medial claws for trimmed and un-trimmed cows (Raven 1989; Peterse 1986; Scott 1986; and van der Tol et al., 2001). The reason for the greater pressures in the lateral claws of the front foot of the trimmed group obtained in this experiment may be explained, in part by a greater surface contact area of the medial claws obtained with trimming treatment resulting in peak smaller pressures but nevertheless still bearing a greater force.

The pressure analysis for the three different points of the stance phase, demonstrated, in a general form, that there are small changes in the way the pressure is distributed after trimming the claws. From the normalized pressure analysis at midstance, the greater impact of trimming is reflected in some increase in the pressure concentration on the medial sole of the four legs for the trimmed group accounting for both claws.

The redistribution of the pressures in midstance, although small, seems to be transferred to the sole medial region. This trend is shown in the G*L*R interaction (p <0.0043) in Figure 4-10, which shows visually a slight approximation of the average pressures among regions 2, 3, and 4 in a general form accounting for the four legs for group 2 (trimmed/balanced). This trend is desired for trimmed claws and the closer the average pressures among the regions of a claw are, the better is the balancing of the claw pressure distribution obtained.

The increases were shown in Figures 4-9 and 4-10. The values of increased pressure on the sole medial region (R2) for the front left limb corresponded to an increase of 11.6 to 21% of total pressure on that limb for un-trimmed to trimmed group respectively. The right limb medial sole region had an increase from 14.2 to 15.15% in the front left leg. The hind limbs presented increases of 11.52 to 17.53% on the left side from untrimmed to trimmed group on R2 and right side from 8 to 14.5%. The average pressure increase on the medial sole (R2) accounting for the four legs was relatively small (6%) and was not demonstrated by orthogonal contrasts.

The least square means depicting the four-ways interaction G*L*C*R (Figures 4-11 to 4-18) reveals in more detail the changes in average pressure distribution already pointed out in figure 4-10.The decrease in the length of the wall at the sole lateral region, reduced sole thickness and decrease in length of the toe seemed to have caused a slight shift of pressures from heel and lateral sole towards the medial sole of the outer claw rather than a uniform distribution on both claws.

In the loading response phase analysis, the distribution of the total pressure among the 4 regions of interest had similar proportions as in midstance (region (R) main effect significance level of $p < 0.0001$ for both analyses) but were not different between the two analyses for the individual regions (i.e. heel region (R3) for the midstance analysis averaged 271.1±18 KPa vs. 283.4±18 KPa for loading response and so forth)

At loading response, it would be expected that the heel would carry higher pressure as compared to midstance. This is due to the fact that at heel strike (IC), as the name implies, the heel is the first to contact the ground and rapidly transfers the forces forward as the weight is being accepted in loading response towards midstance (Chow 2002, Exercise and Sports Sciences Department. University of Florida. Gainesville, FL, personal communication).

However, the changes were not large enough between midstance and loading response phases to prove that heel is the major region that contacts the ground at heel strike in loading response. As an example, in the left front limb, the pressure value of the heel at midstance for un-trimmed was 28% of total pressure on that leg vs. 30% of total pressure applied on that leg during LR, both accounting for lateral and medial claws. Followed by Front right 26% vs. 27%, rear left 28.76% vs. 28.5% and rear right with 26.09% vs. 30.3% of total pressure per foot. The trimmed group presented similar results. These values can be found in Figures 4-9 and 4-10 (midstance analysis) and Figures 4-25 and 4-26 (LR analysis).

This present study did not test the initial contact (IC) of the foot with the ground and what region contacted the ground first. However, it seems from the data at LR phase, which follows right after the initial contact and differs from it by a fraction of second, that the sole lateral (weight bearing border) may be the part of the foot that is involved in initial contact as well. Van der Tol et al. (2002) (Pathobiology Department. Veterinary Medicine School. University of Utrecht, Utrecht, The Netherlands, personal communication) presented similar trends when analyzing five moments of the stance phase of the cow's stride. From their data, it seems that more than the heel contact region is loaded (also lateral sole) in the so-called heel strike. An analysis for this particular phase (initial contact (IC)) of the stance may be performed in the future using the data set used for this experiment.

In the push-off analysis, the 3-way interaction G*L*R ($p < 0.0262$) shows that front legs load more the sole lateral and toe regions (i.e., front left foot: 229.6±32.9 KPa and 232.6 ±32.9 KPa for sole lateral and toe respectively compared to 72.9±32.9 KPa and 137.2±32.9 KPa for medial sole and heel respectively) and the rear legs load more the sole lateral and showed higher peak pressures for heel region rather than toe in the un-trimmed group (i.e., rear left foot: 284.3±42.5 KPa and 239.9±42.5 KPa for sole lateral and heel respectively compared to 100.6±42.5 KPa and 180.1±42.5 KPa for sole medial and toe respectively). This trend seemed to be more evident (graphic visualization) for the left foot than the right foot. Trimmed cows consistently load the sole lateral and toe region more (although the average pressures among regions were closer to each other) irrespective of the leg (i.e., front left foot: 469.6±43.2 KPa and 332.4±43.2 KPa for sole lateral and toe respectively compared to 285.3±43.2 KPa and 249.6±43.2 KPa for sole medial and heel respectively and similarly, rear left foot: 365.1±39.9 KPa and 253.1±39.9 KPa for lateral sole and toe compared to 158.2±39.9 KPa and 225.7±39.9 KPa for medial sole and heel respectively).This interaction is presented in Figures 4-30 and 4-31. Figures 4-34 and 4-35 show the same visual trends expressed as percentages of the total pressure applied on the claws.

The detail of this trend is further clarified by the G*L*C*R interaction for this particular analysis and is depicted in Figures 4-36 to 4-43, where the differences in pressure distribution between heel and toe for front and hind legs of untrimmed group seem to occur, like midstance analysis, on the lateral claw. From this set, it is possible to see that rather than balance between heel and toe, what happened in reality is that hind lateral claws tended to load the sole lateral and heel more in untrimmed cows. The trimmed group, presents an overall better balance between regions, nevertheless the highest pressures are in the lateral sole and toe of both front and hind limbs. Orthogonal contrasts for pressure analysis at three different phases of the stance were performed for main factors region (R) and leg (L) and 2-ways interactions (G*C), (G*R) and (C*R). Region (R) was the only significant main effect obtained for midstance analysis and showed that regions are significantly different from each other. Interaction (G*C) was significant for midstance as well showing evidence that claws are different between the two groups. Regions (R2) and (R4), medial sole and toe respectively, orthogonal contrasts were also significant in midstance analysis between lateral and medial claws ((C*R) interaction). These contrasts are presented in Table 4-3.

Loading response phase main effects region (R) and leg (L) were statistically significant in the orthogonal contrasts tested. Regions were different from each other for both groups and front right leg (L2) was significantly different from rear legs (L3 and L4). The 2-way interactions tested were not statistically significant. Contrasts for this analysis are presented in Table 4-9. Push-off analysis orthogonal contrasts were significant for the region main effects only.

Gait linear kinematics analysis showed that un-trimmed cows tended to have a significantly longer stride time ($p < 0.0857$) than trimmed (1.45sec vs. 1.299sec for untrimmed vs. trimmed respectively). The least squares means for velocity between groups were 1.17m/s vs. 1.29m/s for untrimmed and trimmed respectively. Stride velocity analysis was not statistically significant ($p < 0.1773$). These data agree with previous studies for stride duration (Rajkondawar et al., 2001, Flower et al., 2003) and stride velocity (Flower et al., 2003). It can be speculated from these values that claw trimming could have provided a slightly more comfortable gait for cows, mostly during push off where the hind limbs are more involved in propulsion of the body forward (Scott 1988). The un-trimmed group seemed to maintain pressures in the heel and lateral sole even during the push-off phase where pressures would be expected to increase at the toe for propulsion.

Angular kinematics analyses showed statistical significance ($p < 0.0045$) in midstance phase for the fetlock joint relative extension angle (Figure 4-48). Trimmed cows presented a higher degree of fetlock joint angle extension (162±1.05°) as compared to untrimmed cows (157±1.05°). The increased extension angle at the fetlock joint shown by the trimmed cows may be due to the effects of trimming. Speculation about this result leads to the assumption that trimming the claw brings the sole more parallel (level) with the floor, thus extending the two leg segments, anterior and posterior to the fetlock joint. The range of fetlock joint relative angle values obtained for trimmed cows had overall higher maximum extension angles in all three phases of stance (Figure 4-47).

In conclusion, this study attempted to balance the claws by trimming and reducing the claw horn overgrowth using a method developed by Raven seemed to achieve small differences in the redistribution of pressures within the claw. Statistical analysis (PROC MIXED (SAS®)) found significant differences for many interactions that tested the distribution of pressures between groups. However, the higher order (3 and 4-way) significant interactions were not tested with orthogonal contrasts. Therefore, most of the discussion and conclusions presented here are speculative and based only on least square means, standard errors and previous understanding of biomechanical mechanisms.

Speculation obtained about the data analysis may leads to an assumption that even by trimming the claw, the heel and lateral sole still maintain the major pressure peaks. In addition, small changes in pressure concentration from the heel and lateral sole towards the medial sole area (site of vulnerable spot – Raven 1989) after trimming, may increase stresses in the medial sole area rather than relieve its burden.

Gait analysis has been done in a preliminary basis using video capturing and editing technology with minimum requirements for this type of analysis. The results supported trends occurring in the pressure analysis and indicated that trimming may benefit cows. The increased velocity and greater extension of the fetlock joint at midstance are results that tended to affect gait of trimmed cows. However, in the angular kinematics analyses, frame-by-frame manual digitizing was difficult to interpret. An ideal manual digitizing procedure can be obtained if reflective markers on the body landmarks are used. Automated tracking systems are the most reliable method of digitizing kinematic data and the results obtained with these systems are very accurate. Unfortunately, they are very expensive systems and are performed in only few biomechanical laboratories for human motion.

According to the data obtained in this study, claw trimming may provide some balance to the pressures applied to various regions of the lateral claws of the front feet and the hind feet by redistributing some of these pressures to the medial sole area. However, it is questionable whether shifting pressures from weight-bearing border (lateral sole) towards the softer portion of the sole in order to achieve balance is the correct approach. Lameness of biomechanical origin is thought to be related to the overburdening of soft tissues in the axial region of the claw anterior to the heel bulb caused by claw overgrowth under confinement housing conditions. This particular region (typical sole lesion spot, Raven 1989) did not appear to be obviously overloaded in un-trimmed claws as expected. However, the claw divisions used in this experiment did merge the sole with the heel region. According to the data obtained in this experiment, the heel was the major weight bearing portion of the claws in the un-trimmed group as compared with trimmed group. The result of pressure distribution between these two groups combined with limited support from the joint angular kinematics leads to the assumption that there may be an area of overburdened soft sole at the vulnerable spot region. Further, it is assumed that the high pressures at this spot may be mitigated by claw trimming that tends to increase contact surface area at that spot. However, data here suggest that these pressures are not redistributed evenly towards the anterior part of the medial sole region and are instead redirected towards the vulnerable region where sole ulcer occurs. If this is the case, trimming the cows according to the Toussaint Raven method may not accomplish the desired effects (redistribution of weight-bearing away from the vulnerable area).

Performing other analyzes with data obtained from different approaches can be useful to clarify overall findings obtained in studies such as that described here. Some of these approaches include the following.

First, the development of a recording system that would better define another subdivision of the medial sole towards the vulnerable (fragile) spot. This would permit the assessment of pressures for the anterior and posterior portions of the medial sole. Second, calculations of the center of pressure (COP) trajectory during gait is another possible analysis that may help to clarify this issue. Because part of the sole that is not in contact with the ground can be overstressed as well due to the suspended structures (suspensory apparatus) within the claw, a follow up analysis of the trajectory of the center of pressure under the claw could be the next step in order to supplement the findings obtained with pressure analysis. Finally, orthogonal contrasts of the higher order significant interactions need to be performed in order to properly compare the visual trends obtained so far.

REFERENCES

Bartel, D. L., F. Schryver, J. L. Lowe, and R. A. Parker. 1978. Locomotion in the Horse: A Procedure for Computing the Internal Forces in The Digit. Am. J. Vet. Res. 39: (11), 1721-1727.

Carter, E. J., L. D. Galuppo, J. R. Snyder, and N. H. Willits. 2001. Evaluation of an In-Shoe Pressure Measurement System in Horses. Am. J. Vet. Res. 62:(1), 23-27.

Clayton, H. M., E. Hodson, and J. L. Lanovaz. 2000. The Forelimb in Walking Horses: 2. Net Joint Moments and Joint Powers. Equine Vet. J. 32: (4), 295-299.

Dalin, G., and L. B. Jeffcott. 1985. Locomotion and Gait Analysis. Vet. Clinics of North Am.: Equine Practice.1:(3), 549-569.

Dammrich, K. 1986a. Aetiology of Disorders of Skeletal Structures. In Cattle Housing Systems: Lameness and Behavior. Martinus Nijhoff Publishers-Netherlands, 8-13.

Dammrich, K. 1986b. The Reaction of the Leg (Bone, Joints) to Loading and the Consequences to Lameness. In Cattle Housing Systems: Lameness and Behavior. Martinus Nijhoff Publishers-Netherlands, 50-55.

Hall, M. B. 2002. Rumen Acidosis: Carbohydrate Feeding Consideration. Proceedings of the 12th International Symposium on Lameness in Ruminants. Orlando-Florida. 51-61.

Harris, G. F., and J. J. Wertsch. 1994. Procedures for Gait Analysis. Arch. Phys. Med. Rehab. 75: 216-225.

Hendry, V. J, L. E. Green, R. W. Blowey, A. J. Packington, and R. H. C. Bonser. 2002. Tensile Strength of the White Line in the Claw of Dairy Cows Supplemented With Biotin. Proceedings of the 12th International Symposium on Lameness in Ruminants. Orlando-Florida. 167-170.

Hodd D. M., I. P. Wagner, D. D. Taylor, G. W. Brumbaugh, and M. K. Chaffin. Voluntary Load Distribution in Horses with Acute and Chronic Laminitis. Am. J. of Vet. Res. 62:(9), 1393-1397.

Hodson E., H. M. Clayton, and J. L. Lanovaz. 2000. The Forelimb in Walking Horses: 1. Kinematics and Ground Reaction Forces. Equine Vet. J. 32:(4), 287-294

Leach, D. H. 1987. Locomotion Analysis Technology for Evaluation of Lameness in Horses. Equine Vet. J. 19: (2), 97-99.

Lischer Ch. J. and P. Ossent. 2002. Pathogenesis of Sole Lesions Attributed to Lameness in Cattle. Proceedings of the 12th International Symposium on Lameness in Ruminants. Orlando-Florida. 82-89.

Khumsap, S., M. C. Hilary, and J. L. Lanovaz. 2001. Effect of Walking Velocity on Ground Reaction Force Variables in the Hind Limb of Clinically Normal Horses. Am. J. Vet. Res., 62: (6), 901-906.

Martin R. B., D. B. Burr, N. A. Sharkey. 1998a. Skeletal Tissue Mechanics. Chapter 1: Forces in Joints. New York: Springer-Verlag, 20-23.

Martin R. B., D. B. Burr, N. A. Sharkey. 1998b. Skeletal Tissue Mechanics. Chapter 5: Fatigue and Fracture Resistance of Bone. New York: Springer-Verlag, 183-191.

Martin R. B., D. B. Burr, N. A. Sharkey. 1998c. Skeletal Tissue Mechanics. Chapter 7: Synovial Joint Mechanics. New York: Springer-Verlag, 275-287.

Merkens, H. W., and H. C. Schamhardt. 1988. Distribution of Ground Reaction Forces of the Concurrently Loaded Limbs of the Dutch Warmblood Horse at the Normal Walk. Equine Vet. J. 20: (3), 209-213.

Merkens, H. W., H. C. Schamhardt, W. Hartman, and W. Kersjes. 1985. Ground Reaction Force Patterns of Dutch Warmblood Horses at Normal Walk. Equine Vet. J. 18: (3), 207-214.

Peterse D. J. 1986a. Aetiology of Claw Disorders in Dairy Cattle. In Cattle Housing Systems: Lameness and Behavior. Martinus Nijhoff Publishers-Netherlands, 3-7.

Peterse D. J. 1986b. Influence of Loading on Claw Disorders. In Cattle Housing Systems: Lameness and Behavior. Martinus Nijhoff Publishers-Netherlands, 45-49.

Phillips C. J. C., and I. D. Morris. 2000. The Locomotion of Dairy Cows on Concrete Floors that are Dry, Wet, or Covered with Excreta. J. Dairy Sci. 83, 1767-1772.

Rajkondawar, P. G., U. Tasch, A. M. Lefcourt, B. Erez, R. M. Dyer, M. A. Varner. 2001. A System for Identifying Lameness in Dairy Cattle. Applied Engineering in Agriculture. ASAE, 18:(1), 87-96.

Raven E. T. 1989. Cattle Foot Care and Claw Trimming. Farming Press. Ipswich, UK. 19-33.

Reilly, J. D., H. Newlyn, B. Cope, L. J. Lathan, S. Collins, and L. Hopegood. 2002. A Comparison of Different Moisture-Loss Methods for Measuring Hoof Wall Moisture Content. Proceedings of the 12th International Symposium on Lameness in Ruminants. Orlando-Florida. 193.

Riemersma, D. J., A. J. van den Bogert, H. C. Shamhardt, and W. Hartman. 1988. Kinetics and Kinematics of the Equine Hind Limb: In Vivo, tendon Strain and Joint Kinematics. Am. J. Vet. Res. 49: (8), 1353-1359.

Scott, G. B. 1986. Variation in Load Distribution under the Hooves of Friesian Heifers. In Cattle Housing Systems: Lameness and Behavior. Martinus Nijhoff Publishers-Netherlands, 29-36.

Scott G. B. 1988. Studies of the Gait of Friesian Heifer Cattle. Veterinary Record:123, 245-248.

Shearer, J. K. and S. R. Van Amstel, 2000. Manual for The Master Hoof Care Technician Program. Department of Large Animal Clinical Sciences-College of Veterinary Medicine, University of Florida-Gainesville, FL. 6-14.

Shearer, J. K., Beede, D. K., Bray, D. R., and Bucklin, R. A. 1999. Managing During Heat Stress. Proceedings of the 1999 Tri-State Dairy Nutrition Conference. Fort Wayne-IN, 5-18

Van Amstel, S. R., F. L. Palin, and J. K. Shearer. 2002. Claw Trimming: An Adaptation of the Dutch Method. Proceedings of the 12th International Symposium on Lameness in Ruminants. Orlando-Florida. 127-130.

Van der Tol, P. P. J., J. H. M. Metz, and E. N. Noordhuizen-Stassen. 2002. The Pressure Distribution Under the Bovine Claws During Square Standing on a Flat Substrate. J. Dairy Sci. 85: 1476-1481.

Weishaupt, M. A., H. P. Hogg, T. Wiestner, J. Denoth, E. Strussi, and J. A. Auer. 2002. Instrumented Treadmill for Measuring Vertical Groung Reaction Forces in Horses. Am. J. Vet. Res. 63: (4), 520-526.

Whittle, M. W., 1996. Gait Analysis-An Introduction. Butterworth-Heinemann. 58-69

BIOGRAPHICAL SKETCH

Victor Ricardo Ciaco de Carvalho was born in Mogi-Guaçu-SP, Brazil in 1969. He attended primary and secondary schools in Mogi-Guaçu. He is the second of three children of Ana Maria Ciaco de Carvalho and José Augusto de Carvalho Neto. In 1989 he began college studies at Octavio Bastos Veterinary Medicine School, graduating in 1994 with the degree of Doctor of Veterinary Medicine. He then worked at the family dairy farm in Sao Paulo state, Brazil. In June of 1997 he enrolled in the English Language Institute at the University of Florida to continue his English studies. In January of 1998 he began his Master's degree program in the Department of Agricultural and Biological Engineering and graduated with a Master of Science degree in May 2000. In August 2000 he began his Doctor of Philosophy degree in the Department of Agricultural and Biological Engineering. He will graduate with a Doctor of Philosophy degree in May 2004.

I certify that I have read this study and that in my opinion it conforms to acceptable standards of scholarly presentation and its fully adequate, in scope and quality, as a dissertation for the degree of Doctor of Philosophy.

Ray A. Bucklin, Chair
Professor of Agricultural and
Biological Engineering

I certify that I have read this study and that in my opinion it conforms to acceptable standards of scholarly presentation and its fully adequate, in scope and quality, as a dissertation for the degree of Doctor of Philosophy.

J. K. Shearer

Jan K. Shearer
Professor of Large Animal
Clinical Sciences

I certify that I have read this study and that in my opinion it conforms to acceptable standards of scholarly presentation and its fully adequate, in scope and quality, as a dissertation for the degree of Doctor of Philosophy.

H Herbert Head

H. Herbert Head
Professor Emeritus of Animal
Sciences

I certify that I have read this study and that in my opinion it conforms to acceptable standards of scholarly presentation and its fully adequate, in scope and quality, as a dissertation for the degree of Doctor of Philosophy.

James D. Leary
Lecturer of Agricultural and
Biological Engineering

I certify that I have read this study and that in my opinion it conforms to acceptable standards of scholarly presentation and its fully adequate, in scope and quality, as a dissertation for the degree of Doctor of Philosophy.

Roger A. Nordstedt
Professor of Agricultural and
Biological Engineering

This dissertation was submitted to the Graduate Faculty of the College of Agricultural and Life Sciences and to the Graduate School and was accepted as partial fulfillment of the requirements for the degree of Doctor of Philosophy.

May 2004

E. Jane Luzar

Dean, College of Agricultural
and Life Sciences

Dean, Graduate School